CONSTRUCTION OF INELASTIC RESPONSE SPECTRA FOR SINGLE-DEGREE-OF-FREEDOM SYSTEMS

COMPUTER PROGRAM AND APPLICATIONS

By S.A. Mahin and J. Lin

A report on research sponsored by the

National Science Foundation

Report No. UCB/EERC-83/17

Earthquake Engineering Research Center

College of Engineering

University of California

Berkeley, California

June, 1983

6
1 a

50272-101

REPORT DOCUMENTATION PAGE	1. REPORT NO. NSF/CEE-83030	2.	3. Recipient's Accession No. PB84 208834
4. Title and Subtitle: CONSTRUCTION OF INELASTIC RESPONSE SPECTRA FOR SINGLE-DEGREE-OF-FREEDOM SYSTEMS: Computer Program and Applications			5. Report Date: June 1983 6.
7. Author(s): S.A. Mahin and J. Lin			8. Performing Organization Rept. No. UCB/EERC-83/17
9. Performing Organization Name and Address: Earthquake Engineering Research Center University of California 1301 South 46th Street Richmond, CA 94804			10. Project/Task/Work Unit No. 11. Contract(C) or Grant(G) No. (C) (G) CEE-8208079
12. Sponsoring Organization Name and Address: National Science Foundation 1800 "G" Street NW Washington, DC 20550			13. Type of Report & Period Covered 14.

15. Supplementary Notes

16. Abstract (Limit: 200 words)

This report describes a computer program written to analyze the inelastic response of viscously damped single-degree-of-freedom systems to either support excitation or external loadings. Various methods of developing design aids based on computed inelastic response are discussed. The computer program has been written to allow the user to conveniently obtain detailed information regarding the inelastic response of a system and to study systematically the effect of variations in the mechanical and dynamic characteristics of the system and of different excitations.

Theoretical formulations and solution schemes used in the computer program are described. The definitions and limitations of different response indicies, including various types of ductility factors, are examined. Procedures for constructing ductility-based response spectra appropriate for design are presented. Several examples of using the computer program for generating response of single-degree-of-freedom systems and response spectra are presented for illustration. Observations regarding inelastic behavior of structures are also described. Conclusions regarding the applicability of these results and the need to extend these methods to multiple-degree-of-freedom systems are offered.

17. Document Analysis a. Descriptors

b. Identifiers/Open-Ended Terms

c. COSATI Field/Group

18. Availability Statement: Release Unlimited	19. Security Class (This Report)	21. No. of Pages 96
	20. Security Class (This Page)	22. Price

ABSTRACT

This report describes a computer program written to analyze the inelastic response of viscously damped single-degree-of-freedom systems to either support excitation or external loadings. Various methods of developing design aids based on computed inelastic response are discussed. The computer program has been written to allow the user to conveniently obtain detailed information regarding the inelastic response of a system and to study systematically the effect of variations in the mechanical and dynamic characteristics of the system and of different excitations.

Theoretical formulations and solution schemes used in the computer program are described. The definitions and limitations of different response indicies, including various types of ductility factors, are examined. Procedures for constructing ductility-based response spectra appropriate for design are presented. Several examples of using the computer program for generating response of single-degree-of-freedom systems and response spectra are presented for illustration. Observations regarding inelastic behavior of structures are also described. Conclusions regarding the applicability of these results and the need to extend these methods to multiple-degree-of-freedom systems are offered.

ACKNOWLEDGEMENTS

The research presented in this report has been sponsored by the National Science Foundation. The support is gratefully acknowledged. Opinions, findings, and conclusions or recommendations expressed in this publication are those of the authors and do not necessarily reflect the views of the National Science Foundation or the Earthquake Engineering Research Center, University of California, Berkeley.

Credits are given to Mr. R. Herrera who was involved in the early development of the computer program and to Mr. R. Klingner who developed the variable time step algorithm used in the computer program. The drafting was prepared by Ms. G. Feazell. The contributions of these persons to the publication of this report are appreciated.

Table of Contents

1 INTRODUCTION

1.1 Introductory Remarks

Buildings and other structures are often designed to respond inelastically when they might be subjected to rare and unusually intense dynamic loads during their service life. This results in considerable economic savings relative to designing for such loading on an elastic basis. Such structures, however, must be designed, detailed and constructed to develop the required inelastic deformations. When this is done properly, the structures will sustain the dynamic loading with local damage but without collapse.

This design philosophy is often adopted in design of conventional earthquake-resistant buildings and of impact- or blast-resistant structures. However, inelastic dynamic response is complex and difficult to predict using conventional design and analysis methods based on elastic dynamic behavior [10]. Consequently, it is desirable to have design-oriented analytical tools capable of accounting for the inelastic dynamic response of structures.

General purpose, finite element analysis, computer programs have been developed to predict the inelastic dynamic response of two- and three-dimensional assemblages of structural components [1,2,9,11,13,14,20] While such programs are useful in assessing the reliability of a final design where the geometry and member properties are known, they are generally unsuitable for preliminary design. In the initial stages of design little information is available regarding the structure's mechanical or dynamic characteristics. The designer in this case needs basic guidance in selecting the overall stiffness and strength of a system in order to limit its inelastic deformations to accceptable levels. Alternatively, the designer may wish to quickly assess the sensitivity of the overall response of a proposed structure to uncertainties in its mechanical and dynamic characteristics or to different excitations. General purpose programs can provide little guidance in such cases.

Fortunately, it may be feasible to represent certain multiple-degree-of-freedom structures as equivalent single-degree-of-freedom systems [16,21,22,23 and Appendix B]. In this case, a

variety of parametric studies can be easily and economically performed using simple structural models. To facilitate such analyses and the development of general design guidelines, it is desirable to have a computer program capable of efficiently computing the inelastic response of such structural models to various dynamic excitations.

1.2 Objectives And Organization

The objectives of this report are to describe a computer program written to analyze the inelastic responses of viscously damped single-degree-of-freedom systems to either base input accelograms or direct external load inputs (Fig. 1) and to discuss various methods of developing design aids based on computed inelastic response. The computer program has been written to allow the user to conveniently obtain detailed information regarding the inelastic response of a system and to study systematically the effect of variations in the mechanical and dynamic charateristics of the system and of different excitations.

In Chapter 2, the governing equations of motion for the systems considered are described, and normalized forms of these equations are derived to illustrate the generalization of the computed responses for a particular system to a family of related systems. The numerical method used in the program is also described in that chapter with a brief discussion on the accuracy and stability of the method. Section 2.3 describes the self-adjusting time step scheme adopted in the program to solve the equations of motion. This method reduces the number of times steps needed in numerically integrating the equations of motion and automatically controls the accuracy of the solution when inelastic events occur.

The two nonlinear force-deformation models incorporated in the program are described in Chapter 3. These hysteretic idealizations, the bilinear and stiffness degrading models shown in Fig. 2, are commonly used to analyze many types of structures. However, they are relatively simple compared to the inelastic behavior exhibited by some types of structures. The use of seperate subroutines for state determination with each model makes it convenient for the user to add additional hysteretic models. The last section of Chapter 3 includes a discussion of the application of the available hysteretic models to account for P-Delta effects due to gravity loads.

In many cases, it is infeasible to inspect the entire response history and a few numerical indicies are desirable to summarize the response. In Chapter 4, various response indicies to quantify inelastic response are discussed. The response indices discussed and incorporated in the program include maximum response displacement, residual displacement, displacement ductility, cyclic ductility, accumulative displacement ductility, normalized hysteretic energy ductility, number of yield excursions and yield reversals, number of zero crossings, and various energy indices.

Development of design guidelines for inelastic systems by means of response spectra is discussed in Chapter 5. The capability of the computer program in generating different kinds of response spectra is discussed. The program can automatically compute the responses of systems obtained by permuting all combinations of user-specified lists of periods, yield strengths and damping values. Alternatively, the user can list the specific combinations of these parameters to be analyzed. These features are useful in constructing constant strength, constant ductility and other types of response spectra described in Chapter 5.

Examples of using the computer program for generating responses of single-degree-of-freedom systems and response spectra are given in Chapter 6. Observations regarding inelastic behavior of structures are also offered. Conclusions and recommendations are offered in Chapter 7.

In Appendix A, program input specification and output are discussed, and in Appendix B, modeling of multiple-degree-of-freedom systems by single-degree-of-freedom systems is discussed.

2 SOLUTION OF EQUATIONS OF MOTION

2.1 Basic Form of Equation

As mentioned in Chapter 1, the program calculates the response of viscously damped, inelastic, single-degree-of-freedom systems. For a system subjected to an external forcing function (see Fig. 1), the governing equilibrium equation at time t is

$$M\ddot{u}(t)+C\dot{u}(t)+R(t)=P(t) \tag{1}$$

where M is the mass of the system, C is the system's damping coefficient, $R(t)$ is its restoring force and $P(t)$ is the load acting on the system. As shown in the Fig. 1, the displacement of the system with respect to its fixed base is denoted as $u(t)$.

In the case of horizontal earthquake ground motion excitations (Fig. 1) we may write Eq. 1 in the form:

$$M\ddot{u}(t)+C\dot{u}(t)+R(t)=-M\ddot{u}_g(t) \tag{2}$$

where $M,C,R(t)$ are the same as before. In this case, $u(t)$ denotes the displacement of the system relative to the ground and $u_g(t)$ is the displacement of the ground relative to a fixed reference axis.

By comparison of Eqs. 1 and 2, one can note that the equation of motion for a seismically excited system is the same as that for an externally loaded system if the load $P(t)$ equals $-M\ddot{u}_g(t)$. However, the precise meaning of $u(t)$ in each case must be remembered. When Eq. 1 is applied to a seismically excited system, $u(t)$ represents the displacement of the system with respect to an accelerating base and the total displacement is $v(t) = u(t)+ u_g(t)$; however, when the equation is applied to an externally loaded system, $u(t)$ also represents the total displacement of the system since the base is fixed.

2.2 Normalized Form of Equations of Motion

Although Eqs. 1 and 2 can be solved directly for the response of a particular system, it is frequently desirable to express these equations in a normalized form. In this manner, the specific parameters that influence response can be more readily identified. In addition, the

computed responses can be applied to a family of related systems thereby facilitating the development of design aids. It is convenient to write Eqs. 1 and 2, respectively, as

$$\ddot{u}(t)+2\omega\xi\dot{u}(t)+\frac{1}{M}R(t)=\frac{P(t)}{M} \tag{3}$$

$$\ddot{u}(t)+2\omega\xi\dot{u}(t)+\frac{1}{M}R(t)=-\ddot{u}_g(t) \tag{4}$$

where ω is the natural circular frequency of the system ($\omega^2 = K/M$) and ξ is its viscous damping ratio (expressed as a fraction of the critical damping ratio). In the case of elastic systems, where $R(t)=K\times u(t)$, Eqs. 3 and 4 reduce, respectively, to

$$\ddot{u}(t)+2\omega\xi\dot{u}(t)+\omega^2u(t)=\frac{P(t)}{M} \tag{5}$$

$$\ddot{u}(t)+2\omega\xi\dot{u}(t)+\omega^2u(t)=-\ddot{u}_g(t) \tag{6}$$

In this way, only a single analysis is needed to determine the responses of all elastic systems having the same frequency and damping ratio subjected to the same excitation. The responses of the related systems can be conveniently summarized by response spectra (Chapter 5) which plot, as an example, the maximum responses against frequencies for a constant amount of damping.

To develop design aids for inelastic systems, it is desirable to normalize equations of motion for inelastic systems similiarly. In the case of external loadings, it has been suggested [4] to normalize the hysteretic loops as follow:

$$\mu(t)=\frac{u(t)}{u_y} \quad \text{and} \quad \rho(t)=\frac{R(t)}{R_y} \tag{7}$$

where u_y and R_y are the yield displacement and force of the system, respectively. The value of $\mu(t)$ is often called the displacement ductility of the system and is useful in designing structures. For example, the maximum value of displacement ductility, μ_{max}, that the system undergoes indicates how tough the structure must be detailed to be.

If we additionally define $\gamma=\frac{t}{T}$, where T is the structural period ($T=2\frac{\pi}{\omega}$), then

$$\dot{u}(t)=\frac{du(t)}{dt}=\frac{du}{d\gamma}\frac{d\gamma}{dt}=\frac{u_y}{T}\frac{d\mu(\gamma)}{d\gamma} \tag{8a}$$

$$\ddot{u}(t)=\frac{d^2u(t)}{dt^2}=\frac{u_y}{T^2}\frac{d^2\mu(\gamma)}{d\gamma^2} \tag{8b}$$

and Eq. 3 becomes

$$\frac{u_y}{T^2}\frac{d^2\mu(\gamma)}{d\gamma^2}+2\omega\xi\frac{u_y}{T}\frac{d\mu(\gamma)}{d\gamma}+\frac{R(\gamma)}{M}=\frac{P(\gamma)}{M} \tag{9}$$

Since

$$R_y=Ku_y \quad \text{and} \quad T^2=4\pi^2\frac{M}{K} \tag{10}$$

we get

$$\frac{R_y}{4\pi^2 M}\frac{d^2\mu(\gamma)}{d\gamma^2}+2\xi\frac{R_y}{2\pi M}\frac{d\mu(\gamma)}{d\gamma}+\frac{R(\gamma)}{M}=\frac{P(\gamma)}{M} \tag{11}$$

or

$$\frac{1}{4\pi^2}\frac{d^2\mu(\gamma)}{d\gamma^2}+\frac{\xi}{\pi}\frac{d\mu(\gamma)}{d\gamma}+\frac{R(\gamma)}{R_y}=\frac{P(\gamma)}{(R_y)} \tag{12}$$

If we rewrite $P(\gamma)$ as $\frac{P(\gamma)}{P_{\max}}P_{\max}$, we get

$$\frac{1}{4\pi^2}\frac{d^2\mu(\gamma)}{d\gamma^2}+\frac{\xi}{\pi}\frac{d\mu(\gamma)}{d\gamma}+\frac{R(\gamma)}{R_y}=\frac{P_{\max}}{R_y}\frac{P(\gamma)}{P_{\max}} \tag{13a}$$

which can be simplified by introducing the definition

$$\kappa=\frac{R_y}{P_{\max}} \tag{14}$$

where κ expresses a measure of the system's strength relative to the maximum applied load. In this case, we get

$$\frac{d^2\mu(\gamma)}{d\gamma^2}+4\pi\xi\frac{d\mu(\gamma)}{d\gamma}+4\pi^2\rho(\gamma)=4\frac{\pi^2}{\kappa}\frac{P(\gamma)}{P_{\max}} \tag{13b}$$

In this way, the displacement ductility responses of all systems having the same shape of resisting force versus displacement curves, the same shape of loading function, the same ratio of maximum load over yield force, κ, and the same ratio of loading duration over structural period can be determined from a single analysis, and can be conveniently summarized in chart form [4].

In the case of inelastic seismic response, Eq. 4 can also be normalized by dividing by the yield displacement of the system and we get

$$\frac{\ddot{u}(t)}{u_y}+2\omega\xi\frac{\dot{u}(t)}{u_y}+\frac{R(t)}{Mu_y}=-\frac{\ddot{u}_g(t)}{u_y} \tag{15}$$

Although others [18] have suggested dividing by the peak ground displacement, the above equation is more useful in assessing the structural behavior for design purposes. Making the variable substitutions introduced previously and noting that the terms

$$\frac{R(t)}{Mu_y}=\frac{K}{M}\frac{R(t)}{Ku_y}=\omega^2\frac{R(t)}{R_y}=\omega^2\rho(t) \tag{16}$$

$$\frac{\ddot{u}_g(t)}{u_y}=\frac{K}{K}\frac{\ddot{u}_g(t)}{u_y}=\frac{\omega^2 M\ddot{u}_g(t)}{R_y} \tag{17}$$

Eq. 15 becomes

$$\ddot{\mu}(t)+2\omega\xi\dot{\mu}(t)+\omega^2\rho(t)=-\omega^2\left(\frac{M}{R_y}\right)\ddot{u}_g(t) \tag{18}$$

As in the case of external loading, it is helpful to define a nondimensional parameter, η, to simplify the right-hand side of Eq. 18.

$$\eta=\frac{R_y}{M\ddot{u}_{g_{\max}}} \tag{19}$$

which expresses a system's yield strength relative to the maximum inertia force of an infinitely rigid system. Alternatively, if we define the structure's yielding seismic resistance coefficient, C_y, such that

$$R_y=C_y\cdot W=C_y\cdot M\cdot g \tag{20}$$

then

$$\eta=\frac{C_y}{\ddot{u}_{g_{\max}}/g} \tag{21}$$

and η reveals the strength of the system as a fraction of its weight relative to the peak ground acceleration expressed as a fraction of gravity. In this case, we get

$$\ddot{\mu}(t)+2\omega\xi\dot{\mu}(t)+\omega^2\rho(t)=-\frac{\omega^2}{\eta}\frac{\ddot{u}_g(t)}{\ddot{u}_{g_{\max}}} \tag{22}$$

which is similiar in form to Eq. 13(b). In this final form, the displacement ductility responses of all systems having the same natural frequency, the same hysteretic characteristics and the same strength over inertia force index (η) subjected to ground motions having the same shape can be determined from a single analysis and can be used to summarize the ductility responses of a family of systems in an efficient way (see Chapter 5).

2.3 Numerical Method

Closed form solutions of the equations of motion only exist for a few types of excitations; in most cases, numerical methods must be employed. For inelastic systems, the analysis of the structural responses is usually carried out by step-by-step integration of the equations of motion. In this approach, the analysis over the entire duration of excitation is divided into a series of sequential analyses over smaller intervals of time. The response is evaluated at the end of each time increment (Δt) based on the conditions existing at the beginning of the increment and the assumed response mechanism during the time increment. For the computer program, the response acceleration is assumed to vary linearly while the properties of the system are assumed to remain constant during the time increment. Because of the assumptions regarding the system's properties and the response mechanism, dynamic equilibrium will not always be met by the computed responses at the end of a time increment. In particular, large changes in the stiffness of the structure due to inelasticity within steps can result in substantial equilibrium violations. To obtain dynamically meaningful responses, the program can repeat the step using sufficiently small time intervals to achieve the desired level of convergence (see Section 2.4) and the response acceleration at the end of that time increment is adjusted so as to satisfy dynamic equilibrium (see Section 2.5). The responses at the end of next time increment can be calculated repeating the same procedure.

There are many other integration methods for solving the equations of motion numerically besides the linear acceleration method used in this computer program. The choice of the integration method depends on the efficiency, accuracy and stability associated with the particular method chosen. Most of the available numerical integration methods assume some form of variation of the response acceleration between the integration time step leading to the associated efficiency, accuracy and stability characteristics. Recently, an integration method was developed for bilinear stiffness systems (which include also elasto-perfectly plastic systems) by taking advantages of the piece-wise linear characteristics of the force-deformation relationship [15]. It appears that this integration method might be faster than the linear acceleration

method, particularly for stiff structures. However, because this computer program is oriented toward generating and obtaining detailed information regarding response (the various reponse indicies which will be discussed in Chapter 4), considerable amount of effort is spend in computing these response indicies besides integrating the equation of motion. Consequently, it is believed that the efficiency of the integration methods in solving the equation of motion is not a very critical factor in overall efficiency of the computer program. For ths reason, the more commonly used linear acceleration method is adopted for this computer program.

The normalized forms of equations of motion are useful in illustrating the applicability of the responses of a particular system to a family of related systems. However, in the computer program the actual numerical solution of the equations of motion are obtained using the original Eqs. 1 and 2. This permits calculations to be performed for a particular system. However, if desired, input can be specified in terms of the normalized variables indicated previously.

At any instant of time t, Eqs. 1 and 2 can be written as

$$M\ddot{u}(t)+C\dot{u}(t)+R(t)=P(t) \tag{23}$$

where $P(t)=-M\ddot{u}_g(t)$ for seismically excited systems. While at t+ Δt they are (assuming that the time increment is small enough such that the system's properties remain constant)

$$M\ddot{u}(t+\Delta t)+C\dot{u}(t+\Delta t)+R(t+\Delta t)=P(t+\Delta t) \tag{24}$$

Subtracting the equations, we get

$$M[\ddot{u}(t+\Delta t)-\ddot{u}(t)]+C[\dot{u}(t+\Delta t)-\dot{u}(t)]+[R(t+\Delta t)-R(t)] =[P(t+\Delta t)-P(t)] \tag{25}$$

and denoting

$$\Delta\ddot{u}(t)=\ddot{u}(t+\Delta t)-\ddot{u}(t) \tag{26a}$$

$$\Delta\dot{u}(t)=\dot{u}(t+\Delta t)-\dot{u}(t) \tag{26b}$$

$$\Delta u(t)=u(t+\Delta t)-u(t) \tag{26c}$$

$$\Delta R(t)=R(t+\Delta t)-R(t) \tag{26d}$$

$$\Delta P(t)=P(t+\Delta t)-P(t) \tag{26e}$$

Eq. 11 reduces to

$$M\Delta\ddot{u}(t)+C\Delta\dot{u}(t)+\Delta R(t)=\Delta P(t) \tag{27}$$

If $\Delta R(t)$ is denoted as $K_T \Delta u(T)$, the Eq. 27 becomes

$$M\Delta\ddot{u}(t)+C\Delta\dot{u}(t)+K_T\Delta u(t)=\Delta P(t) \tag{28}$$

where K_T is a tangent stiffness of the structure between times t and t+ Δt, (if K_T is assumed constant during a step). This last equation together with the assumption of linearly varying acceleration is used to obtain the incremental acceleration, $\Delta\ddot{u}(t)$, along with $\Delta\dot{u}(t)$ and $\Delta u(t)$. The actual values of the displacement, velocity are obtained by

$$\dot{u}(t+\Delta t)=\dot{u}(t)+\Delta\dot{u}(t) \tag{29a}$$

$$u(t+\Delta t)=u(t)+\Delta u(t) \tag{29b}$$

Instead of calculating acceleration in similiar manner, the actual acceleration is calculated based on Eq. 14, Sec 2.5, to correct any equilibrium violation. For ground excited structures, $v(t+\Delta t) = u(t+\Delta t) + u_g(t+\Delta t)$. For more details on the numerical integration, see Chapter 8 of Dynamics of Structures [7].

The accuracy and stability of the integration method is of important concern. The linear acceleration method used is only conditionally stable. That is, for elastic systems, results may diverge rapidly from the true solution if the integration time step exceeds the period of the system divided by π [7]. Stability limits have not been established for inelasitc systems. For accuracy of the integration method, a time increment not exceeding one tenth of the structural period is a good rule of thumb [7] for elastic systems. For inelastic systems changes in stiffness within a step can result in equilibrium violations which must be accounted for to prevent instability or divergence from the correct solution. Two methods to prevent this are discussed in the next two sections.

2.4 Time Step Selection

One of the features of the program is the use of a varible time increment (Δt). One method for minimizing equilibrium violations due to stiffness changes within a step is to use a very small Δt. This results in a large number of incremental calculations and it is difficult to know *a priori* what the time increment should be to achieve the desired level of accuracy. By varying the time increment, the number of steps (calculations) required can be reduced while

maintaining the desired level of accuracy.

At the beginning of each time step, denoted as time t, a new time increment (Δt) is selected based on four criteria. The first criterion requires that Δt should never exceed $\Delta\tau$ which is specified by the user during input. This quantity $\Delta\tau$ should be selected to achieve the desired accuracy if the system were to respond elastically.

The second criterion is that Δt should never be more than the time it would take to reach the next excitation digitizaton point (these digitizaton points refer to the discretization of a physically continuous event - the ground movement or the loading on the structure). Thus, the program will consider the actual record as input, unlike methods which modify the input by "clipping" peaks in records originally digitized at unequal intervals or at intervals different from those used in the analysis.

The third criterion is that Δt should never be more than the time it would take to reach the next output time specified. The computed responses can be output at time intervals that are specified by the user in input as a fraction of $\Delta\tau$.

The last criterion concerns the convergence of the results when stiffness changes. Fig. 3 shows instances where the computed responses "overshoot" when the stiffness changes. The solid lines in the figures represent the paths followed by the computed responses when convergence tolerances are met. The dashed lines represent the correct paths the responses should have taken. To prevent excessive "overshoot" error, convergence tolerances can be specified by the user. Overshooting also modifies the shape of the hysteretic curves as seen in Fig. 3.

A convergence tolerance, TCONV, can be specified to minimize the amount of overshoot and the resulting distortion of hysteretic curve. Convergence tolerance is checked when the system yields, unloads from a yielded state, changes from a reduced stiffness state to another stiffness state for a stiffness degrading model (defined in Section 3.3), or changes stiffness while crossing the displacement axis during a step for a stiffness degrading model.

These checks are illustrated in Fig 3. In general, the overshoot convergence tolerance is assumed to be satisfied in each case if the displacement at the end of a step during which a

change in stiffness occurs does not differ by more than TCONV$\times u_y$ from the displacement at which the stiffness should have changed. The user can select the value of TCONV to achieve the desired level of convergence.

If the convergence tolerance is not met, the step is discarded and the program returns to time t to repeat the calculation again with a smaller time increment. In the program, the step is reduced by a factor of 10. With such a reduction in the time step, the repeated time step may not encounter a stiffness change. In that case, the reduced time step is used for all subsequent steps until the change in stiffness is again encountered. If the convergence tolerance is satisfied for the reduced time step, the program continues but reverts to the original time step selection procedure. If the tolerance is still violated, the program disregards the very last time step and starts from the beginning point of that step using a time step one tenth of the last one (i.e., one hundredth of the original). This process is repeated until the tolerances are satisfied or the time step is reduced 5 times without convergence at which time the program stops and notifies the user of the failure for convergence in the program output. The variable time step algorithm is illustrated in Fig. 4.

In summary, the current time increment actually used must meet the following four criteria:

(1) It does not exceed $\Delta\tau$

(2) It does not exceed the time it takes to reach the next excitation digitization point

(3) It does not exceed the next output time specified

(4) Convergence tolerance is met when applicalbe.

The first three criteria for selecting the time increment are checked before the step begins; while the last criterion is checked at the end of the step.

2.5 Equilibrium Correction

When equilibrium violations are detected by the program and the user specified loading and unloading tolerances are satisfied, the program automatically imposes equilibrium by

modifying the acceleration at the end of the step [7]. This is done using the equation

$$\ddot{u}(t+\Delta t)=\frac{P(t+\Delta t)-C\dot{u}(t+\Delta t)-R(t+\Delta t)}{M} \tag{30}$$

3 STIFFNESS MODELS

3.1 Introduction

Two of the more commonly used nonlinear force-deformation models have been implemented in the program and are described in this chapter. The types of structures that are found to be adequately represented by these hysteretic idealizations are also discussed.

The effects of gravity loads result in changes in stiffness and hysteretic behavior of a system. In this chapter, the effects of gravity loads on the two force-deformation models mentioned in Sections 3.2 and 3.3 are examined.

3.2 Bilinear Stiffness Model

Bilinear models are frequently used in modeling structures that exhibit stable and full hysteretic loops. The bilinear stiffness model is defined by three parameters : the yield point, initial stiffness, and the post-yield stiffness. The bilinear model is graphically shown in Fig. 2a. Notice that the yielding always occurs on the two dashed lines - the yielding envelop curves, and the system always unloads with the initial stiffness until it reaches one of the two yielding envelop curves. The elastic and elasto-perfectly plastic models are special cases that can be considered by using appropriate input values. The post-yield stiffness can be of negative value.

3.3 The Stiffness Degrading Model

Stiffness degrading models of the type incorporated are used commonly to represent reinforced concrete structures that do not exhibit substantial degradation due to shear and/or bond deterioration [6,22]. In these cases, the hysteretic loops would be spindle shaped or pinched [19,22]. The stiffness degrading model also uses a bilinear envelop curve defined by three parameters : the yield point, the initial stiffness and the post-yield stiffness. The stiffness degrading characteristics during load reversals are graphically shown in Fig. 2b. There are two primary differences between this stiffness degrading model and that proposed by Clough and Johnston shown in Fig. 5. In the Clough and Johnston model [6], the post-yield stiffness is

assumed to be always zero, while the current stiffness degrading model allows non-zero post-yield stiffness (either positive or negative). Also, as shown in Fig. 2b, for the current stiffness degrading model, after the initial yielding, the loading is directed toward the last unloading point in the direction of motion. The Clough and Johnston model always loads toward the furtherest unloading point in the direction of motion which can result in unrealistic loops (Fig. 5).

Just like the bilinear stiffness model, the stiffness degrading system will always unload with the initial elastic stiffness; however, the stiffness degrading system changes its stiffness when it crosses the displacement axis (zero crossing point) and starts loading in the opposite direction. There is evidence that the unloading stiffness slope should degrade with cycling and maximum peak displacement. However, analyses [5] indicate that this degraded unloading stiffness does not generally have a significant effect on seismic response. After it crosses the displacement axis, it heads straight toward the last yield point as shown in Fig. 2b.

3.4 Inclusion of P-Delta Effects

Gravity loads can effect the apparent mechanical characteristics of a structure when the system is displaced horizontally. This geometric nonlinearity is often called the "P-Delta" effect. The P-Delta effect decreases the system's tangent stiffness by P/L where P is the gravity load and L is the system's height as shown in Fig. 6.

The P-Delta effects can be incorporated into the program by changing the input for the primary envelops for the bilinear and stiffness degrading model. When P-Delta effects are considered, the yield displacement u_y remains the same, while the new initial period (T_o), the initial stiffness (K_o), the post-yield stiffness (PK_o), the yield strength (R_{y_o}) and η-value (η_o) are changed as follow:

$$T' = T_o \sqrt{\frac{1}{(1-\frac{P}{LK_o})}} \tag{31a}$$

$$K' = K_o (1-\frac{P}{LK_o}) \tag{31b}$$

$$PK' = PK_o\left(1 - \frac{P}{LK_o}\right) \tag{31c}$$

$$R'_y = R_{y_o}\left(1 - \frac{P}{LK_o}\right) \tag{31d}$$

$$\eta' = \eta_o\left(1 - \frac{P}{LK_o}\right) \tag{31e}$$

This does not exactly produce the correct effect on stiffness degrading models. Notice that in Fig. 6, the "zero crossing" point for the stiffness degrading model should be shifted away from the displacement axis by the P-Delta effects. This can not be taken into account by the current version of the computer program. Instead, the program assumes the stiffness changes at the zero crossing point and follows the dashed path shown in the figure. Although not strictly correct, the responses calculated this way are probably of sufficient accuracy for most practical values encountered for P-Delta effects.

4 RESPONSE INDICES

4.1 Introduction

While hysteretic curves and response time histories contain all the information on response, it may not be possible or desirable to inspect these curves for every system analysed. Consequently, it is useful to define a few simple indices to characterize the response. The maximum displacement ductility is commonly used to describe the response of an inelastic system. It is especially useful for structures with stable hysteretic loops subjected to impulsive loads. However, when cyclic inelastic action is likely, other indices may provide additional insight into the behavior of the system. A number of indicies that have been incorporated in the computer program are discussed in this chapter.

4.2 Ductility Factors

(a) Maximum Displacement Ductility Factor

Displacement ductility is defined as the maximum absolute value of the displacement response normalized by the yield displacement of the system. This definition of displacement ductility gives a simple qualitative indication of the severity of the peak displacement relative to the displacement necessary to initiate yielding and is illustrated graphically in Fig. 7. A maximum displacement ductility less than unity represents elastic response; while a value greater than unity indicates inelastic response.

For monotonic loading conditions, the maximum displacement ductility factor is a good index of inelastic deformation; however it does not by itself indicate the amount and severity of inelastic deformations under cyclic deformation histories. In this case the largest inelastic deformation in a cycle, the number of yield events and reversals and the total amount of inelastic deformation can be substantially larger than indicated by the maximum displacement. These factors can be important in structures with limited inelastic dissipation capacities.

(b) Cyclic Displacement Ductility Factor

To get an idea of te severity of the worst inelastic excursion, a cyclic displacement ductility factor is defined as the largest cyclic displacement excursion normalized by u_y. As shown in Fig. 7, the origin used to define the cyclic ductility is shifted to account for the prior inelastic action. Mathematically, the value of ductility is computed as

$$u_a = \begin{cases} u_{\max} & \text{if} u_{\max} > u_y \\ u_y & \text{if} u_{\max} \leqslant u_y \end{cases}$$

$$u_b = \begin{cases} -u_{\min} & \text{if} u_{\min} < -u_y \\ u_y & \text{if} u_{\min} \geqslant -u_y \end{cases}$$

$$u_c = \frac{u_a + u_b}{u_y} - 1 \geqslant 1.0$$

Since measuring the total amount of inelastic deformation under cyclic deformation histories is the main goal in defining the cyclic displacement ductlity, a value of unity is output by the computer program if the response remains elastic.

(c) Accumulative Displacement Ductility Factor

For structures susceptible to low cycle fatigue failures, accumulative inelastic displacements maybe more important than the inelastic deformation in one direction or in one cycle. To assess the accumulative inelastic displacement, the absolute values of all inelastic deformations are summed and normalized by u_y and, in order for this index to be comparable to the maximum displacement ductility and for the accumulative ductility to equal one at first yield, a value of one is added to the above ratio. This is illustrated in Fig. 8. This ductility gives a measure of the total amount of inelastic deformation the system has experienced.

(d) Normalized Hysteretic Energy Ductility Factor

The amount of the energy dissipated through the hysteretic actions is important for assessing the required toughness of a system. The energy dissipated can be visualized as the area within the hysteretic loops developed by the system (see Fig. 9). To express this energy quantity in a more convenient form, the total energy dissipated by the system during all cycles can be divided by twice the energy absorbed at first yield plus one. In this form, the ductility

factor represents the maximum displacement ductility of an equivalent elasto-perfectly plastic system that dissipates under monotonic loading the same amount of hysteretic energy (represented by the shaded areas) as the actual system. This is a convenient way of visualizing this factor.

For elasto-perfectly plastic models, the normalized hysteretic energy ductility factor should equal the accumulative displacement ductility defined in the previous section. However, because of differences in computational methods for the two quantities, the results may be slightly different depending on the converenge tolerance used. Fortunately, for most cases, the differences in the ductilities are insignificant.

(e) Comments on Ductility Factors

Because ductility factors are attempting to simplify a complex response, they must be used with caution. In general there is little agreement on the precise definition of ductility and scant data on the ductility capacity of a structure. Moreover, it must be recognized that the ductility based on local response (plastic hinge rotation, strain, etc.) will usually be substantially larger than those based on displacement.

While the definitions introduced above have precise meanings for the single-degree-of-freedom systems considered, this is not necessarily so for multiple degree of freedom systems or structures that do not exhibit definite yield points. However, use of the above definitions individually and in, particular, by comparing them can give a designer a good idea of the type of response expected of a system [12]. See the examples in Chapter 6 for a comparison of various definitions of ductility as applied to several structures.

The various ductility factors introduced have been defined to result in identical numerical values for a monotonic response excursion. In addition, a value of one or less indicates elastic response in each case. This overcomes some of the difficulties in comparing values that would result from other methods of normalizing response [8].

The equations of motion were normalized in Section 2.2 in such a way that the values of

the various ductility factors defined previously will be identical for family of systems having the same characteristics as described in Section 2.2 and subjected to excitations of the same shape. However, this does not mean that the displacements or force histories will necessarily be the same. Fortunately, these parameters can be calculated from the definition of ductility and knowledge of the system's mechanical characteristics and the intensity of the excitation (see Section 4.4).

4.3 Number of Yield Events, Yield Reversals and Zero Crossings

In addition to having some measures of the severity of inelastic deformations, it is also desirable to have information on their frequency. To give an indication of any bias in yielding, the number of yield excursions in the positive and negative directions are given seperately. Yielding is defined for these indicies as an excursion on the primary post-yield envelop curve (dashed lines in Fig. 2). Note, small hysteretic loops for the stiffness degrading model that do not contact the primary envelop are not counted. The number of yield reversals is an important quantity. For example, successive yield events can occur in the same direction. Thus, several small yield excursion may have the same effect as one large event. To distinguish this case from cases where cyclic inelastic deformation reversals occur the number of yield reversals is given as well. The number of yield reversals is defined as the number of times the system changes from yielding in one direction to yielding in the opposite direction. Again only contact with the primary yield envelop is counted. Because of the behavior of the stiffness degrading model is hysteretic on all cycles once yielding has occurred, the number of zero crossing (for reversals) is also given. This also gives an indication of the mean frequency of the response which may degrade with inelastic deformation.

The definitions of the number of yield events, yielding reversals and zero crossings are illustrated in Fig. 11. Note that number of events does not change for systems normalized as in Section 2.2 subjected to excitations of the same shape.

4.4 Maximum Response Displacements, Velocities and Accelerations

(a) Displacement

In addition to controlling inelastic deformations, it is also frequently necessary to control the maximum relative displacement of a structure. This is done (1) to control the damages to the nonstructural elements; (2) to mitigate the adverse consequences of P-Delta effects; (3) to reduce human perception of motion; (4) to prevent pounding against adjacent structures (or equipment) and (5) to satisfy prescribed code or other displacement limits. Consequently, information on the maximum displacements of a system are summarized by the computer program.

Although the ductilities computed according to the definitions made in Section 4.2 will be the same for all systems normalized according to Eqs. 13b and 22, the maximum displacements may be considerably different. To relate the maximum displacements to maximum displacement ductilities, it is helpful to re-write the definition of the maximum displacement ductility for seismic excitation as

$$\mu_{max}=\frac{u_{max}}{u_y}=\frac{u_{max}}{R_y/K}=\frac{K\cdot u_{max}}{M\cdot \ddot{u}_{g_{max}}\cdot\eta}=\left(\frac{\omega^2}{\eta}\right)\left(\frac{u_{max}}{\ddot{u}_{g_{max}}}\right) \tag{32a}$$

or solving for displacement

$$u_{max}=u_y\cdot\mu_{max} \tag{32b}$$

or

$$u_{max}=\frac{\eta}{\omega^2}\ddot{u}_{g_{max}}\cdot\mu_{max} \tag{32c}$$

From this last equation, we can see that for normalized structures subjected to the same normalized excitation and having the same values of ω and η, the value of u_{max} is proportional to $\ddot{u}_{g_{max}}$, even though μ_{max} is not. However, η and $\ddot{u}_{g_{max}}$ are related and Eq. 32b is more useful in practice in determining displacements.

For force excited systems, we can also re-write the definition of the maximum ductility as

$$\mu_{max}=\frac{u_{max}}{u_y}=\frac{u_{max}}{R_y/K}=\frac{K\cdot u_{max}}{\kappa\cdot P_{max}}=\left(\frac{K}{\kappa}\right)\frac{u_{max}}{P_{max}} \tag{33a}$$

or

$$u_{max}=\mu_{max}\frac{\kappa}{K}P_{max} \tag{33b}$$

Again, we can see that for normaized structures having the same values of K and κ , the value of u_{max} is proportional to the P_{max}.

If two systems are normalized such that they develop the same ductility, the displacement of one can be determined from that of the other using

$$u_2=u_1\left(\frac{u_{y_2}}{u_{y_1}}\right) \tag{34}$$

This equation is convenient when interpreting the computer output.

(b) Velocity

Maximum total response velocity is important in determining the human perception of motion and maximum relative response velocity is important in determining the strain rate of the deformation. Similiar to the maximum response displacement, the maximum total response velocity and the maximum relative response velocity can be normalized as

$$\dot{u}^t_{max}=u_y\dot{\mu}^t_{max}=\ddot{u}_{g_{max}}\frac{\eta}{\omega^2}\dot{\mu}^t_{max} \tag{35a}$$

$$\dot{u}_{max}=u_y\dot{\mu}_{max}=\ddot{u}_{g_{max}}\frac{\eta}{\omega^2}\dot{\mu}_{max} \tag{35b}$$

or if the velocities are known for a particular system, they can be related to those for a related system with the same η and ω by

$$\dot{u}^t_2=\dot{u}^t_1\left(\frac{u_{y_2}}{u_{y_1}}\right) \quad when\ \dot{\mu}^t_1=\dot{\mu}^t_2 \tag{35c}$$

and

$$\dot{u}_2=\dot{u}_1\left(\frac{u_{y_2}}{u_{y_1}}\right) \quad when\ \dot{\mu}_1=\dot{\mu}_2 \tag{35d}$$

(c) Acceleration

Maximum total response acceleration is important in determining the human perception of the severity of an earthquake and in design of equipments attached to the structure. Similiar to the maximum response displacement and the maximum total and relative response velocity, the maximum total response acceleration can be normalized as

$$\ddot{u}'_{max} = u_y \ddot{\mu}'_{max} = \ddot{u}_{g_{max}} = \frac{\eta}{\omega^2} \ddot{\mu}'_{max} \tag{36a}$$

$$\ddot{u}_{max} = u_y \ddot{\mu}_{max} = \ddot{u}_{g_{max}} \frac{\eta}{\omega^2} \ddot{\mu}_{max} \tag{36b}$$

4.7 Energy Indices

For ground motion excited systems, the computer program will keep track of the amount of energy input, absorbed and dissipated. The amount of input energy can be expressed as the integral of negative of the sum of the resistance force plus the damping force times the ground velocity over time. The derivation of this expression is shown in Fig. 12.

Part of the input energy is stored in the system as strain energy. For systems with no deterioration in unloading stiffness, the recoverable strain energy can be computed as half the square of the force divided by the initial elastic stiffness. Part of the input energy is stored as kinetic energy. It can be expressed as one half the product of the response velocity relative to a stationary reference frame and the mass of the system.

Finally, part of the input energy is dissipated as hysteretic energy and can be computed as the area within the hysteretic loops developed by the system; and the rest of the input energy is dissipated as damping energy through the viscous damping mechanism of the system. It can be expressed, for viscously damped systems, as the integral of the damping coefficient times the square of the response velocity over time. The time histories and maximum values of these energy terms maybe output by the computer program if desired (see Appendix A, Section A.1, Card B.2).

5 RESPONSE SPECTRA

5.1 Introduction

In designing structures, especially in the preliminary stage, one is primarily concerned with the maximum responses rather than the precise details of the response time histories. To facilitate design of structures subjected to severe dynamic excitations, it would be helpful to develop design guidelines which indicate how these peak response parameters vary with the dynamic, mechanical and damping characteristics of the structure for a particular excitation. Such guidelines can be easily formulated for single-degree-of-freedom systems using various options incorporated in the computer program. Various peak response can be tabulated for a set of user specified combinations of stiffness, strength and damping values. Moreover by taking advantage of the various methods of normalizing the equations of motion discribed in Chpater 2, different types of response spectra may be constructed as will be described in this chapter and illustrated in the next. Once constructed, these spectra can be used to derive the response of a particular system to a specific type of excitation; to determine the consequences of different design options; and to identify those combinations of design parameters that satisfy the response criteria. In addition, various spectra can be combined to derive a composite design spectra where uncertainties exist as to the precise nature of the excitation.

5.2 Elastic Response Spectra

The peak responses of elastic systems can be conveniently summarized by plots of elastic response spectra. Stated briefly, an elastic response spectrum is a plot of the maximum response (maximum response displacement, response velocity, total response acceleration, or any other response quantity of interest) to a specified load function plotted as a function of system's period (or frequency). Such plots are possible because, as can be seem from Eqs. 5 and 6 of Section 2.2, the responses of systems subjected to a particular excitation are the same if they have the same frequency and the same amount of damping. Thus, by solving the equations of motion for one system with each combinaton of period and damping values of interest,

one has determined the response of all systems with these values of period and damping. It is convenient to summarize this data as response sepctra in which the maximum responses are plotted against periods for a constant damping value.

Typical elastic response spectra for a seismic excitaion are shown in Fig. 13 for the 1940 El Centro earthquake. The maximum responses are plotted in terms of the pseudo-acceleration (S_a), pseudo-velocity (S_v) and the relative displacement (S_d) in a single graph. Pseudo-velocity is defined as the product of the natural circular frequency of the system and the relative response displacement. Pseudo-acceleration is defined as the product of the natural frequency of the system and pseudo-velocity.

$$S_a = \textit{peak relative displacement} \tag{37a}$$

$$S_v = \omega S_d \tag{37b}$$

$$S_a = \omega S_v = \omega^2 S_d \tag{37c}$$

When defined this way, it is convenient to take advantage of the relationships existing between these three quantities to plot them in a four-way log paper, known as tripartite plot, as shown in Fig. 13.

Elastic response spectra have been widely used in earthquake engineering design [7]. Maximum responses of a single-degree-of-freedom structure subjected to a specific excitation can be conveniently determined from elastic response spectra if only the natural period and damping of the system are known. In addition, the sensitivity of the responses to variations in the period or damping of the system can be easily seen from the spectra. However, the elastic response spectra for different excitations can be sustantially different. Consequently, for design response spectra, a variety of excitations representative of those expected at a site should be considered to obtain a smoothed elastic design response spectra [16]. Methods for doing this are beyond the scope of this report.

5.3 Inelatic Response Spectra

In cases where only maximum response values are of interest, spectral summarization similiar to that of elastic response spectra is helpful and efficient in identifying the parameters

effecting the response of structures. Looking at Eqs. 21 and 22 of Section 2.2, the ductility responses of inelastic systems subjected to a specific excitation are uniquely defined for a specific combination of damping, period and η-value. In design, one is usually interested in controlling displacement ductility values. Consequently, a useful plot would be to graph μ_{max} as a function of period for a constant value of η and ξ. Typically, for a single graph the excitation, damping and hysteretic model are held constant and maximum displacement ductility is plotted as a function of period (frequency) for specified values of η. Usually the curves are plotted on log-log or semi-log scales. Such inelastic response spectra can be called constant strength response spectra. Spectra for maximum displacement ductility for an elasto-perfectly plastic system with 5 percent viscous damping subjected to the north-south component of the 1940 El Centro record are shown in Figs. 20 and 21. To use such spectra, one can determine the maximum ductility or displacement for a particular system for a structure with a period of 1 second and a yield strength of 10 percent of its weight subjected to this record scaled to 50% g (η =0.1/0.5=0.2). The maximum displacement ductility can be read from the graph as 7. In addition, by applying Eq. 32c, the maximum displacement is

$$u_{max}=.5(32.2\times12)(\frac{.2}{(2\pi)^2})\mu_{max}=6.85 \ inches$$

Alternatively, one can specify the maximum ductility for a given period and interpolate between curves to find the required η-value. For example, to limit the same structure to a ductility of 4, one would have to use an η-value of 0.3. For 50% g peak ground acceleration, this corresponds to a yield base shear coefficient of 0.15.

Similiar spectra can be plotted for other response quantities of interests as illustrated in Chapter 6.

Another useful form of inelastic response spectra involves plotting of η-values corresponding to a constant displacement ductility as a functon of period. This form of inelastic response spectra might be called constant ductility response spectra. They are constructed using interpolation between the curves of the constant strength spectra as indicated in the example above. However, as indicated in Fig. 15 and as pointed out in [17], there can be more than one

η-value corresponding to a given displacement ductility. For example for period of 0.7 second, the data in Figs. 20 and 21 results in a relation between μ and T as shown in Fig. 15. It is recommended to take the larger η-value for design.

5.4 Construction of Response Spectra Using Computer Program

The output of the computer program is conveniently organized for constructing elastic response spectra and constant strength inelastic response spectra. As discussed in Appendix A, Section A.2, when more than one system is input, various maximum response indices are tabulated to facilitate plotting of response spectra.

Direct derivation of constant ductility response spectra is not incorporated into the computer program. In order to generate the constant ductility response spectra, the user would have to construct a series of constant strength response spectra, and by interpolation, estimate the constant ductility response spectra.

Inelastic response is very sensitive to the input excitation, and where uncertainty exists as to the nature and characteristics of this excitation, design should not be based on spectra developed for a single excitation. Methods for combining spectra for various types of expected excitatins to produce a composite design response spectra are beyond the scope of this report.

6 EXAMPLES

6.1 Introduction

Several examples are presented to illustrate the capabilities of the program. Moreover, observations related to the nature of inelastic response under different loading conditions are offered. Comparisons of the different response indicies previously defined indicate the complex nature of inelastic response as well as the usefulness in interpreting response.

6.2 Shock Spectra

When systems are subjected to impulsive type of loading, response spectra can be constructed similiar to the more familiar earthquake response spectra. Spectra for impulsive types of loading, frequently referred to as shock spectra, can be constructed using the computer program. For example, consider a load history consisting of a single sine pulse base acceleration time history of duration t_d and magnitude $\ddot{u}_{g_{\max}}$. Shock spectra are constructed for elasto-perfectly plastic systems with no viscous damping. For these spectra, η-values ranging from 0.2 through 2.0 were used.

It has been shown in Section 2.2 that for a loading of a particular shape, the maximum displacement ductility depends only on the η-value, the amount of viscous damping and the parameter $\frac{t_d}{T}$ for elasto-perfectly plastic systems [4], and only on the amount of viscous damping and the parameter $\frac{t_d}{T}$ for elastic system [4,6]. The shock spectra are usually plotted in terms of the displacement ductility, μ, and the nondimensional parameter, $\frac{t_d}{T}$, for a constant value of η. Spectra constructed in this manner can be very useful for design where the assumed load shape can be anticipated or for qualitatively assessing the potential effects of more complex inputs consisting of a sequence of simple shapes.

The shock spectra computed for the sine pulse loading are shown in Fig. 16. As would be expected on the basis of simple elastic shock spectra [7], the η-values must be at least slightly

greater than 2, in order for systems to remain elastic throughout the entire spectrum range. As can be seen from Fig. 16(a), for η-values less than or equal to 0.8, displacement ductilities tend to increase with the parameter $\frac{t_d}{T}$. For η-values greater than 0.8 displacement ductilities initially increase with $\frac{t_d}{T}$ until a peak is reached (between $\frac{t_d}{T}=1$ and 2), and then they decrease with $\frac{t_d}{T}$. Moreover, it is seen that displacement ductility becomes increasingly sensitive to the value of η when t_d exceeds T.

Another interesting aspect of the response can be assessed from plots of normalized peak displacement $(u_{\max}/\ddot{u}_{g_{\max}})$ versus t_d/T for systems with constant η-values. For the case considered, Fig. 16(b) shows that all systems respond identically for small values of t_d/T (they all are elastic in this range); for high t_d/T values inelastic structures with low η-values respond more than stronger elastic systems, but for intermediated t_d/T values structures with low η-values respond less. Similiar trends have been noted previously [16,18]. Interestingly, the weakest structures considered ($\eta=0.2$) develop nearly constant maximum displacements throughout the t_d/T range. This is apparently a result of the fact that a very weak but stiff system will yield early and respond nearly the same as a very flexible but elastic system.

To assess the consequences of this, Eq. 32c is re-written as

$$\frac{u_{\max}}{\ddot{u}_{g_{\max}}}=\eta(2\pi)^2T^2\mu_{\max} \tag{38}$$

or taking the logarithm on both sides

$$\log\left[\frac{u_{\max}}{\ddot{u}_{g_{\max}}}\right]=2\log T+\log(2\pi)^2+\log\mu_{\max}+\log\eta \tag{39}$$

For the shock spectra considered, η is constant. If $u_{\max}/\ddot{u}_{g_{\max}}$ is taken as a constant (as for $\eta=0.2$)

$$\log\mu_{\max}=2\log\frac{1}{T}+\lambda \tag{40}$$

where λ is some constant depending on the value of η and the constant value of $u_{\max}/\ddot{u}_{g_{\max}}$.

Thus, for weak systems we would expect displacement ductility to be inversely related to period (with a slope of 2 on a log-log plot). This general trend can be identified in Fig. 16(a) for η-values less than 0.6.

6.3 Response Time History For Seismic Excitation

Response time histories of a single-degree-of-freedom system can be obtained using the computer program. The response of a system is computed for the 1940 El Centro (N-S) record. The system has an initial elastic stiffness of 1106 kips/in. and a yield displacement of 0.06266 in.. Viscous damping was assumed to be equal to 5 percent of critical. Elasto-perfectly plastic (EPP) and stiffness degrading (SDM) hysteretic idealizations were assumed for the structure. No deformation hardening is considered in either case.

Typical results are shown in Figs. 17 through 19. These figures include time histories of displacement, input energy, recoverable strain energy, hysteretic energy and damping energy. As can be seen from Fig. 17, the maximum displacement is almost the same for both the stiffness degrading model and the elasto-perfectly plastic system. However, the displacement time history of the SDM system consists of less frequent but larger amplitude oscillations than those of the EPP system. After about 6 seconds, both systems vibrate about a permanent deformation of about 0.4 inches and it does not appear as though the maximum displacements would increase with time after 6 seconds ,especially for the EPP system.

From the energy time histories (Fig. 18), we can see that the SDM system would be subjected to considerably more input energy than the EPP system for the same earthquake. For both systems most of the input energy is being dissipated through hysteresis loops and the effects of viscous damping are smaller. The kinetic energy and recoverable strain energy remain relatively small throughout the response. Unlike the displacement time histories which stop increasing with time after about 6 seconds, the hysteretic and damping energy increase at an almost constant rate for both systems. Thus, for systems with limited energy capacity, the duration of the ground motion may have an important effect on the potential failure.

The hysteretic loops for the two systems are plotted in Fig. 19. The figures show many cycles of reversed plastification. Much more hysteretic energy is dissipated for the SDM than the EPP as can be seen visually from the hysteretic loops as well as from Fig. 18.

6.4 Inelastic Response Spectra

Constant strength and constant ductility response spectra were also constructed for the 1940 El Centro (N-S) record. These spectra were calculated for periods range from 0.1 sec to 1.0 sec at 0.05 sec intervals and then up to 2.0 sec at 0.1 sec intervals. Viscous damping was again assumed to be equal to 5 percent of critical and an elasto-perfectly plastic hysteretic idealization was used. For the constant η-value response spectra, defined in Section 5.2, where various response parameters are plotted against period for systems with constant η-values. The η-values range from 0.1 to 1.0. The constant ductility response spectra were constructed by interpolating the constant η-value response spectra and this involved an iterative process. The required η-values are refined so that they would not result in computed ductilities more than one percent different from the desired values. The ductilities considered for the constant ductility response spectra range from 2 to 10.

The response spectra generated are shown in Figs. 20 through 26. All of the spectra are plotted on semi-log scales, except Fig. 20 which is plotted on log-log scale. Shown in Figs. 20 through 23 are the constant η-value response spectra based on displacement ductility, cyclic displacement ductiltity and normalized hysteretic energy ductility, in that order; and shown in Figs. 24 through 26 are the corresponding constant ductility response spectra. For the EPP system considered, the accumulative displacement ductility values equal the normalized hysteretic energy ductility spectra. They are consequently not plotted here. However, for other systems, they provide valuable additional information and it may be desirable to form spectra based on this parameter as well.

As can be seen from the constant η-value spectra (Figs. 20 through 23), the various response ductility factors tend to decrease with increases in η-value and with increases in period. For the constant η-value displacement ductility and cyclic displacement ductility

spectra, lines of constant η occasionally intersect and, in some instances, cross over one another. This results in weaker systems sometimes requiring less ductility than stronger ones. These intersections and cross-overs correspond to a sharp drop and a positive slope in the η-value versus displacement graph shown in Fig. 15. This tendency is the consequency of numerous interrelated factors. The effect of a specific pulse in an earthquake record depends not only on the factors indicated in Fig. 16 (where this same tendency can be noted in some cases), but on the system's acceleration, velocity and displacement at the onset of the pulse. Since these values are very sensitive to prior inelastic action, the effect of a particular pulse may be greater or less than expected based on the characteristics of the isolated pulse.

From the constant ductility spectra (Figs. 24 and 26), it is observed that the η-values for constant ductility generally decrease with increases in ductility and with increases in period. Because the constant ductility spectra are constructed by interpolating and refining the constant η-value spectra, it would be expected that, for constant displacement ductility and constant cyclic displacement ductility spectra, that intersection and cross-over of lines for some period regions might occur. However, when two or more η-values would result in the same ductility the largest value is plotted when constructing these curves. This is believed to be a conservative assumption for design and accounts for the effect of uncertainties in modeling on response. Consequently, the constant ductility curves do not cross over one another.

For the constant strength (η-value) spectra of displacement ductility shown in Fig. 20, it is seen that, on a log-log scale plot, the lines of constant η-value decrease with period in an almost linear fashion, especially for high ductility levels and low values of η. Similiar to the observations in Section 6.2, this observation can be related to how the normalized displacements vary with period. It is observed in Figs. 28 that the normalized displacement, $\frac{u_{\max}}{\ddot{u}_{g_{\max}}}$, varies almost linearly with period with a slope less than 2 on a log-log scale plot. Furthermore, at larger periods the displacements tend to merge as would be expected. Also, as observed in Fig. 16(b), the displacements tend to become nearly constant (independent of period) as the

η-value decreases. To assess the reason for these observations, one refers to Eq. 40. For the constant η-value plot shown in Fig. 28, η is constant. As observed previously, μ varies inversely and approximately linearly with period for constant values of η on a log-log scale plot. That is,

$$\log\mu \approx -\alpha \times \log T \tag{41}$$

where α is a positive constant. Therefore, Eq. 39 can be re-written as

$$\log\left[\frac{u_{\max}}{\ddot{u}_{g_{\max}}}\right] \approx (2-\alpha)\log T + \lambda \tag{42}$$

where λ is some constant depending on the value of η. From Eq. 42, it is obvious why the normalized displacement, $\frac{u_{\max}}{\ddot{u}_{g_{\max}}}$, would vary almost linearly with a slope less than 2 on a log-log scale plot. Similiar conclusion can be made for the variation of normalized displacement versus period for constant values of displacement ductility by simply recognizing that μ is constant and η varies inversely and approximately linearly with period on a log-log scale plot.

6.5 Comparison of Response Indicies

Comparisons between the different definitions of ductility factors are plotted in Fig. 27 for constant η-values of 0.8 and 0.2, respectively. By comparison, it is seen that ductilities are considerably larger for the weaker system. As noted previously, all ductility factors generally decrease with increasing period. The maximum displacement ductility and the cyclic displacement ductility are generally similiar (except for periods between 0.4 and 1.0 seconds) indicating that inelastic deformations occur primarily in one direction. However, the differences between displacement ductility and equivalent hysteretic energy ductility are as large as two or three hundred percent indicating many cycles of load reversals and reversed plastification. More importantly, this difference varies significantly for different periods [10]. This observation is important for structures sensitive to low cycle fatigue and/or with limited energy dissipation capacity, since for a structure with a certain η-value, the designer not only would have to make sure the structure is sufficiently ductile to develop the required maximum displacement ductil-

ity, but also tough enough to dissipate the required hysteretic energy without significant degradation of its restoring force characteristics.

From the constant displacement ductility spectra obtained in Section 6.4, normalized response (as mentioned in Section 4.4) envelopes can also be plotted against periods to facilitate the comparison between the different response indicies at a constant displacement ductility. The envelopes are shown in Figs. 29 through 31 for a displacement ductility of 4. In Fig. 29, differences between the displacement ductility and other ductility factors are shown. Similiar observations as those just observed for constant η-values are evident again for a constant displacement ductility of 4. That is, for structures with limited energy capacity and/or sensitive to low cycle fatigue, certain periods are preferable over others. Minimum requirements for structural toughness occur at periods between 1.0 and 1.5 seconds for this input.

The difference between the displacement ductility and cyclic displacement ductility gives an indication of the directional distribution of the maximum response. The cyclic displacement ductility as defined can be as large as twice the displacement ductility (minus one) when the positive and negative displacements are equal. The cyclic displacement ductility can be as small as the displacement ductility if the inelastic deformation occurs in only one direction or when the response is elastic (the trivial case). From Fig. 29, it is seen that the directional distribution of response is substantially biased in one direction for periods between 0.7 and 1.4 seconds. Furthermore, it is found that the accumulative displacement ductility (and normalized hysteretic energy ductility) are nearly proportional to the cyclic displacement ductility indicating that there is, for this record, some relation between the energy dissipated and the directional distribution of maximum response.

In Fig. 30, the variations of the normalized maximum and minimum displacements and residual displacement versus period are shown for a displacement ductility of 4. Except in a few cases, the displacement in one direction is significantly larger than in the other direction indicating again a bias in the inelastic response. It is noted that the pattern of bias in the inelastic response observed in this figure matches closely with the pattern discussed in the preceeding

paragraph. The normalized residual ductility tends to increase with period as seen in Fig. 30. In addition, normalized residual ductility can be as large as 50% of the peak normalized displacement in some instances. Large residual displacement is undesirable because it may make structural repair infeasible and can accumulate during severe aftershocks leading to structural instability.

In Fig. 31, the number of yield events versus period is shown and the trend shows that for more flexible, longer period structures, the number of yield events decreases as expected. However, there appears to be an even distribution of positive and negative yield events. This is in contrast with the directional distribution of maximum displacements where the displacement in one direction is consistantly larger than the other direction except in a few cases as shown in Fig. 30. Thus, the number and magnitude of yield events may not be related. For the EPP medel, the sum of number of positive yield excursions and number of negative yield excursion minus the number of yield reservals indicates the number of time the system yielded successively in one direction only. It can be inferred from Fig. 31 that the number of times the system yielded successively in one direction only is about 30% of the number of positive or negative yield events.

Although comparisions such as those discussed in this section can give much insight into inelastic response, caution should be exercised in generalizations drawn from a single record. A statistical study of trends based on realistic structural models and on an appropriately selected ensemble of ground motion records is required.

6.6 Construction of Evolutionary Spectra

Because the response spectra presented previously relate only the maximum response to period, the relationship that exists between the response time history and the features of the excitation time history that cause this response is necessarily absent. One of the ways to incorporate the temporal nature of response and to display the relationship between response time history and excitation time history is through an evolutionary spectrum. An evolutionary spectrum is a two dimensional contour plot of the response showing the time of the first occurance

of each level of the contour. Usually the x-axis refers to time and the y-axis refers to period of the structure.

The evolutionary spectra shown in Fig. 32 are constructed by the computer program. The systems are assumed to be elasto-perfectly plastic with viscous damping of 5%. The periods are selected evenly from 0.1 to 1.0 seconds at 0.05 second interval; from 1.1 to 2.0 seconds at 0.1 second interval. The η-values used are based on the Newmark-Hall inelastic design response spectra [16], for a specified displacement ductility of 4. Consequently, actual maximum ductility demands are not exactly equal to 4 [10]. The excitation used is the 1940 El Centro (N-S) record. The response quantity shown in the evolutionary spectra is the equivalent hysteretic energy ductility. Other response quantities can be used to construct similiar evolutionary spectra. Pre-determined contour levels are selected corresponding to equivalent hysteretic energy at 0.5 interval from 1.0 to 14.5.

7 CONCLUSIONS

This report describes a computer program for the analysis of inelastic viscously damped single-degree-of-freedom systems to either support excitations or external loadings. The program is best utilitized when used to study the sensitivity of the overall response of a proposd structure to uncertainties in its mechanical and dynamic characteristics or to variation in excitation. Useful definitions of response quantities are introduced in connection with the various methods of developing design aids based on computed inelastic response discussed.

The computed responses by the computer program have shown excellent agreement with results by other computer programs. Improvements and further extension of the computer program are possible. For example, inclusion of hysteretic idealizations other than the bilinear and stiffness degrading models is desirable. Studies on methods for combining response spectra for different excitations and for normalizing excitations are needed. In addition, studies to assess methods of applying these methods to systems subjected to biaxial excitations and to complex multiple-degree-of-freedom systems are needed.

8 REFERENCES

(1) ANSYS, Engineering Analysis Systems Users's Manual, Swanson Analysis system, Inc., Pennsylvanis, U.S.A.

(2) Bathe, K.J., "ADINA - A Finite Element Program for Automatic Dynamic Incremental Nonlinear Analysis," Report 82448-1, Accoustics and Vibration Lavaratory, Department of Mechanical Engineering, Massachusetts Institute of Technology, 1975.

(3) Bertero, V.V., and Zagajeski, S.W., "Computer Aided Seismic-Resistant Design of Reinforced Concrete Multistory Frames," Proceedings of the 6th European Conference on Earthquake Engineering, Vol. II, Dubrovnik, Yugoslavia, September 1978.

(4) Biggs, J.M., "Introduction to Structural Dyanmics," McGraw-Hill, New York, 1964.

(5) Chen, D. "Spectrum of Ductility for Earthquake Resistant Structure," Technical Report TR-1, Research Labaratory of Earthquake and Blast Resistant Engineering, Qinhua University, Beijing, 1980.

(6) Clough, R.W., and Johnston, S.B., "Effect of Stiffness Degradation on Earthquake Ductility Requirements," Proceedings of Japan Earthquake Engineering Symposium, 1966.

(7) Clough, R.W., and Penzien, J., Dynamics of Structures, McGraw-Hill, New York, 1975.

(8) Goel, S.C., "Response of Multistory Steel Frames to Earthquake Forces," AISI, Bulletin No. 12, November 1968.

(9) Guendelman-Israel, R., and Powell, G.H., "DRAIN-TABS : A Computer program for Inelastic Earthquake Response of Three Dimensional Buildings," EERC Report 77-08, University of California, Berkeley, 1977.

(10) Mahin, S.A., and Bertero, V.V., "An Evaluation of Inelastic Seismic Design Spectra," Journal of The Structural Division, Proceedings of the Am. Soc. of Civil Engineers, Vol. 107, No. ST9, Sep. 1981.

(11) Mahin, S.A., and Bertero, V.V., "An Evaluation of Some Methods For Predicting Seismic Behavior of Reinforced Concrete Buildings," EERC Report 75-5, Earthquake Engineering Research Center, University of California, Berkeley, 1975.

(12) Mahin, S.A., and Bertero, V.V., "Problems in Establishing and Predicting Ductility in Aseismic Design," Proceedings of the International Symposium on Earthquake Structural Engineering, St. Louis, August 19-21, 1976, Vol. I.

(13) Mondkar, D.P., and Powell, G.H., "ANSR-I General Purpose Computer Program for Analysis of Non-linear Structural Response," EERC Report 75-37, Earthquake Engineering Research Center, University of California, Berkeley, 1975.

(14) Mondkar, D.P., and Powell, G.H., "ANSR-II, Analysis of Nonlinear Structural Response, Users Manual," EERC Report 79-17, Earthquake Engineering Research Center, University of California, Berkeley, 1979.

(15) Nau, J.M., and Hall, W.J., "An Evaluation of Scaling Methods For Earthquake Response Spectra," Civil Engineering Studies, Structural Research Series, No. 499, University of Illinois, Urbana, May 1982.

(16) Newmark, N.M., and Hall, W.J., "Procedures and Criteria for Earthquake Resistant Design," Building Practices for Disaster Mitigation, Building Science Series 46, U.S. Department of Commerce, National Bureau of Standard, Washington, D.C., Febuary 1973.

(17) Newmark, N.M., and Riddell, R., "Statistical Analysis of the Response of Nonlinear Sys-

tems Subjected to Earthquakes," Civil Engineering Studies, Structural Research Series, No. 468, University of Illinois, Urbana, August 1979.

(18) Newmark, N.M., and Veletsos, A.S., "Effect of Inelastic Behavior on the Response of Simple Systems of Earthquake Motions," Proceedings, Second World Conference on Earthquake Engineering, 1960.

(19) Park, R., and Pauley, T., Reinforced Concrete Structures, John Wiley & Sons, 1975.

(20) Powell, G.H., "Drain-2D Users Guide," EERC Report 73-22, Earthquake Engineering Research Center, University of California, Berkeley, October 1973.

(21) Saiidi, M., and Sozen, M.A., "Simple and Complex Models for Nonlinear Seismic Response of Reinforced Concrete Structures," Civil Engineering Studies, Sturctural Research Series, No. 465, University of Illinois, Urbana, August 1979.

(22) Saiidi, M., and Sozen, M.A., "Simple Nonlinear Seismic Analysis of R/C Structures," Journal of Structural Division, ASCE, Vol. 107, No. ST5, May 1981.

(23) Shibata, A., and Sozen, M., "Substitute-Structure Method for Seismic Design in R/C," Journal of the Structural Division, ASCE, Vol. 102, No. ST1, Jan. 1976.

(24) Tansirikongkol, V., and Pecknold, D.A., "Approximate Modal Analysis of Bilinear MDF Systems Subjected to Earthquake Motions," Civil Engineering Studies, Structural Research Series, No. 449, University of Illinois, Urbana, August 1978.

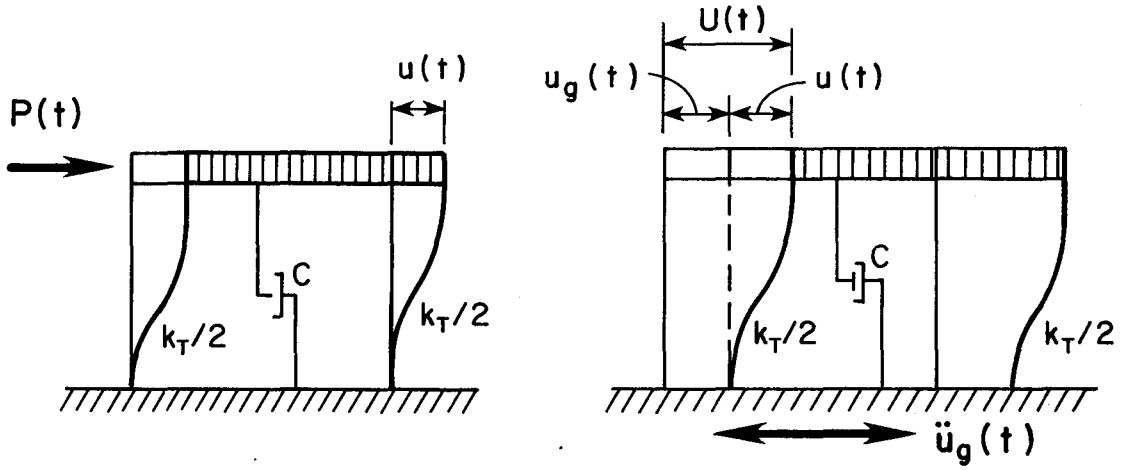

(A) External Load (B) Ground Acceleration

FIG. 1 Single-Degree-Of-Freedom Systems Considered In Analysis

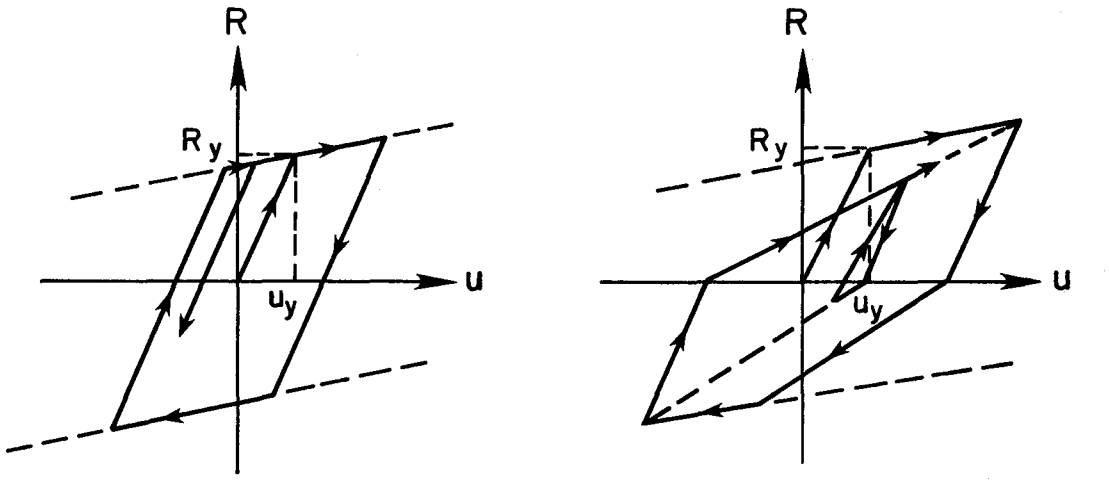

(A) Bilinear Model (B) Stiffness Degrading Model

FIG. 2 Resisting Force Relationships Considered

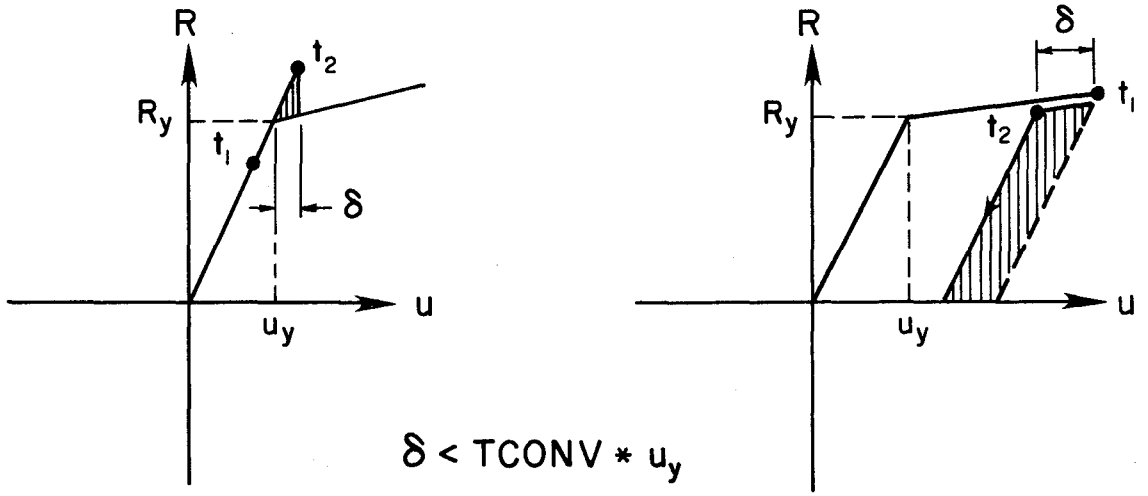

(A) Loading To Yield Envelop (B) Unloading From Yield Envelop

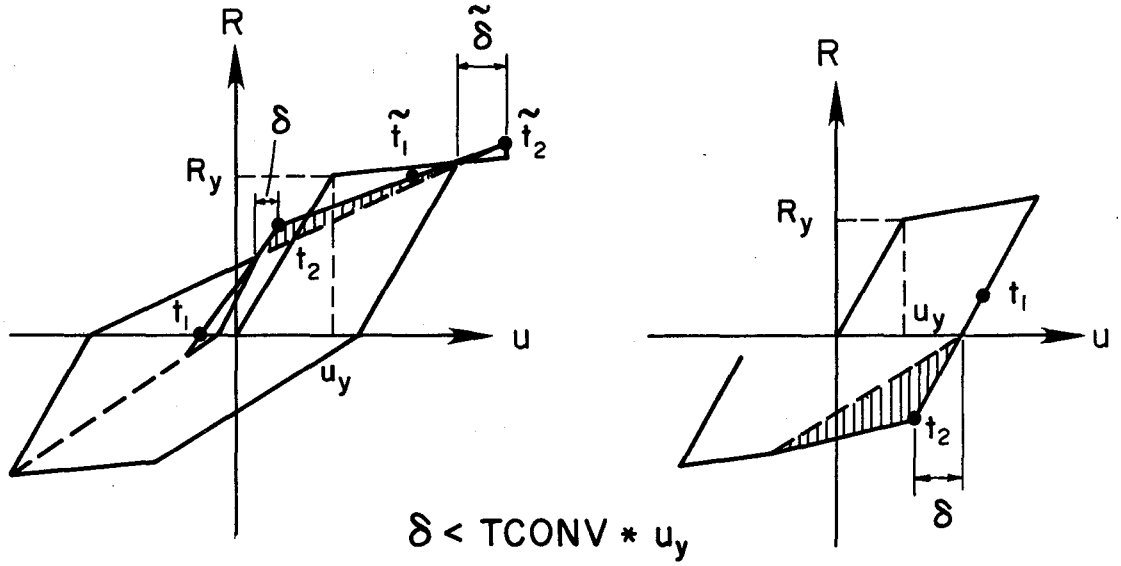

(C) Loading In Stiffness Degrading Model

(D) Unloading In Stiffness Degrading Model

FIG. 3 Convergence Tolerances And Modifications Of Hysteretic Shape Due To Overshoot

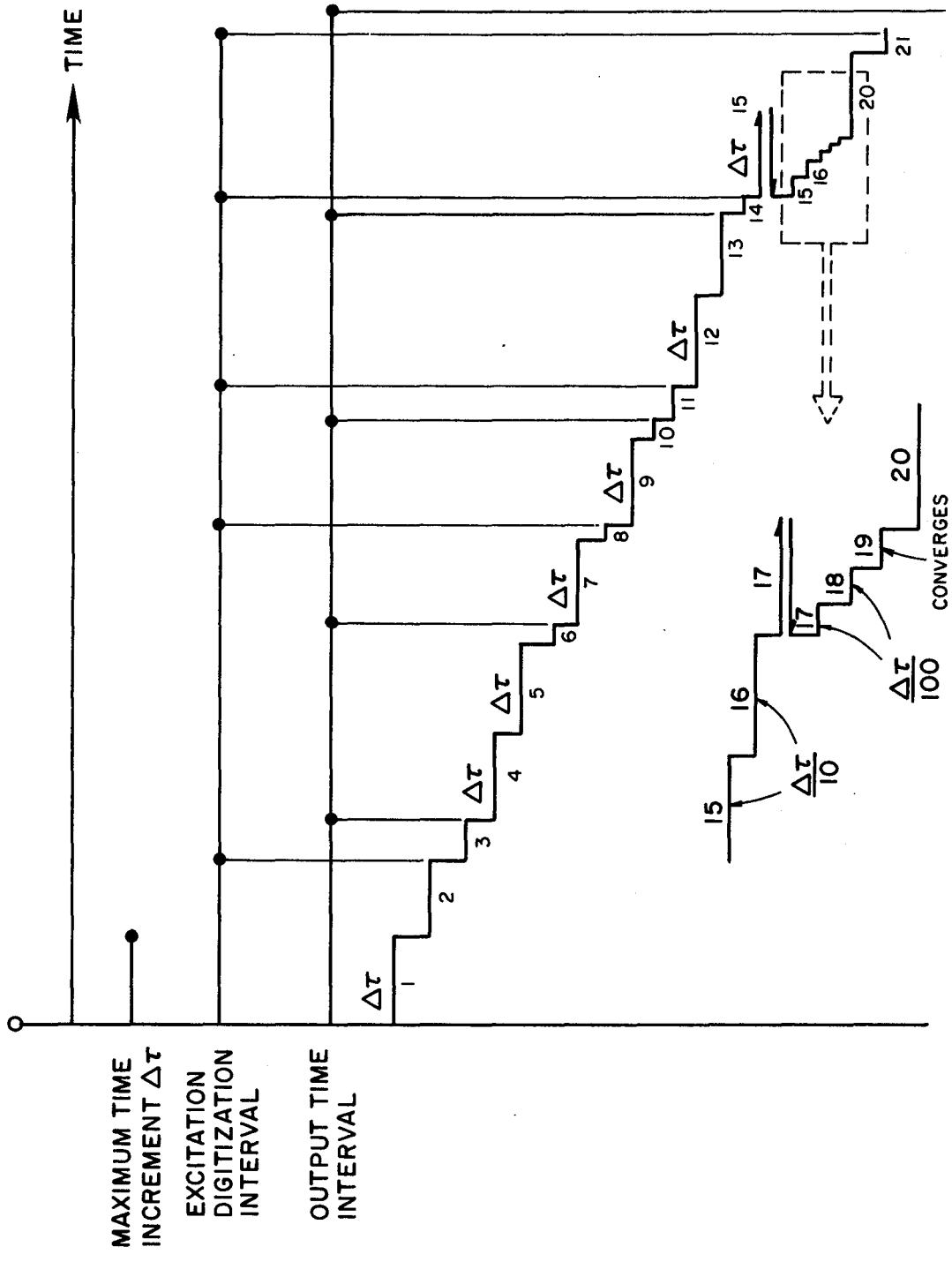

FIG. 4 Variable Time Step Algorithm

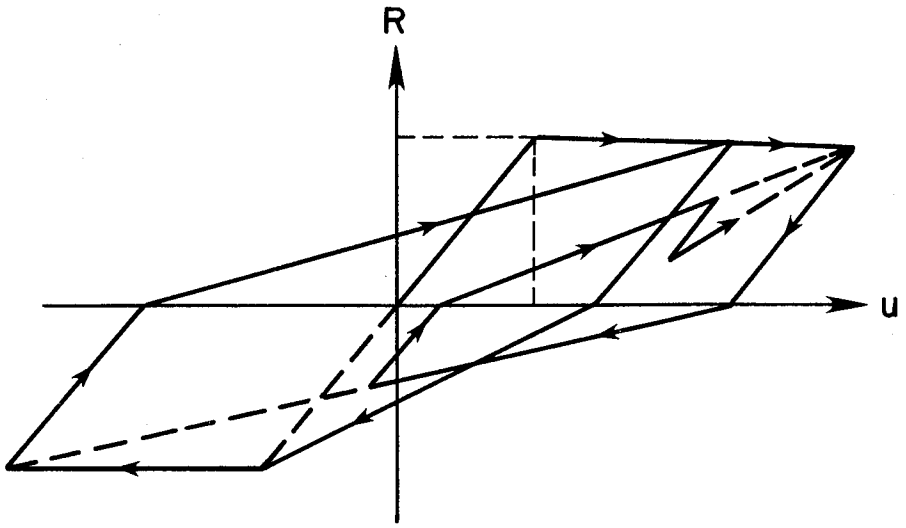

FIG. 5 Stiffness Degrading Model (Clough And Johnston)

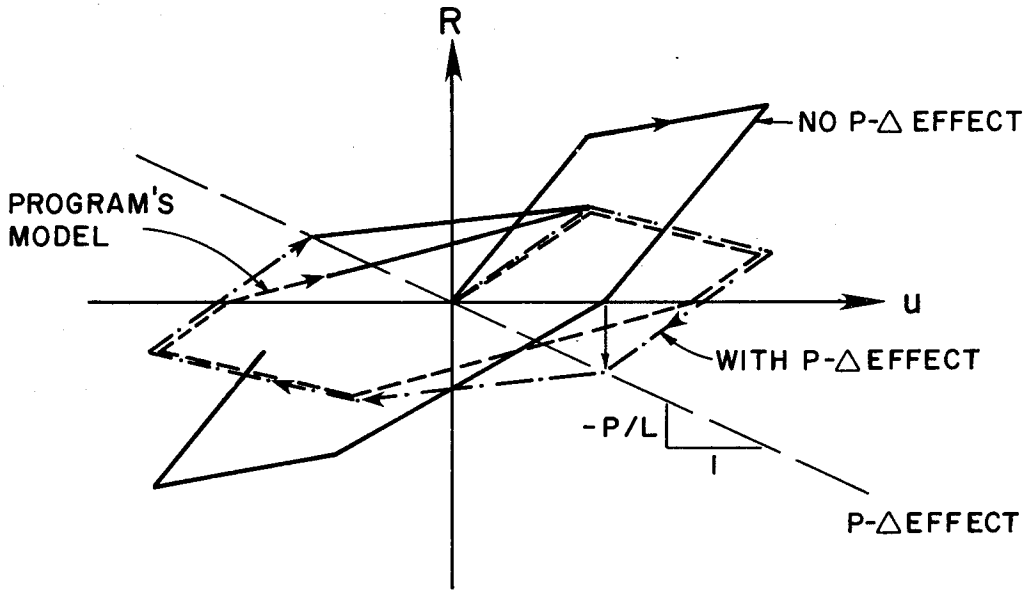

FIG. 6 P-δ Effect On Stiffness Degrading Model

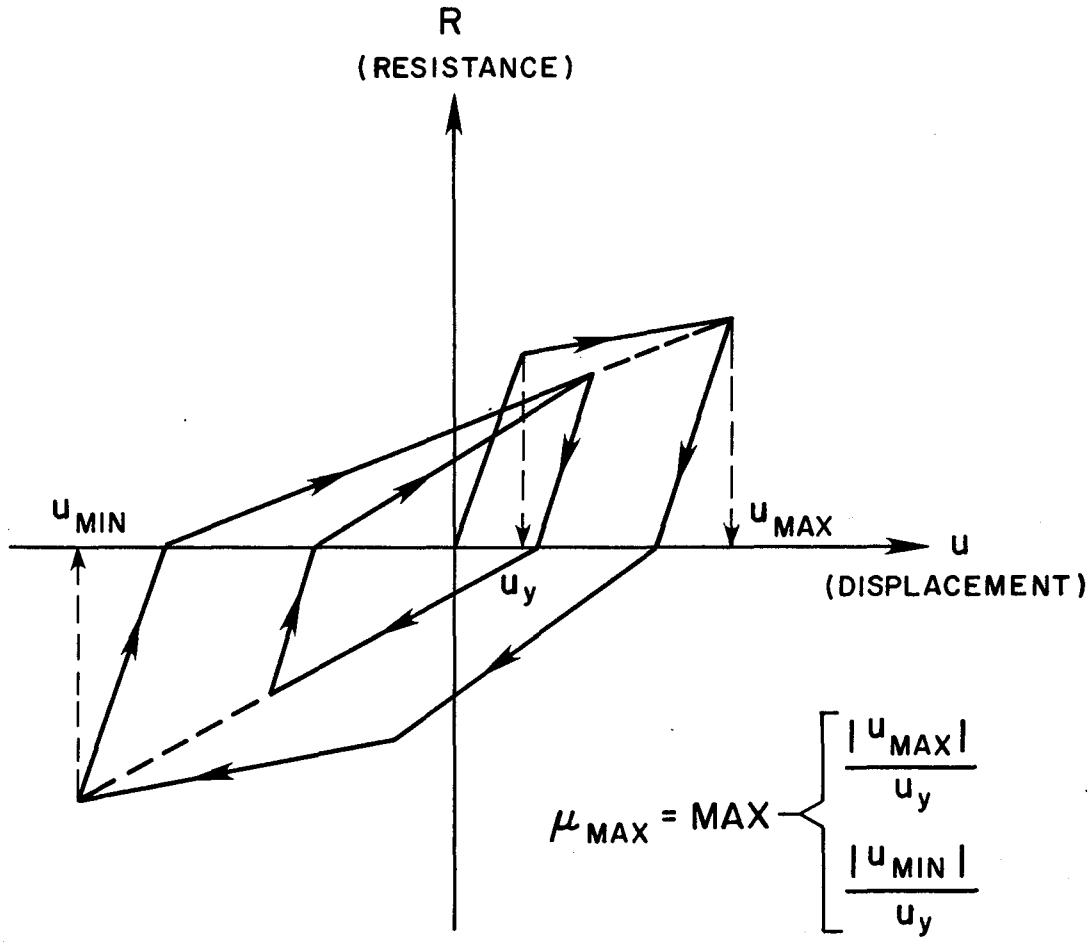

FIG. 7 Definition Of Displacement Ductility

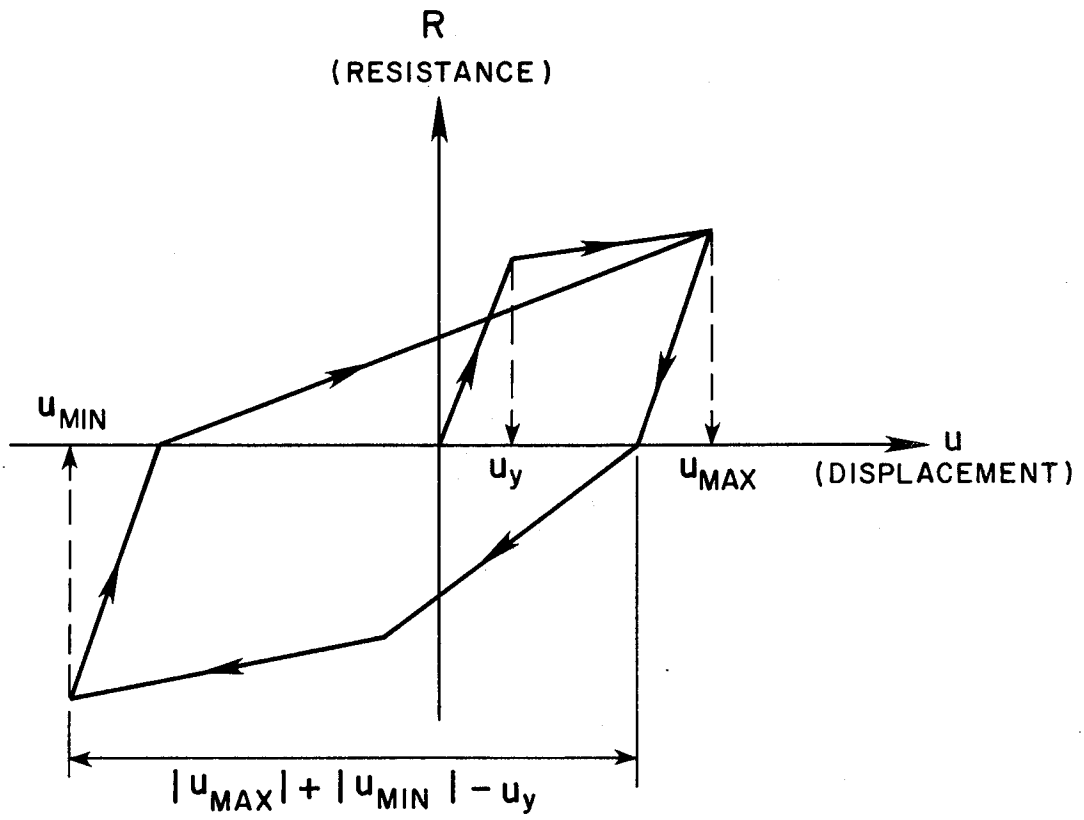

$$u_a \begin{cases} u_{MAX} & \text{IF } u_{MAX} > u_y \\ u_y & \text{IF } u_{MAX} \leq u_y \end{cases}$$

$$u_b \begin{cases} -u_{MIN} & \text{IF } u_{MIN} < -u_y \\ u_y & \text{IF } u_{MIN} \geq -u_y \end{cases}$$

$$\text{CYCLIC DUCTILITY} = \frac{u_a + u_b}{u_y} - 1 \geq 1.0$$

FIG. 8 Definition Of Cyclic Displacement Ductility

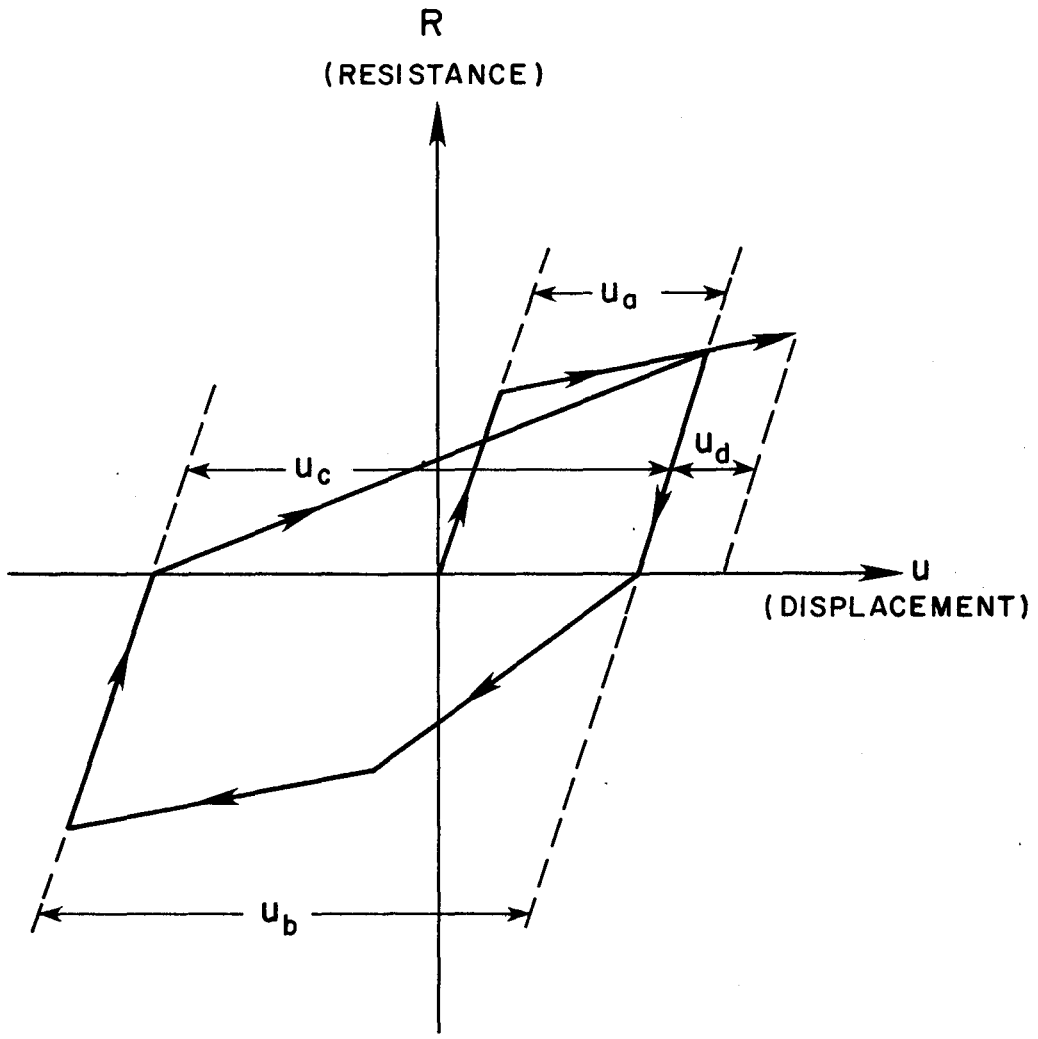

$$\text{ACCUMULATIVE DUCTILITY} = \Sigma\,(upl)_i / u_y + 1$$

$$= \frac{(|u_a| + |u_b| + |u_c| + |u_d|)}{u_y} + 1$$

FIG. 9 Definition Of Accumulative Displacement Ductility

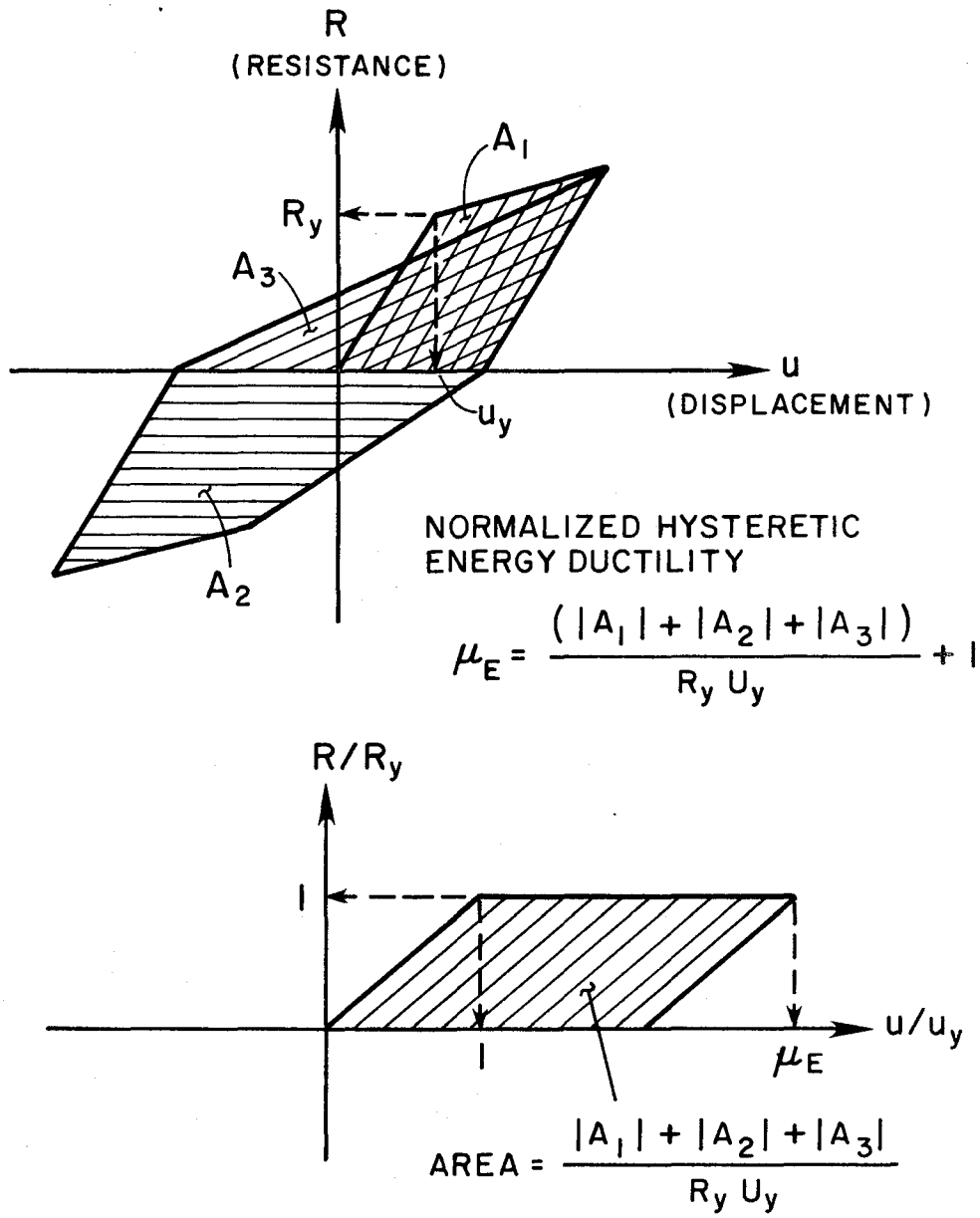

FIG. 10 Definition Of Normalized Hysteretic Energy Ductility

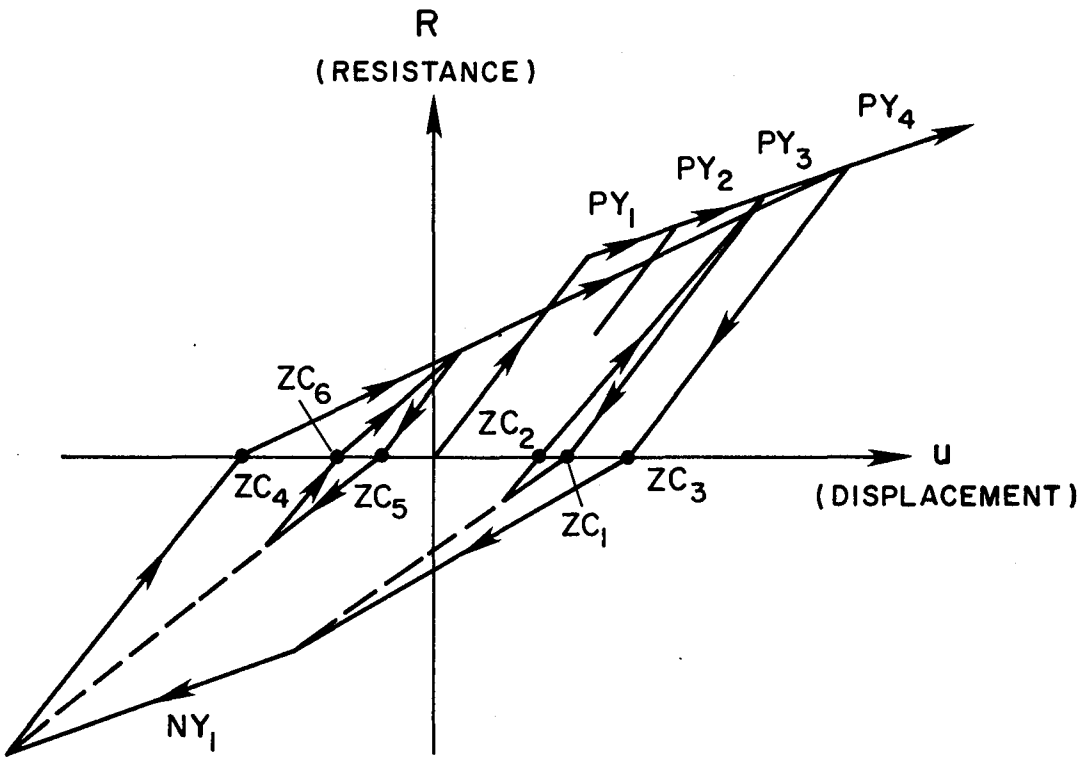

ZERO CROSSINGS (ZC) = 6
NO. OF POSITIVE YIELD EXCURSIONS (PY) = 4
NO. OF NEGATIVE YIELD EXCURSIONS (NY) = 1
NO. OF YIELD REVERSALS = 1

FIG. 11 Definition Of Number Of Yield Events, Yield Reversals And Zero Crossings

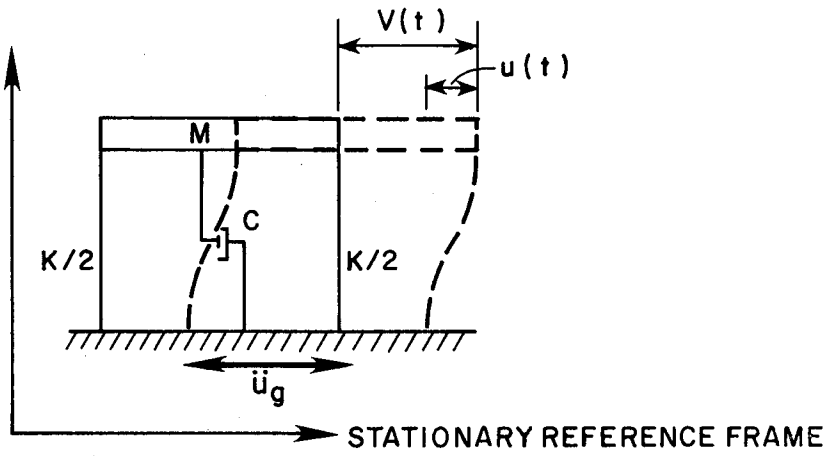

from Figure 1(b)

$$M(\ddot{u}(t)+\ddot{u}_g(t))=-[C\dot{u}(t)+Ku(t)]$$

$$M\ddot{v}(t)=-[C\dot{u}(t)+Ku(t)]$$

So the force on the system, according to Newton's Second Law of Motion (F=Ma), is

$$=-[C\dot{u}(t)+Ku(t)]$$

The work done (equals to the input energy)

$$input\ energy=\int -[C\dot{u}(t)+Ku(t)]\times du_g$$

or

$$input\ energy=\int -[C\dot{u}(t)+Ku(t)]\,\dot{u}_g\,dt$$

FIG. 12 Definition Of Input Energy

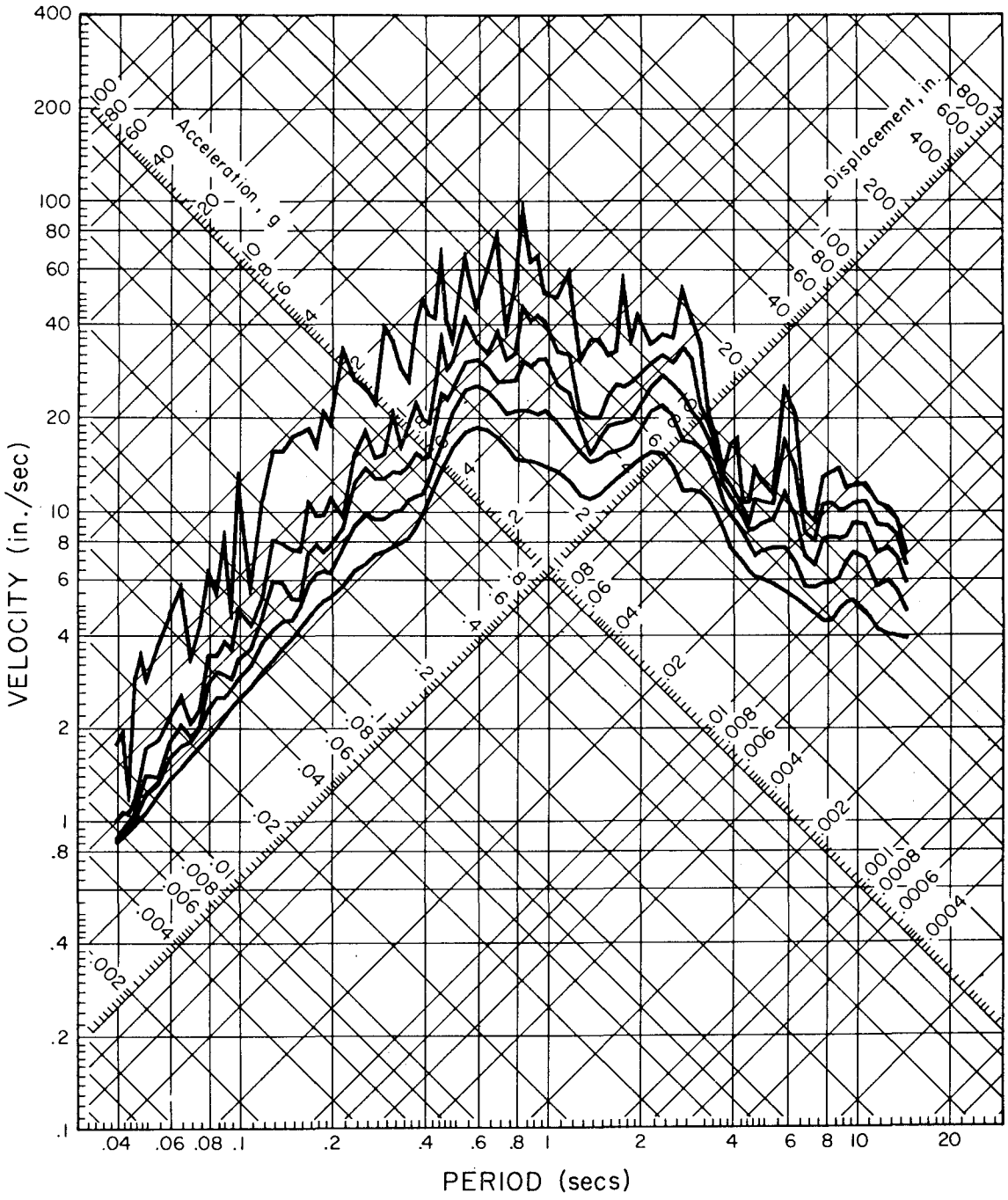

Fig. 13 Elastic Response Spectra For 0, 2, 5, 10 And 20 Percent Damping, 1940 El Centro (S00E) Record

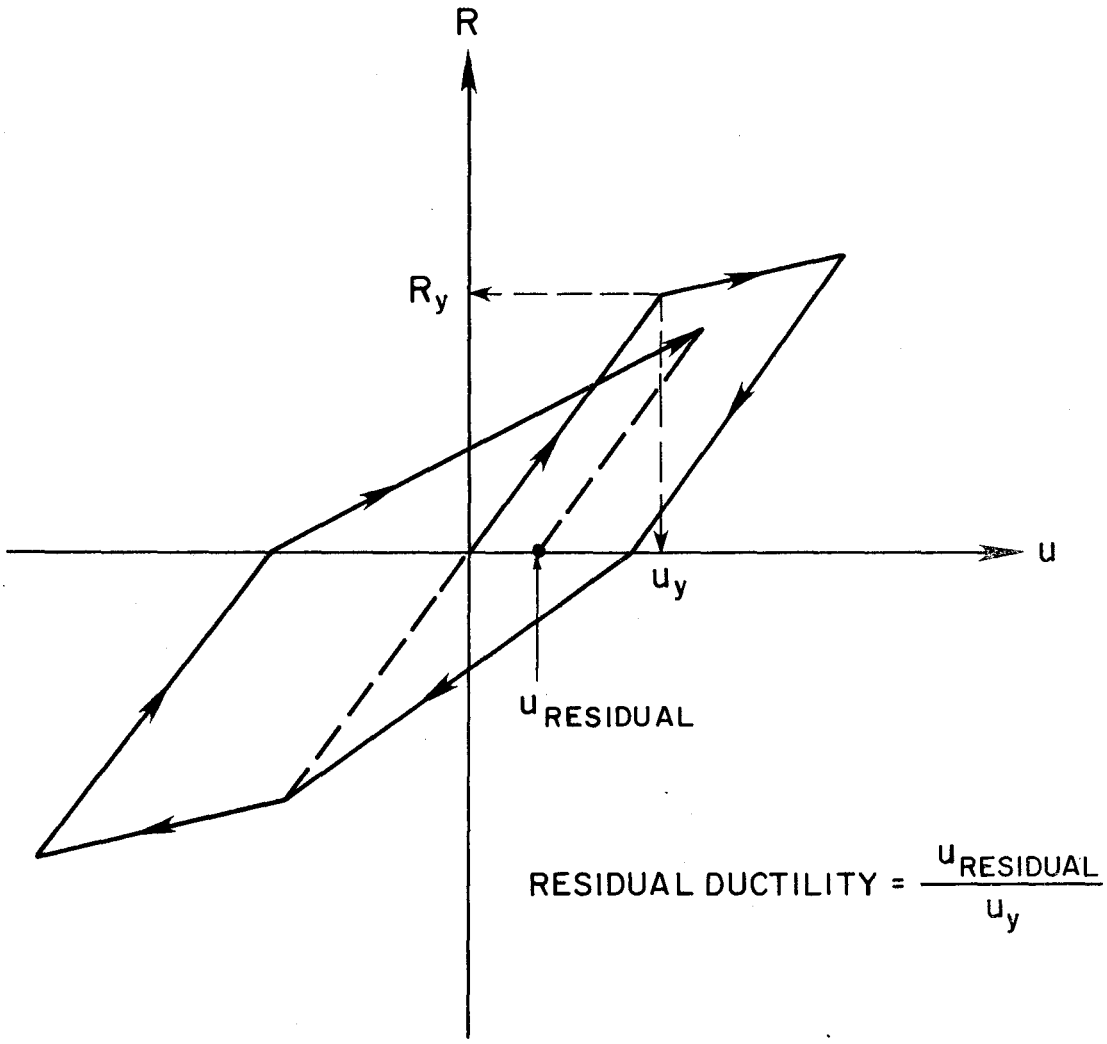

FIG. 14 Definition Of Residual Displacement Ductility

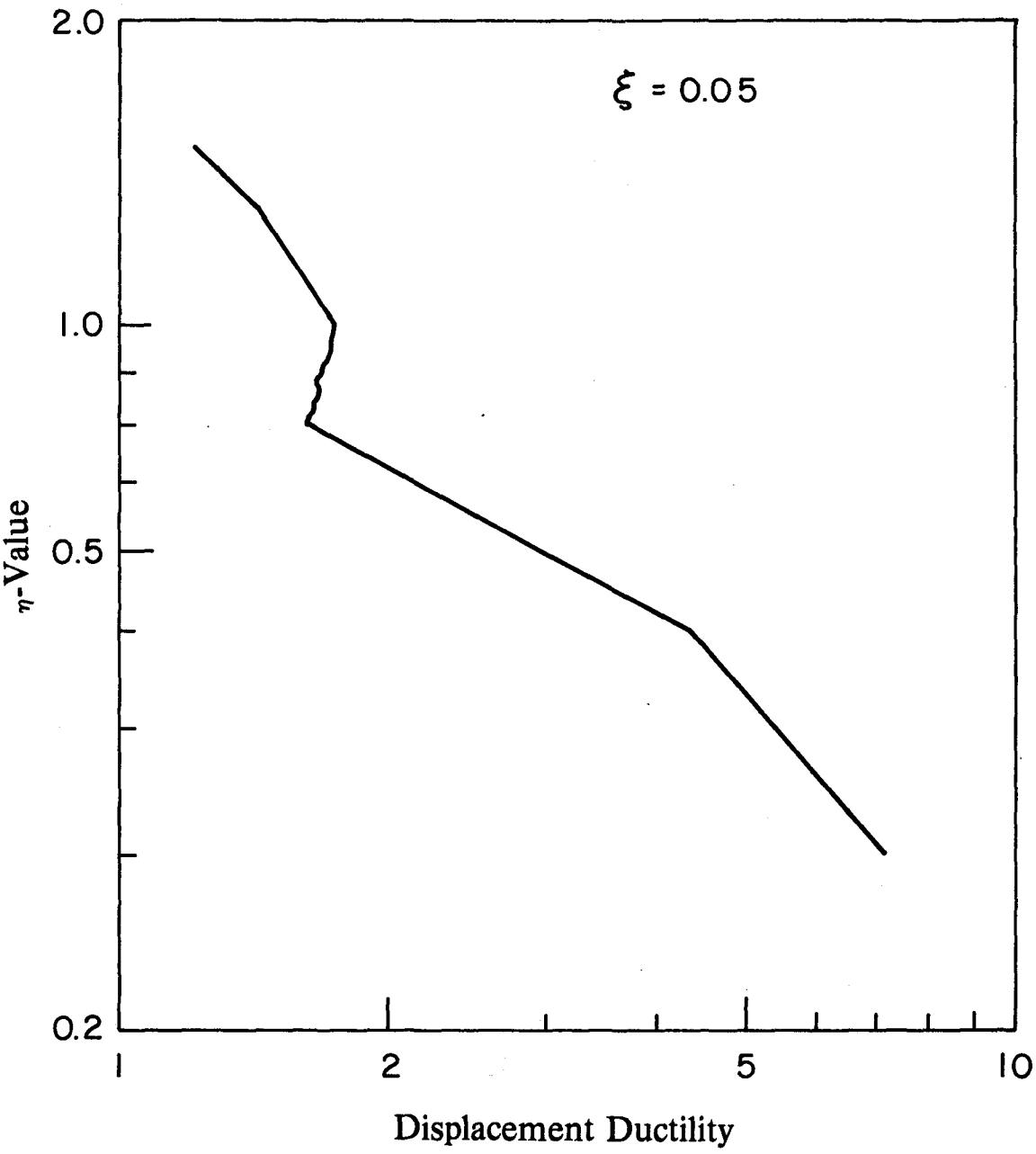

FIG. 15 Relation Between Ductility And η-Values For EPP System With Period 0f 0.7 Sec. - 1940 El Centro (NS) Record

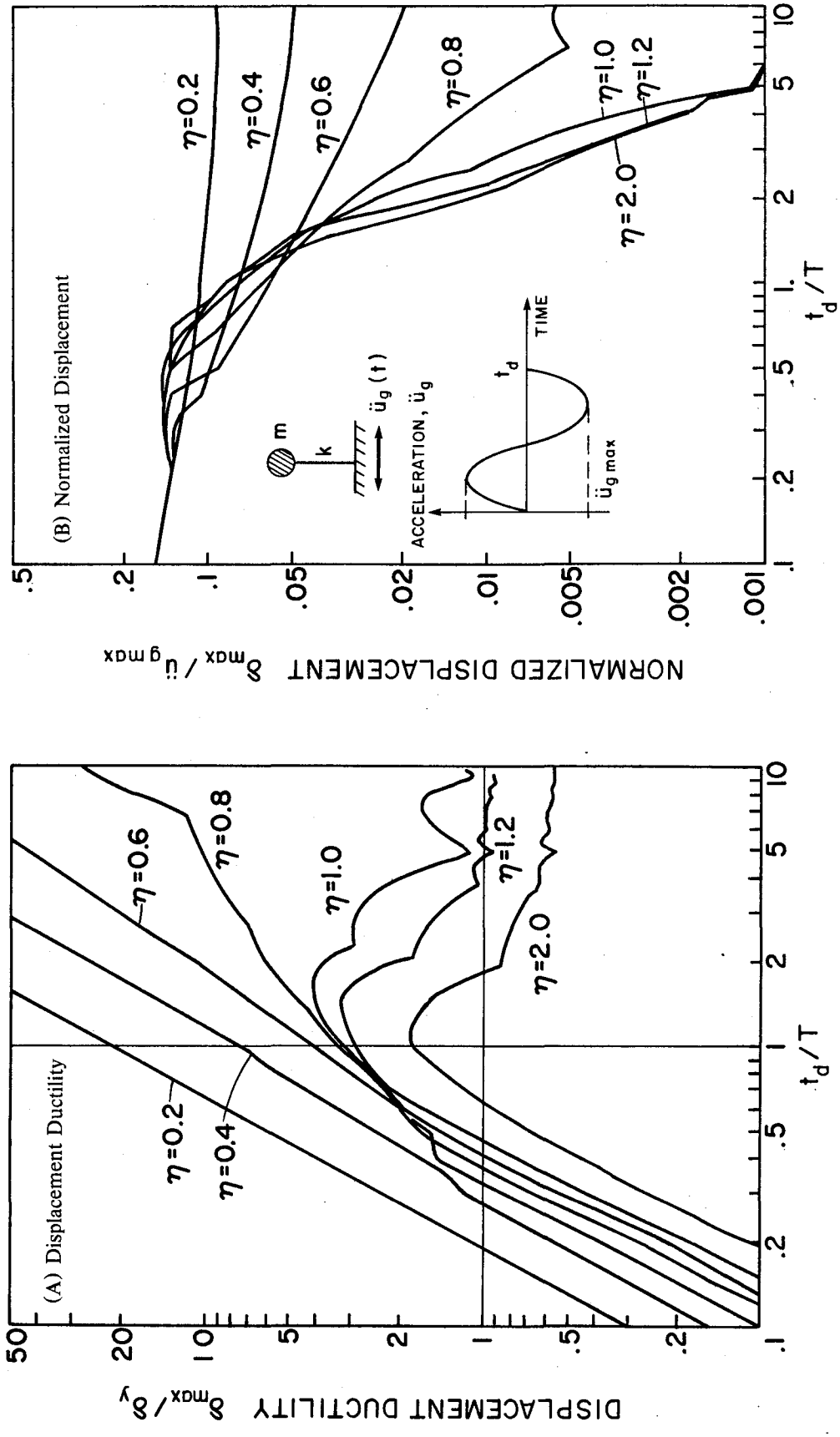

FIG. 16 Shock Spectra For Elasto-Perfectly Plastic Systems With No Damping Subjected To A Sine Pulse

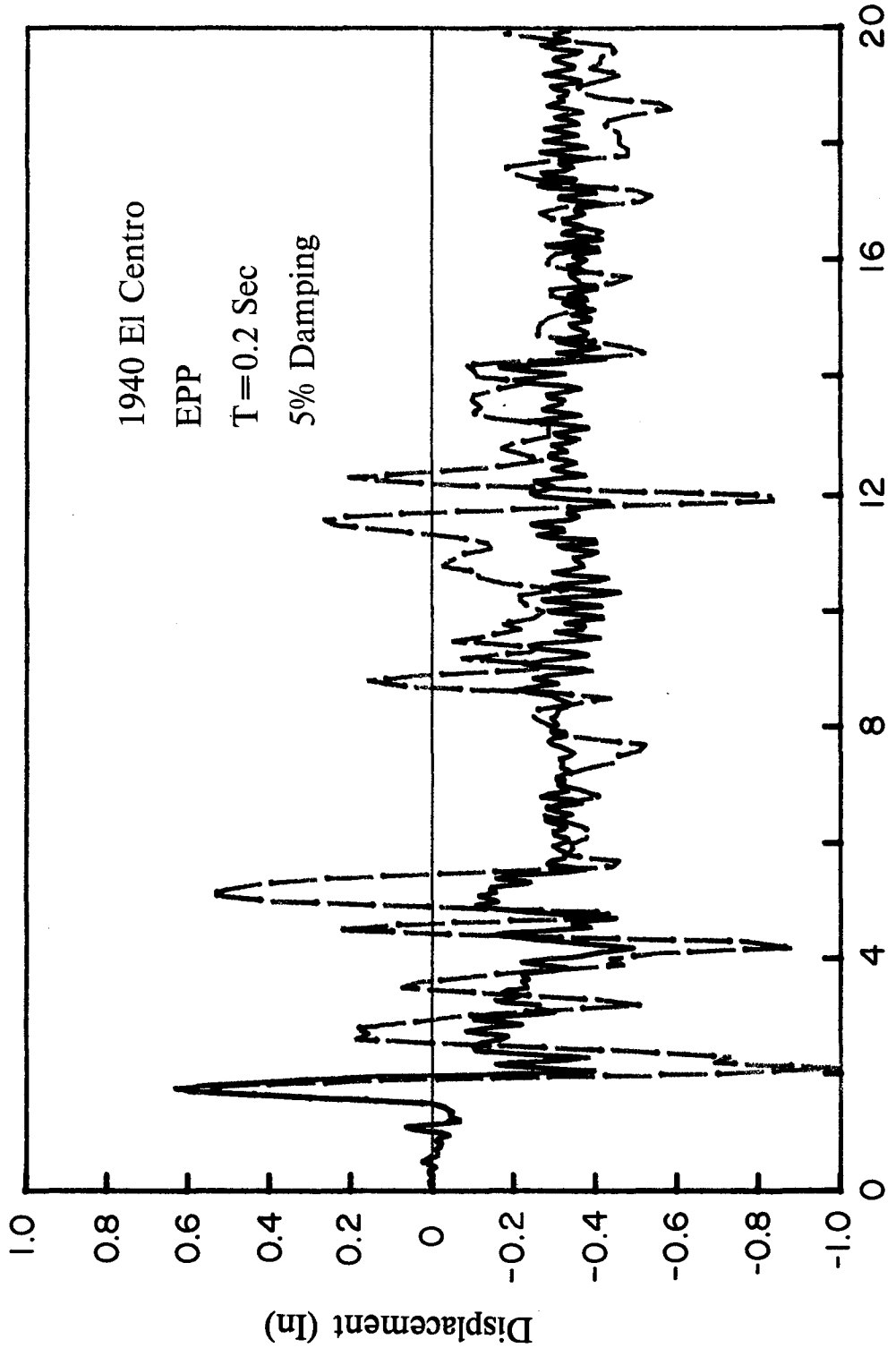

Fig. 17 Response Displacement Time History

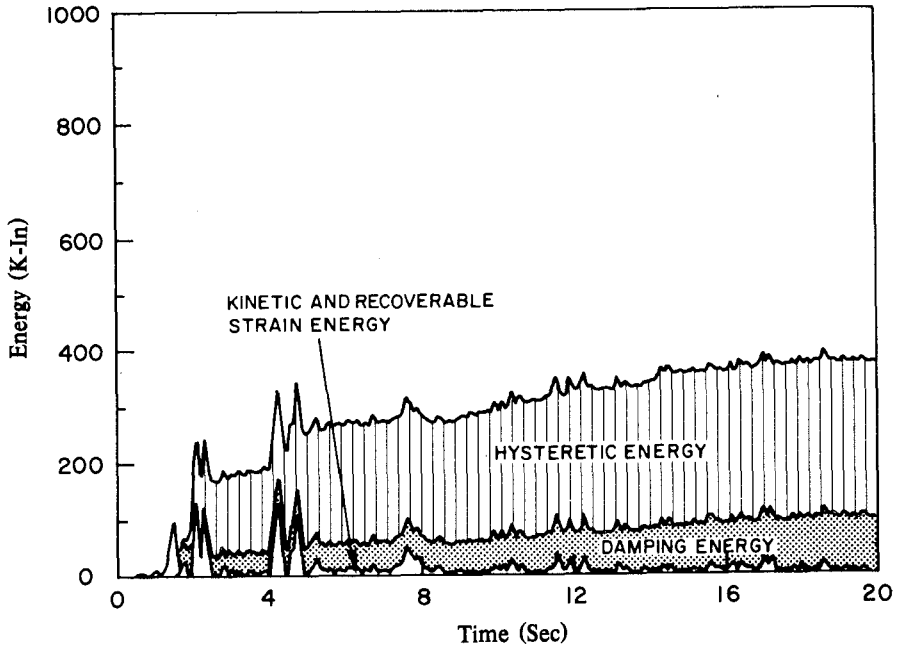

(A) Elasto-Perfectly Plastic

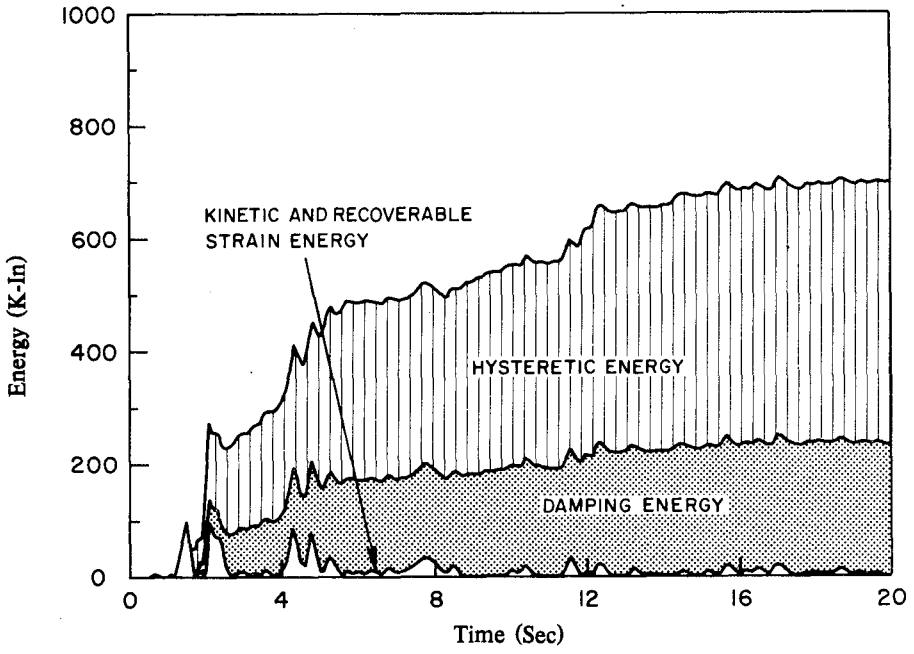

(B) Stiffness Degrading Model

Fig. 18 Energy Time History For Systems With Initial Elastic Period Of 0.2 Sec, 5% Damping And η-value Of 0.48 Subjected To 1940 El Centro (NS) Record

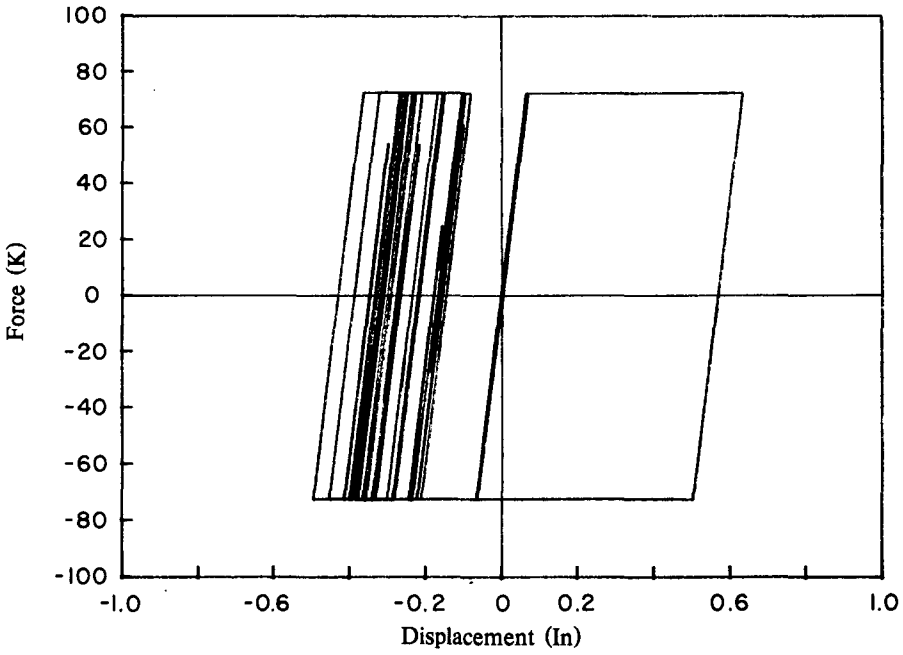

(A) Elasto-Perfectly Plastic

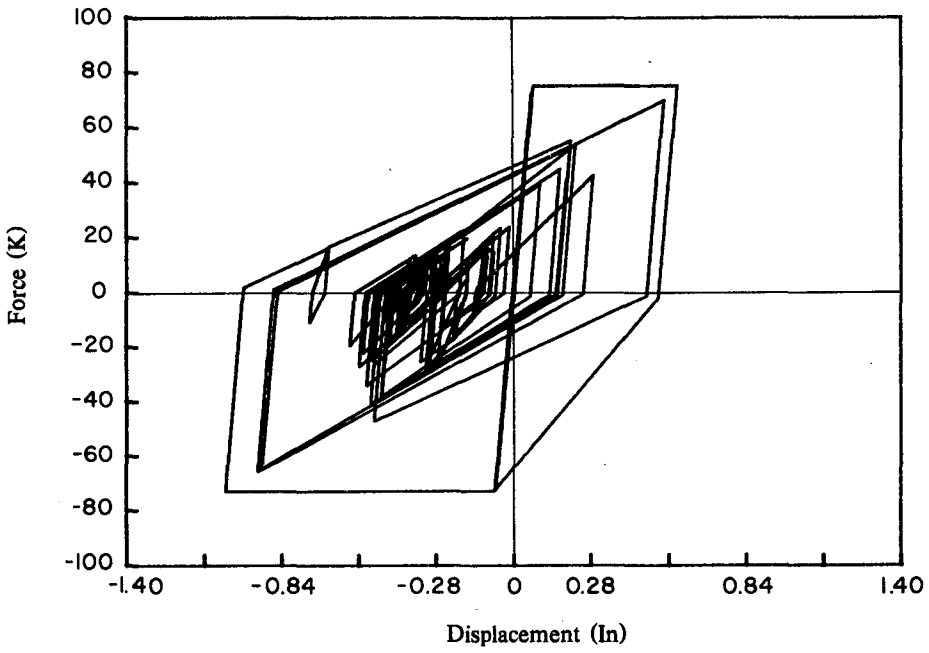

(B) Stiffness Degrading Model

Fig. 19 Hysteretic Loops For Systems With Initial Elastic Period Of 0.2 Sec, 5% Damping And η-value Of 0.48 Subjected To 1940 El Centro (NS) Record

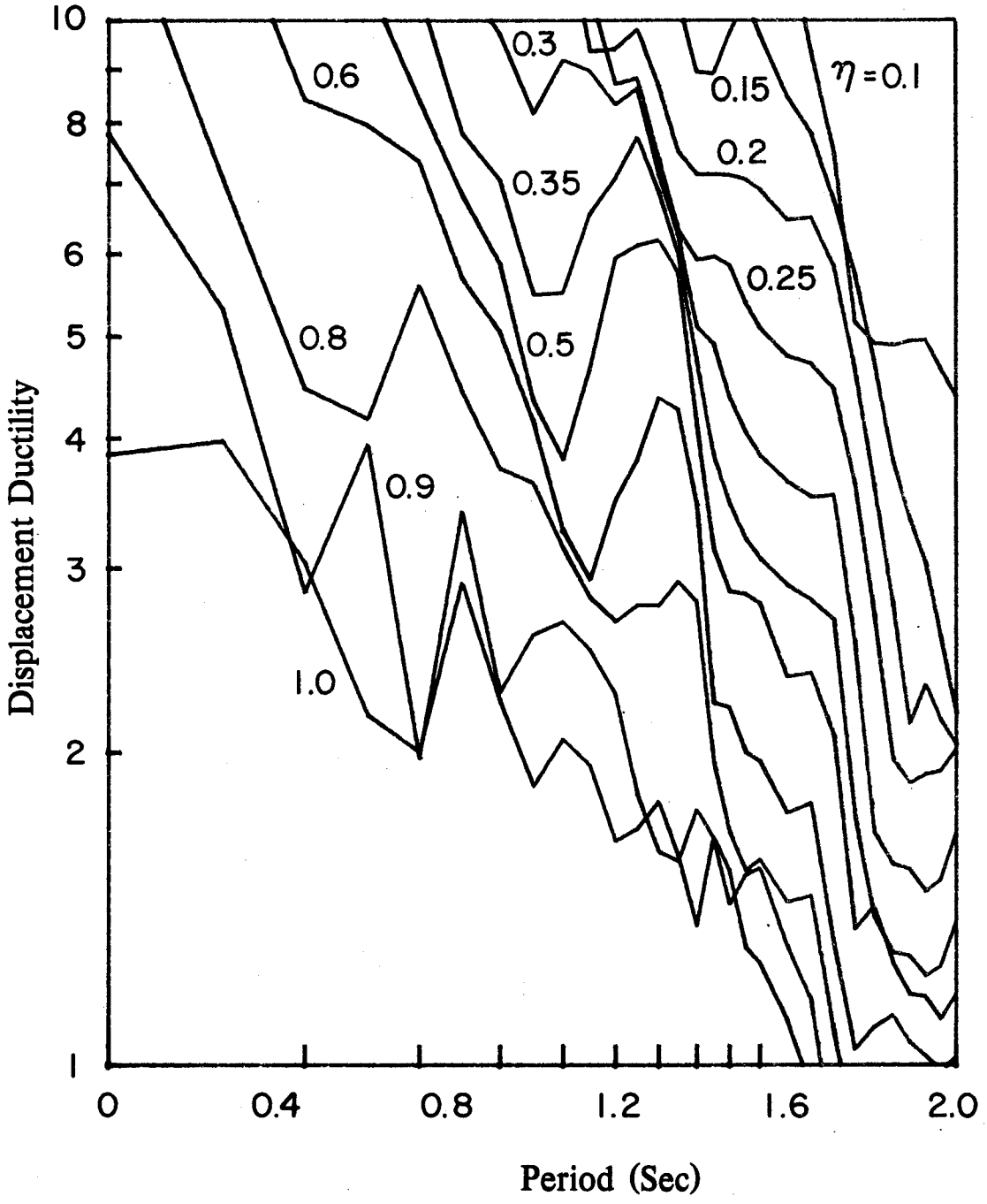

FIG. 20 Displacement Ductility Spectra For Elasto-Perfectly Plastic Systems Of η-Values From 0.1 To 1.0 With 5% Damping Subjected To 1940 El Centro (NS) Record On Log-Log Scale

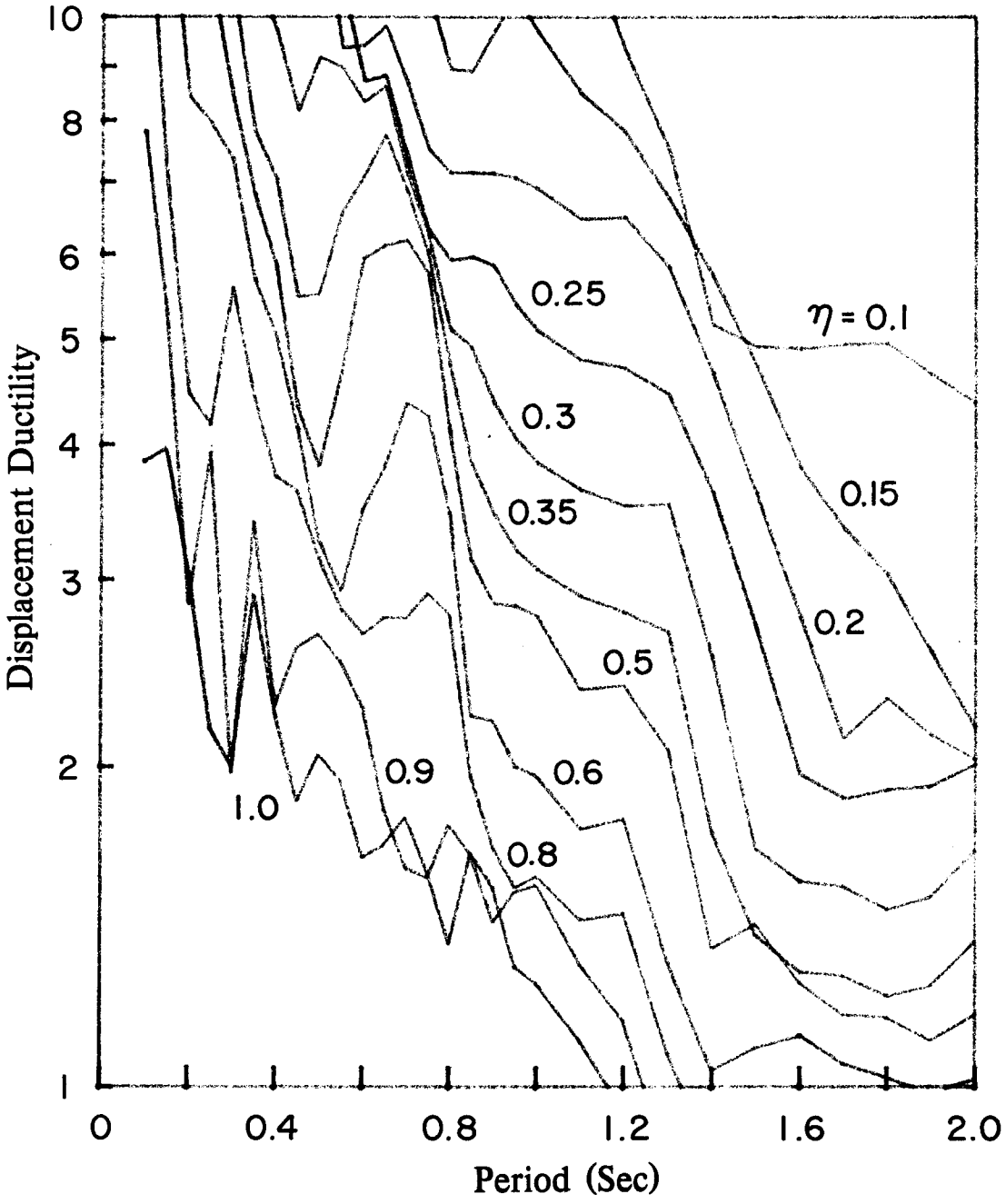

FIG. 21 Displacement Ductility Spectra For Elasto-Perfectly Plastic Systems Of η-Values From 0.1 To 1.0 With 5% Damping Subjected To 1940 El Centro (NS) Record On Semi-Log Scale

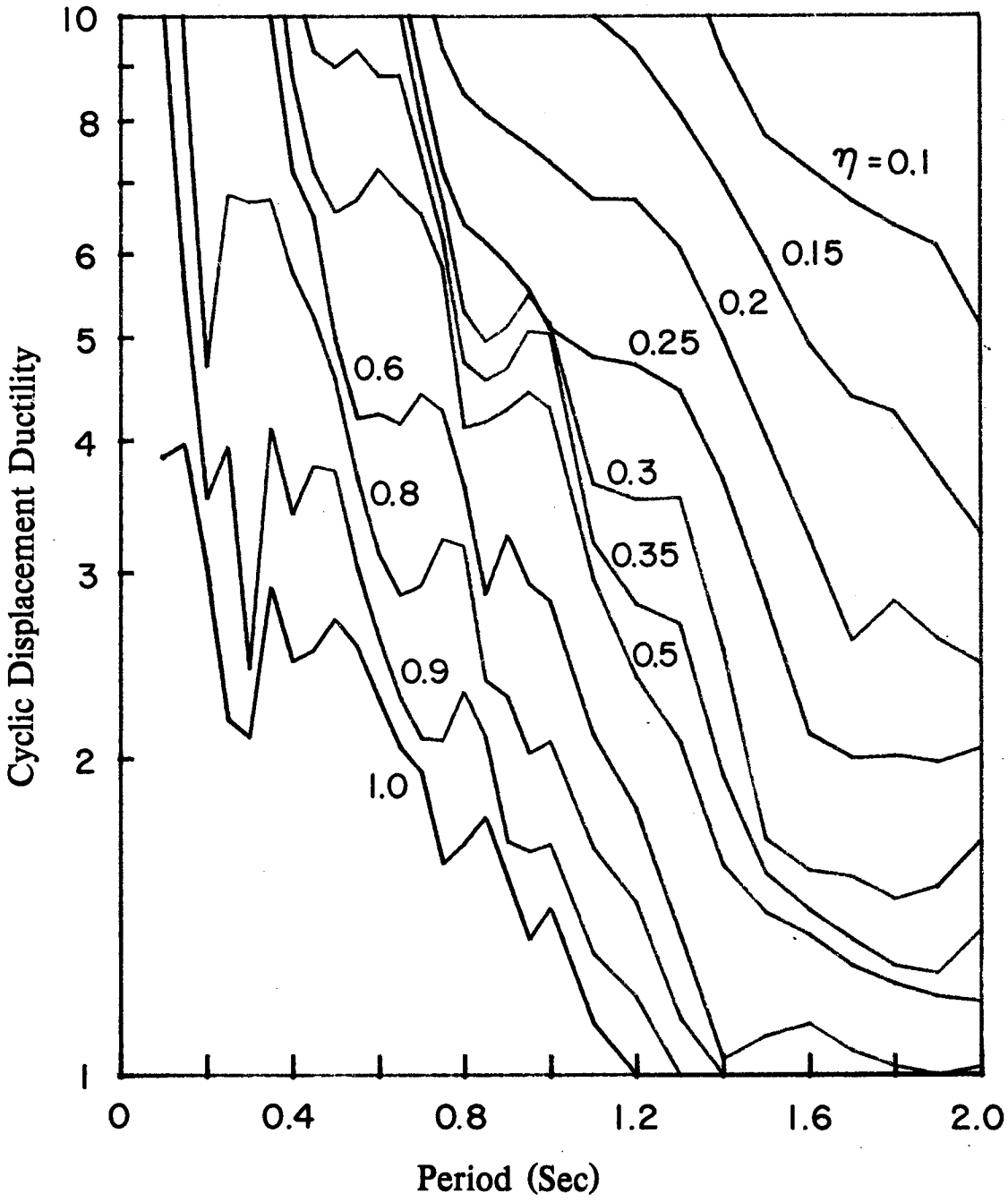

FIG. 22 Cyclic Displacement Ductility Spectra For Elasto-Perfectly Plastic Systems Of η-Values From 0.1 To 1.0 With 5% Damping Subjected To 1940 El Centro (NS) Record

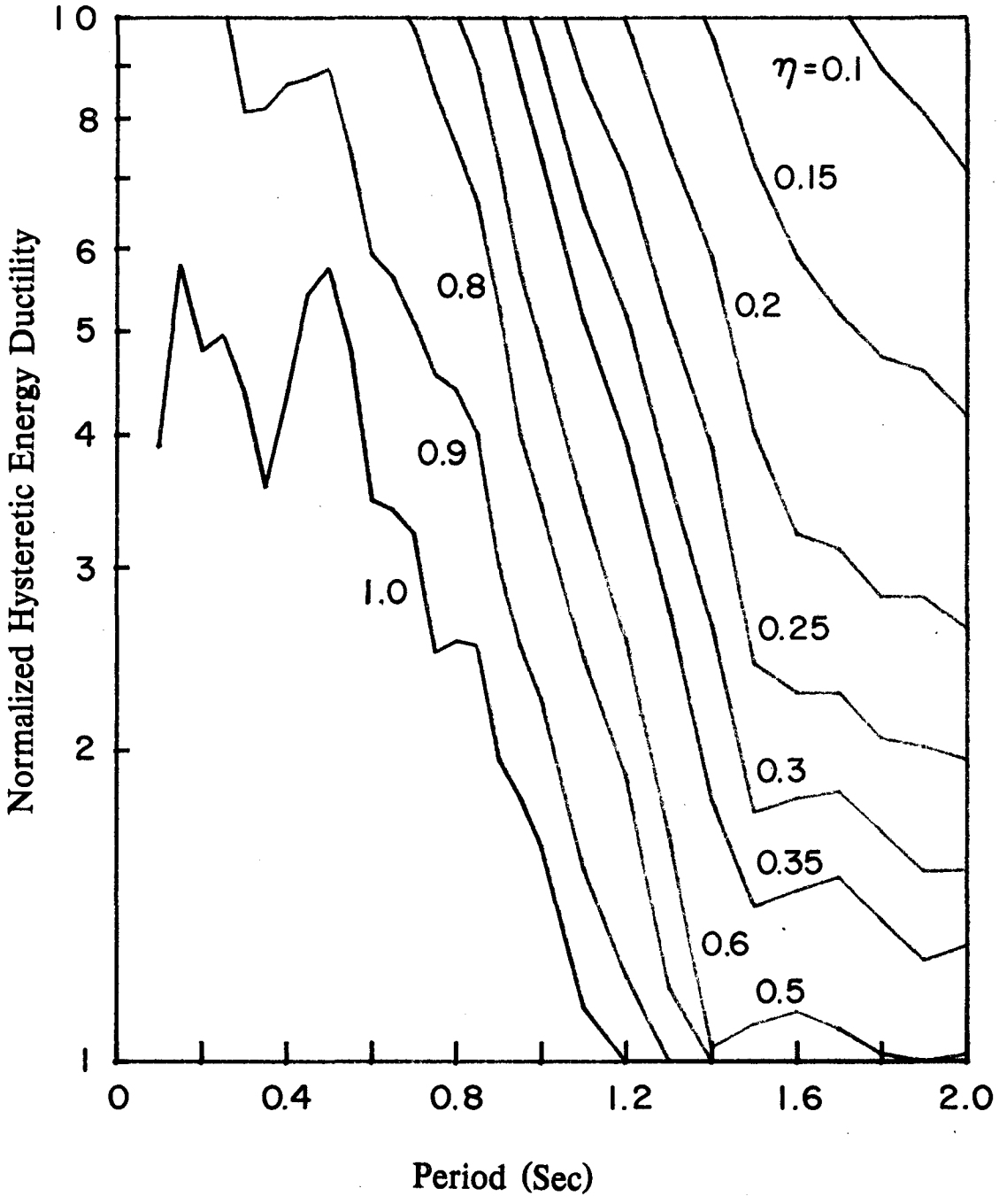

FIG. 23 Normalized Hysteretic Energy Ductility Spectra For Elasto-Perfectly Plastic Systems Of η-Values From 0.1 To 1.0 With 5% Damping Subjected To 1940 El Centro (NS) Record

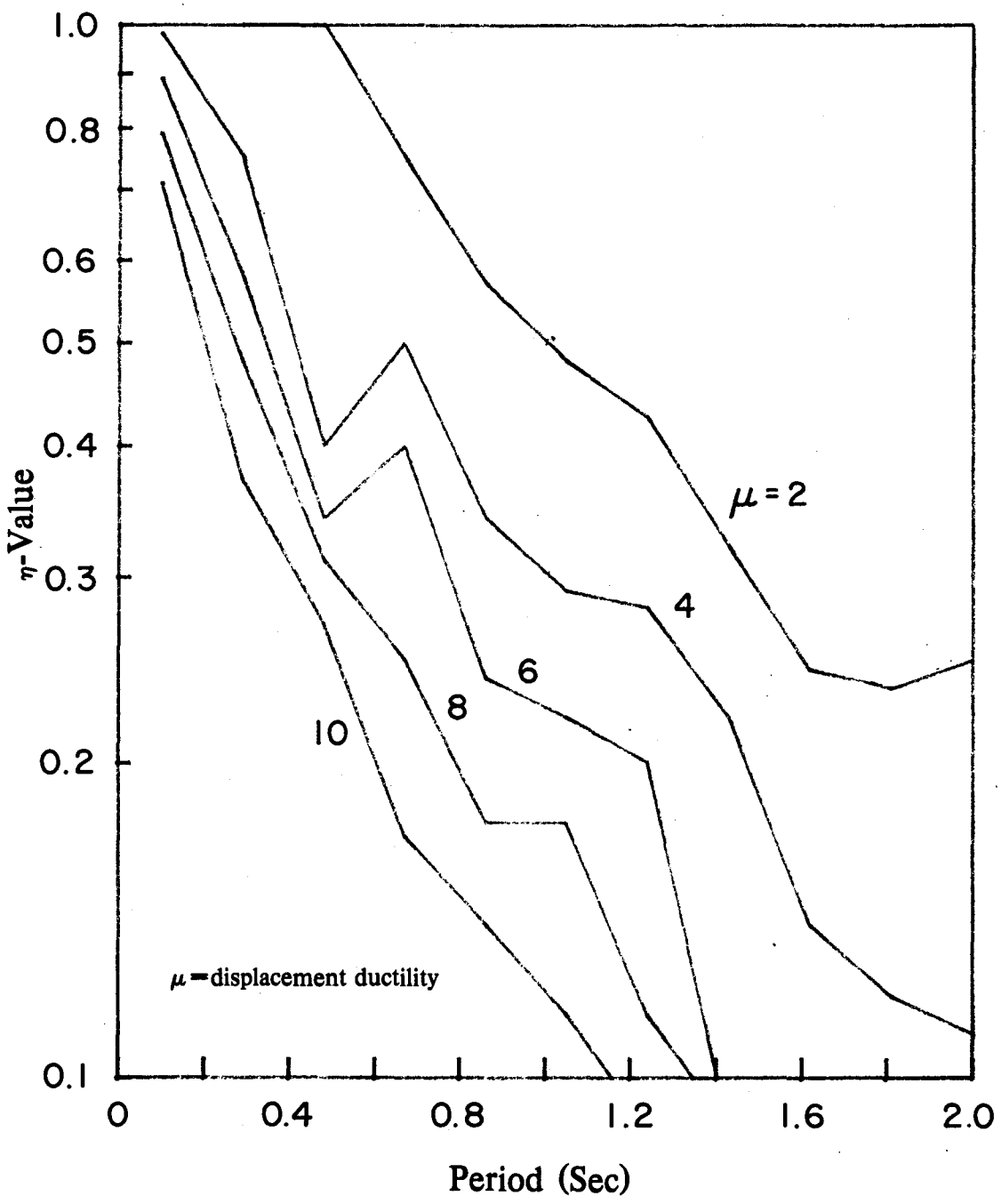

FIG. 24 η-Value Spectra For Elasto-Perfectly Plastic Systems Of Displacement Ductilities From 2 To 10 With 5% Damping Subjected To 1940 El Centro (NS) Record

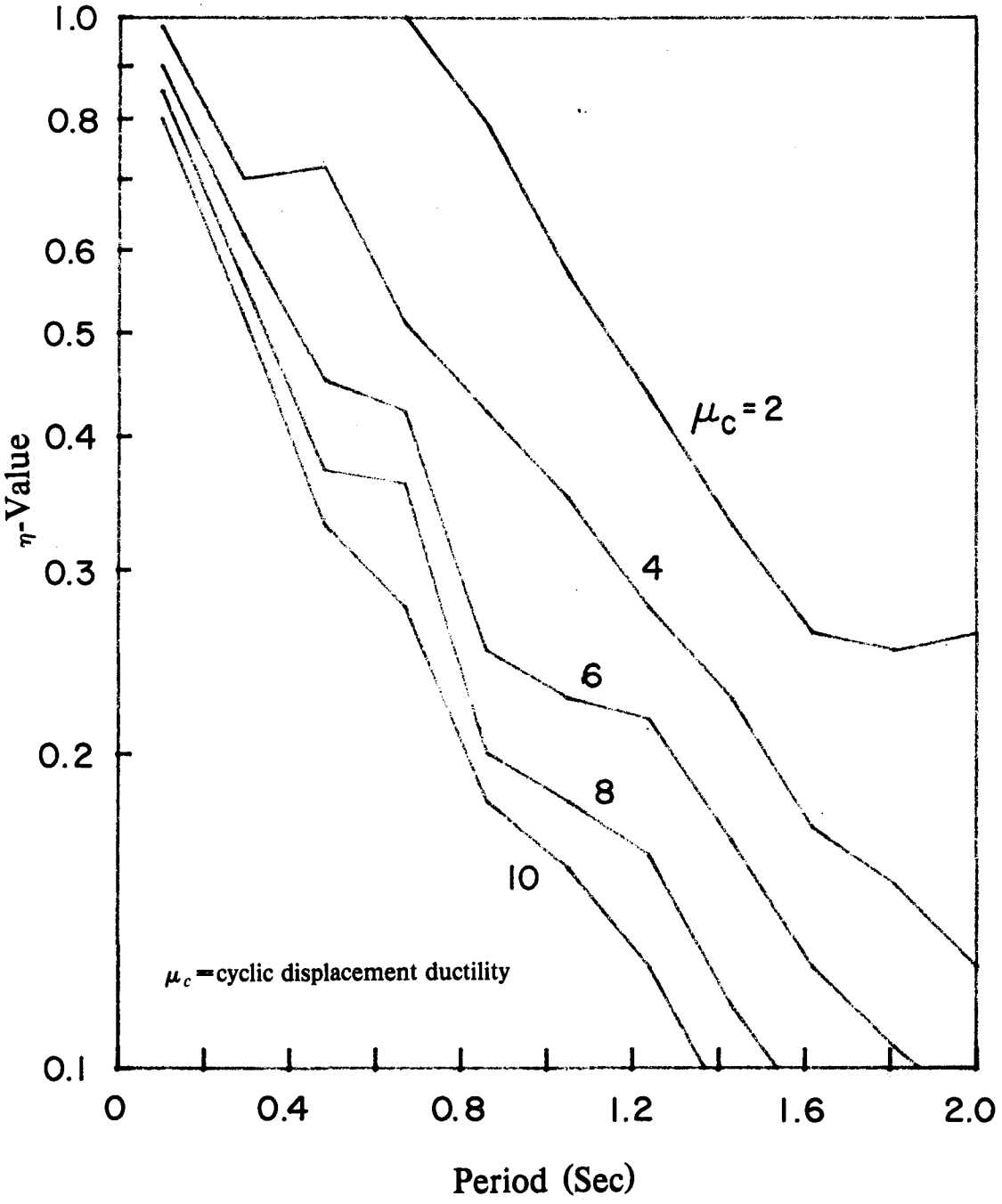

FIG. 25 η-Value Spectra For Elasto-Perfectly Plastic Systems Of Cyclic Displacement Ductilities From 2 To 10 With 5% Damping Subjected To 1940 El Centro (NS) Record

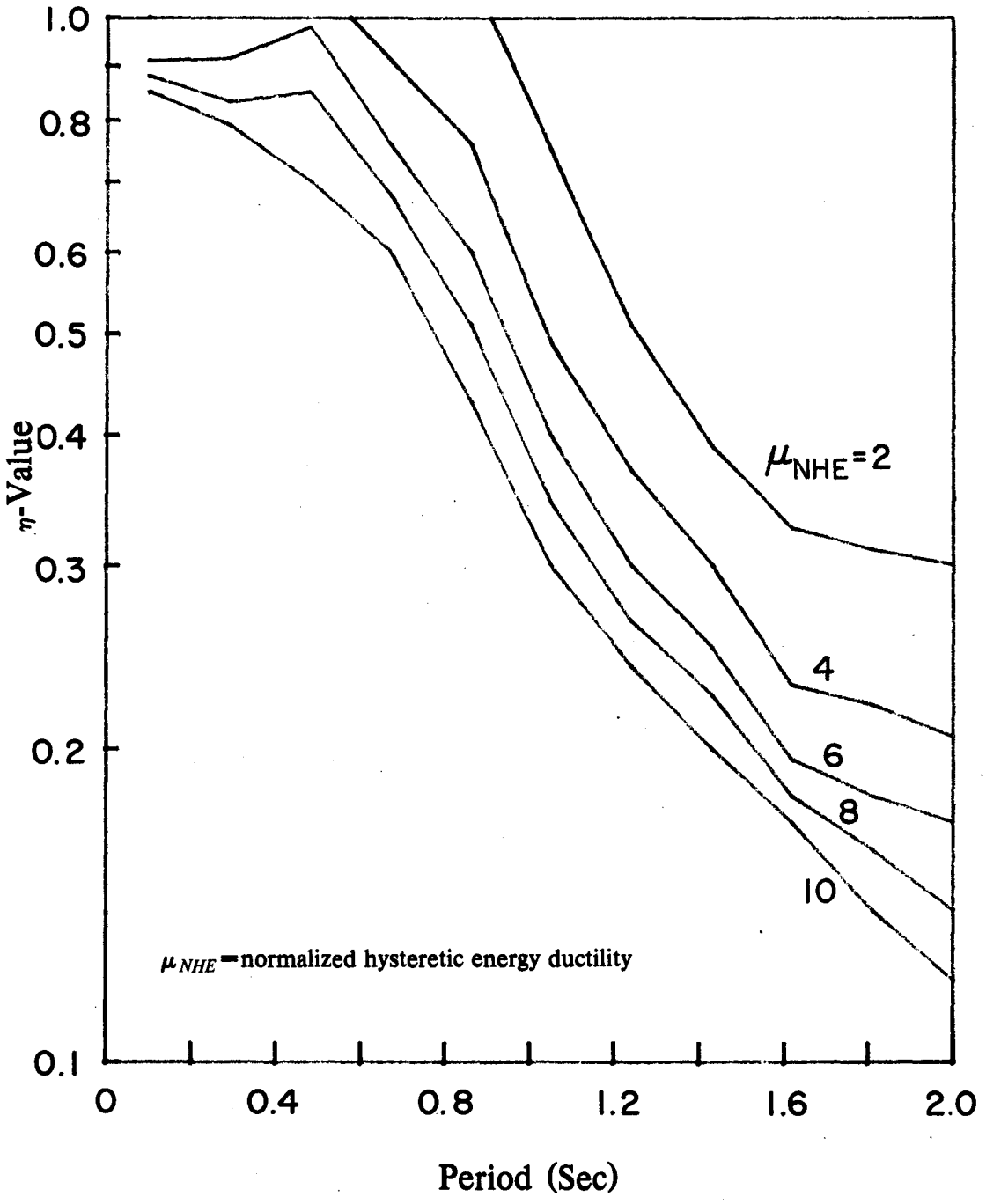

FIG. 26 η-Value Spectra For Elasto-Perfectly Plastic Systems Of Normalized Hysteretic Energy Ductilities From 2 To 10 With 5% Damping Subjected To 1940 El Centro (NS) Record

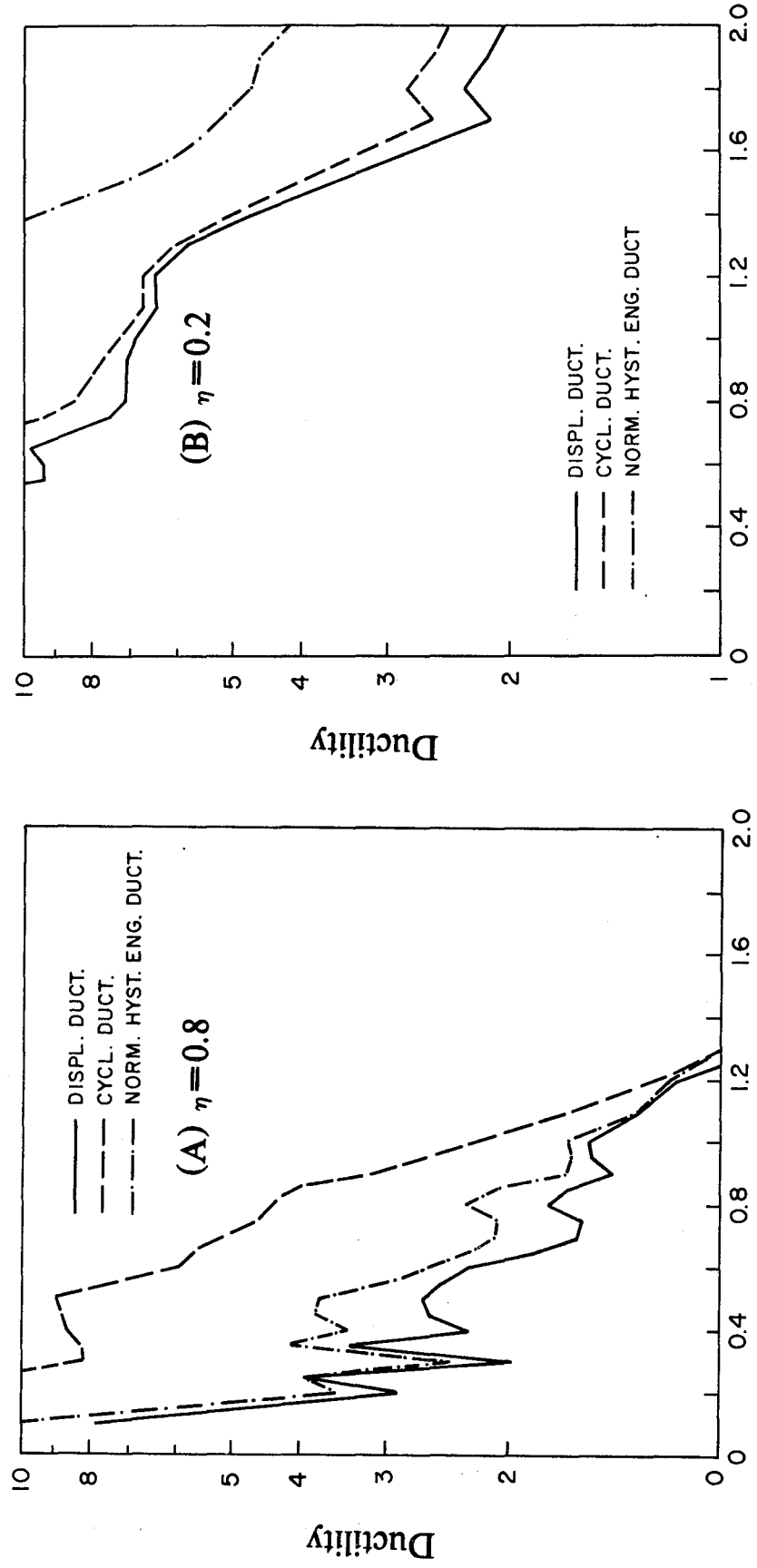

FIG. 27 Comparison Among Daisplacement Ductility, Cyclic Displacement Ductility And Normalized Hysteretic Energy Ductility Spectra For Elasto-Perfectly Plastic Systems Of η-Values of 0.8 And 0.2 With 5% Damping Subjected To 1940 El Centro (NS) Record

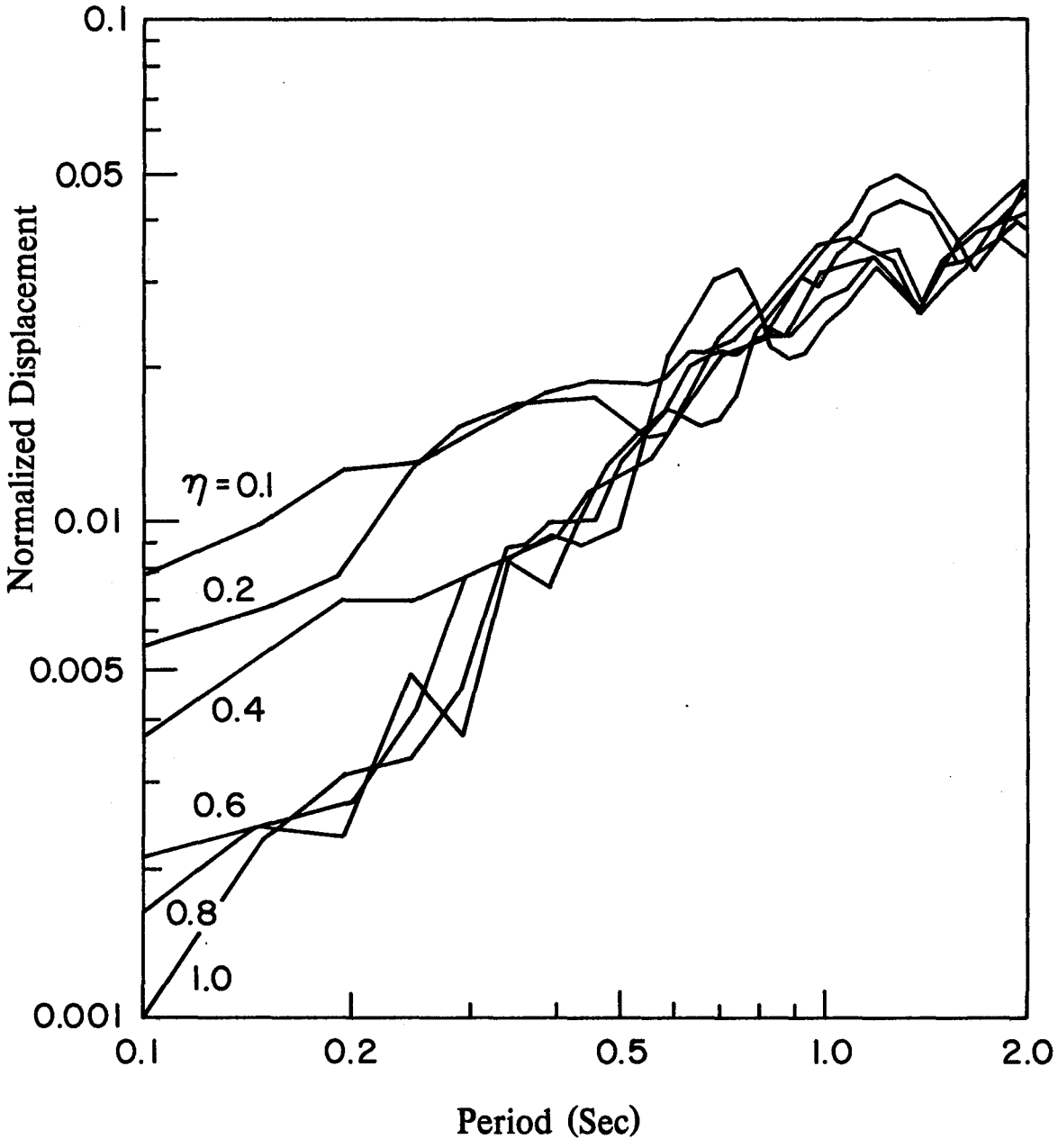

FIG. 28 Normalized Displacements For Elasto-Perfectly Plastic Systems With η-Values 0f 0.1,0.2,0.4,0.6,0.8,1.0 And 5% Damping Subjected To 1940 El Centro (NS) Record

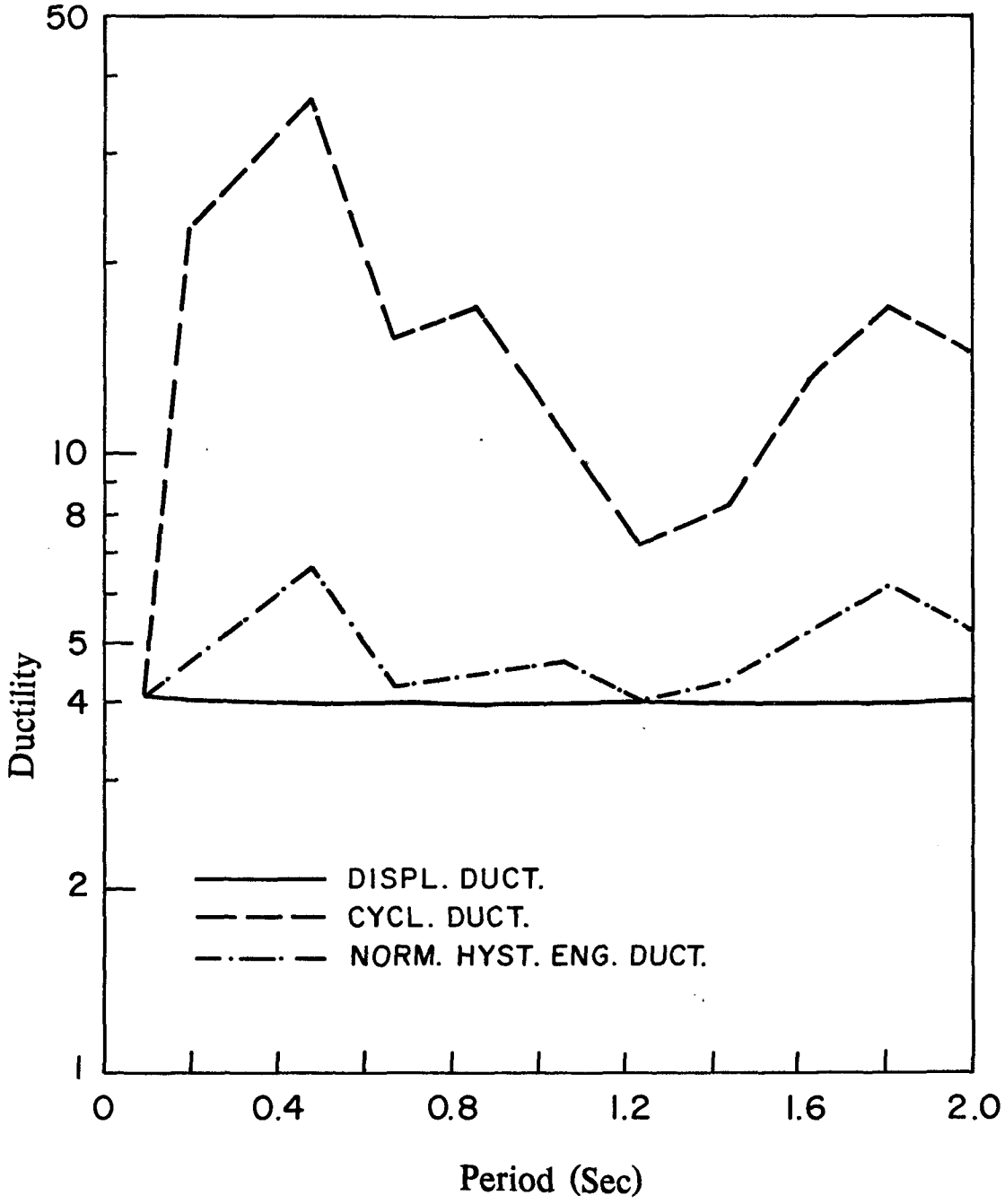

FIG. 29 Comparison Among Displacement Ductility, Cyclic Displacement And Normalized Hysteretic Energy Ductility Spectra For Elasto-Perfectly Plastic Systems Of Displacement Ductility Of 4 And 5% Damping Subjected To 1940 El Centro (NS) Record

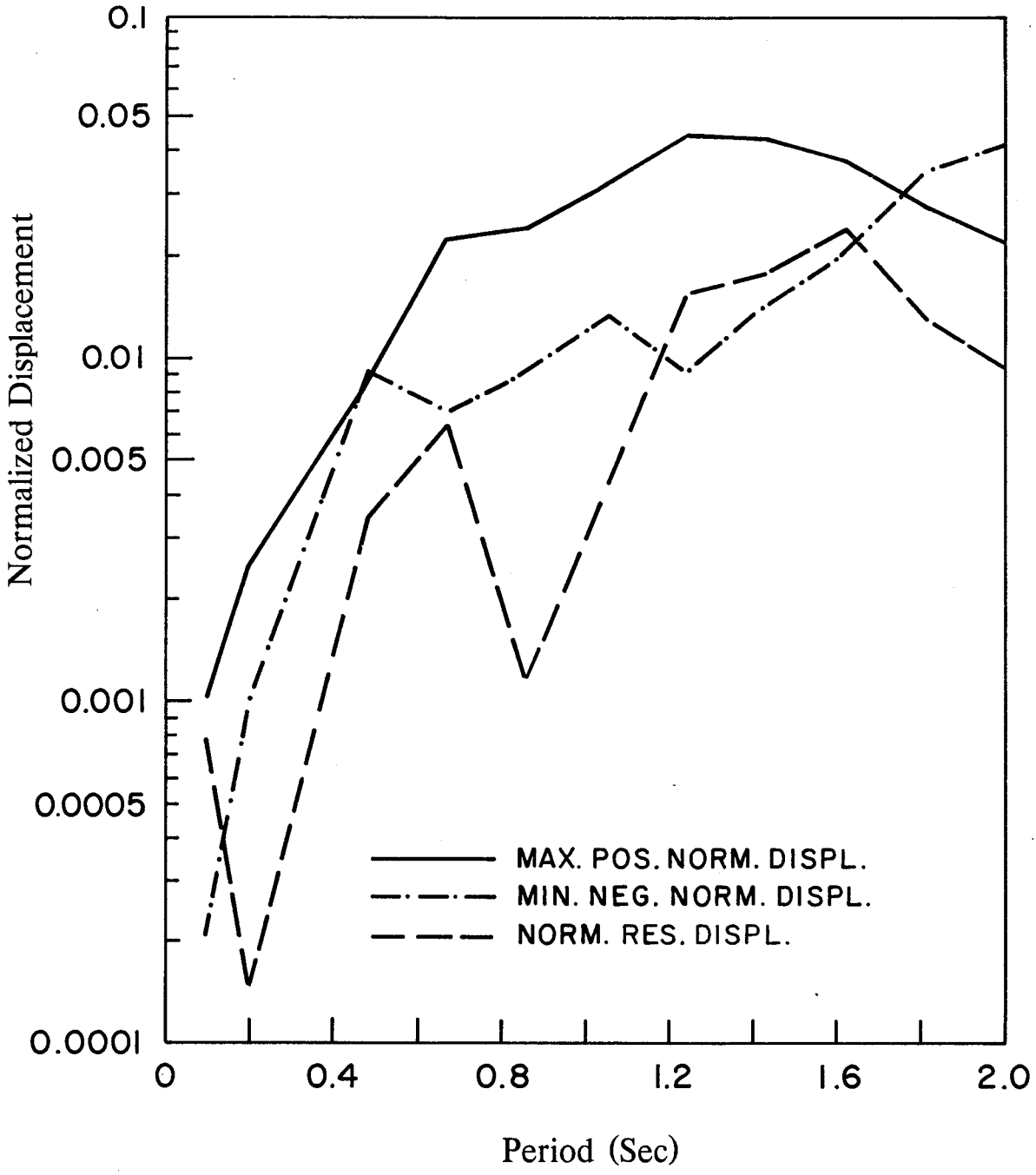

FIG. 30 Maximum Positive And Minimum Negative Normalized Displacement And Normalized Residual Displacement Envelopes For Elasto-Perfectly Plastic Systems Of Displacements Ductility Of 4 With 5% Damping Subjected To 1940 El Centro (NS) Record

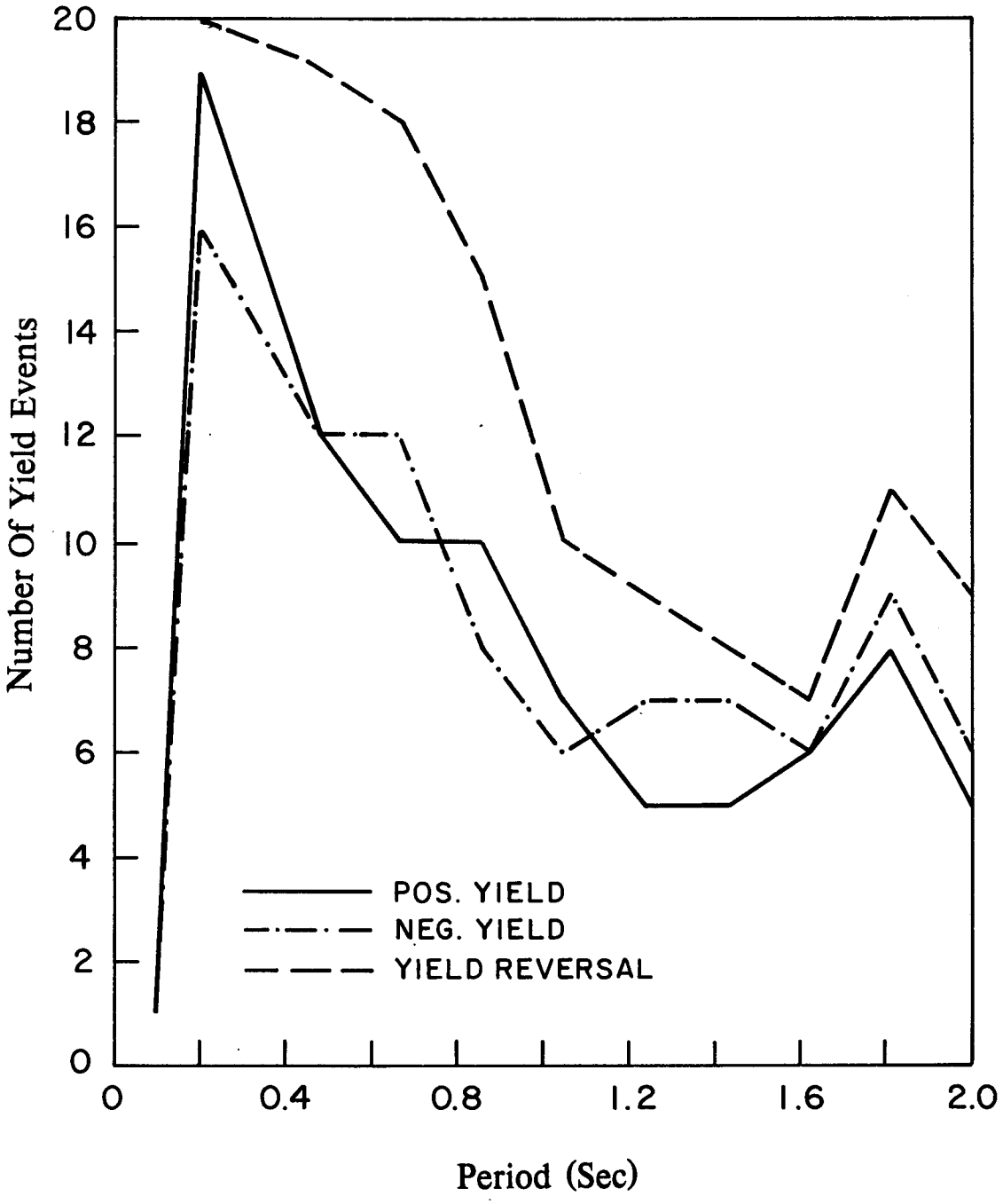

FIG. 31 Number Of Yield Events For Elasto-Perfectly Plastic Systems Of Displacement Ductility Of 4 With 5% Damping Subjected To 1940 El Centro (NS) Record

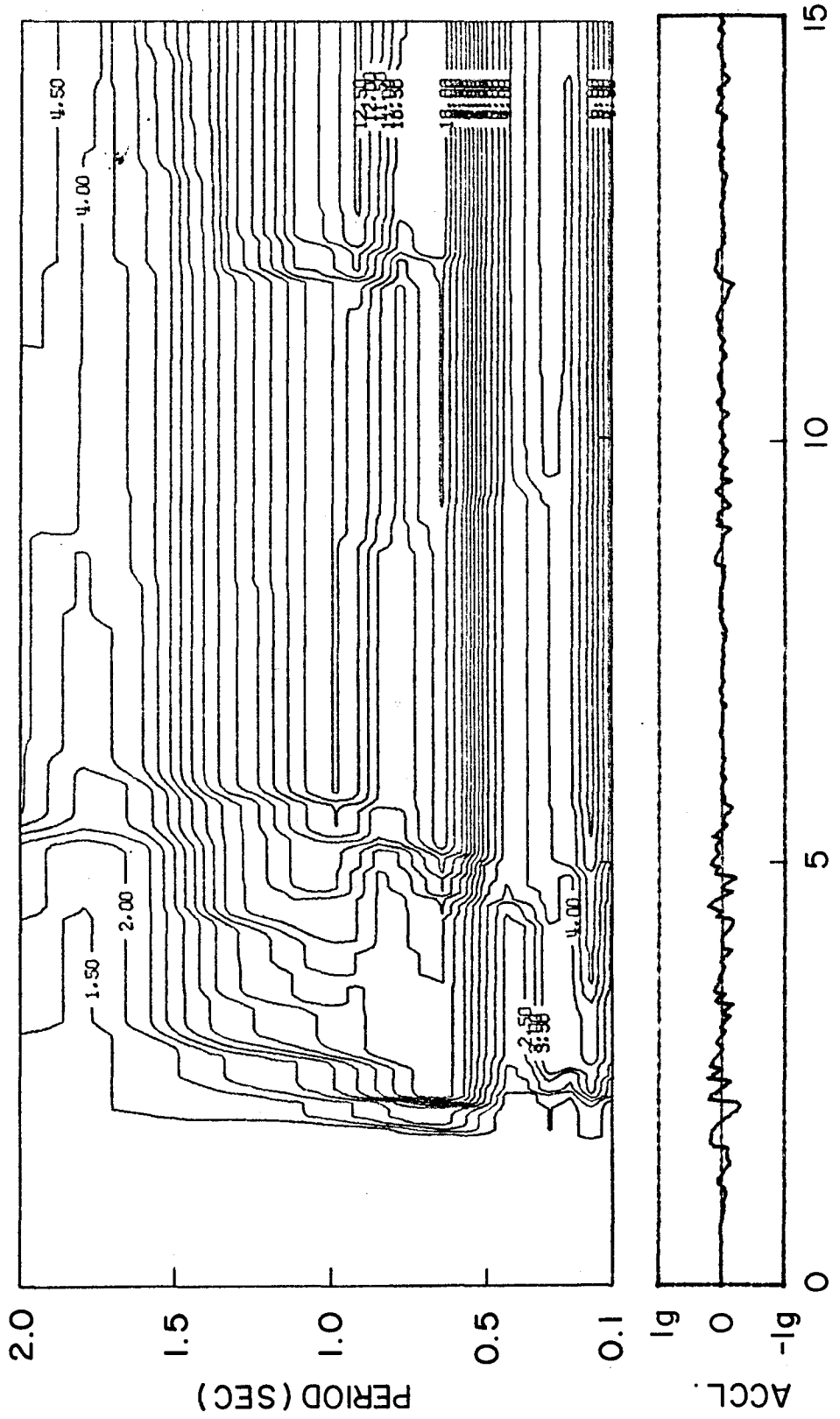

Fig. 32 Normalized Hysteretic Energy Ductility Evolutionary Spectrum

For EPP Structure With 5% Damping Subjected To 1940 El Centro (NS) Record

APPENDIX A : PROGRAM INPUT AND OUTPUT

A.1 Input Specification

The program has been used and tested extensively in mainframe computers like CDC 6400 and CDC 7600 and mini-computers like PDP 11/780, PDP 11/750 and PDP 11/70 using the UNIX operating system. The following input format should be observed when using the computer program. The variable names indicated are those used in the computer program.

A. JOB TITLE (8A10) - ONE CARD

columns 1-80 : Information to be printed in the beginning of the output.

B. SYSTEM DEFINITION

B1. SYSTEM/ANALYSIS INFORMATION (8F10.0) - ONE CARD

columns 1-10 : XMASS. System's mass. If XMASS is positive, then the program will consider all combinations of the stiffness (or period) listed in Section B4 and the yield displacement (or η-value) listed in Section B5 in calculation of responses. If XMASS is negative, then the stiffness (or period) and yield displacement (or η-value) will be considered in pairs in the order they are input. (NOTE: a particular system's mass is not required if η-value and period are specified for the normalized responses of a family of related systems, and can be made equal to one arbitarily. See Section 2.2)

columns 11-20 : PK. Deformation hardening/softening ratio. This ratio should be input as fraction of the initial elastic stiffness, with zero value permitted for the case of elasto-perfectly plastic systems.

columns 21-30 : DELTAT. The maximum time increment to be used in the analysis. However, the program automatically selects smaller time increments to match the loading interval, the output interval, or to obtain the specified convergence tolerance when stiffness changes (see Section 2.4)

columns 31-40 : XOUT. A multiplier for obtaining output interval for response time histories. The output time interval will be determined as output time interval = XOUT * DELTAT. To supress response time histories simply use a sufficiently large XOUT value. (XOUT = 1.0 is the default).

columns 41-50 : TCONV. Convergence tolerance. This tolerance can be used to control the amount of overshoot and distortion of the hysteretic curve shape (see Section 2.4). (TCONV = 0.01 is the default)

B2. SYSTEM/ANALYSIS COMMANDS (10I5) - ONE CARD

columns 1-5 : NSTIFF. Number of stiffness or periods to be specified. A negative value for NSTIFF will result in periods being read in Section B4, while a positive value for NSTIFF results in stiffnesses being read.

columns 6-10 : NUYP. Number of yield displacements or η-values to be specified. A negative value for NUYP will result in η-values being read in Section B5, while a positive value for NUYP will result in yield displacements being read.

columns 11-15 : NDAMP. Number of damping values to be considered. NDAMP = 1 is the default.

columns 16-20 : ITYPE. Hysteretic model identifier.

ITYPE = 1 - bilinear hysteretic model (default)

ITYPE = 2 - stiffness degrading model

columns 21-25 : IENG. Energy computation option.

IENG = 0 - energy computation desired

IENG = 1 - no energy computation desired

Energy computation is made only if the system is excited by ground motions.

columns 26-30 : IPUNCH (output history storage).

IPUNCH = 1 - no output history is desired.

IPUNCH = 2 - the response displacement, resistance force histories are to be saved either on punched cards or on Tape 1 depending on the value of JTAPE (columns 31-35).

IPUNCH = 3 - the response displacement, resistance force, energy ductility and residual ductlity (defined as the residual displacement over the yield displacement, see (Fig. 14) histories are to be saved either on punched cards or on Tape 1 depending on the value of JTAPE(columns 31-35).

IPUNCH = 4 - response displacement, velocity, acceleration, resistance force, input energy, kinetic energy, recoverable strain energy, hysteretic energy, damping energy, energy ductility and residaul ductility histories are to be saved either on punched cards or on tape 1 depending on the value of JTAPE (columns 31-35).

columns 31-35 : JTAPE. File disposition for option associated with IPUNCH.

JTAPE = 1 when file is to be punched.

JTAPE = 0 when file is to be written on Tape 1.

columns 36-40 : IHED. Heading option. If IHED = 0, the information on the first input card will be repeated on the top of each output page. If the value of IHED is non-zero, such heading will only appear on the first page of the output.

columns 41-45 : JPUNCH. For non-negative value of JPUNCH, the spectra (see Appendix A, Section A.2) will be punched on cards, otherwise spectra will only be printed.

columns 46-50 : JPRINT. For JPRINT = 0, the spectra will be written on output file. For non-zero value of JPRINT, the spectra will be written on the output file and on Tape 7. The purpose of writing spectra on Tape 7 is to enable the user to

dispose the detailed output histories and related summaries and the spectra tables to different output devices (e.g. microfiche) when only the information about the spectra is desired.

B3. DAMPING CARDS (8F10.0) - AS MANY CARDS AS ARE NEEDED TO ENTER DATA

Damping values to be considered are expressed as fractions of the critical damping value (defined as two times the product of system's mass and natural circular frequency).

B4. STIFFNESS OR PERIOD (8F10.0) - AS MANY CARDS AS NEEDED

Whether stiffness or period values are input depends on the sign of NSTIFF as described in Section B2.

B5. YIELD DISPLACEMENT OR N-VALUE (8F10.0) - AS MANY CARDS AS NEEDED

Whether yield displacement of η-value are input depends on the sign of NUYP as described in Section B2.

C. LOADING

C1. LOAD CONTROL (2I5,2F10.0,10A5) - ONE CARD

columns 1-5 : KOUNT. Total number of acceleration or external load values to be read. If KNOUT = 0, then the previous record will be used.

columns 6-10 : IND. Excitation indicator flag. When IND = 0, the system is excited by ground motion. When IND = 1, the system is excited by external loads.

columns 11-20 : DT. Time increment between input acceleration or external load values. If DT is non-zero, the program assumes the excitations input occur at constant time interval. If DT = 0, pairs of time-acceleration (or pairs of time-external load) values will be read. The latter case is useful when the excitation is not recorded at equal intervals.

columns 21-30 : FACTOR (excitation scaling factor). To scale input ground acceleration or external loads by a constant FACTOR.

columns 31-80 : FMT. Fortran format specification for inputing excitation. The format must be bracketed within parentheses.

C2. EXCITATION RECORD

As many cards as necessary to read KNOUT number of values according to the specified format in Section C1).

D. EXECUTION DISPOSITION

(1) To terminate execution, place three blank cards after the excitation record.

(2) To proceed to a new problem, repeat data input starting with Card A, but note that record need not be input again if the same excitation is to be considered (see Section C1).

E. STORAGE REQUIREMENT

There are no inherent limits to the number of cases or duration of the record; however, in each case considered, no more than 10,000 blank common can be used. The length of blank common required for any record can be estimated as

$$\textit{length of blank common} = 2\times KOUNT + \left[8\times\frac{DT\times KOUNT}{XOUT\times DELTAT}+2\right]$$
$$+15\times[NSTIFF\times NUYP]+NDAMP+NSTIFF+NUYP+2$$

A.2 Output

The input information is summarized in a table at the beginning of the output for each system followed by the time history of the input excitation. When a family of systems are specified in the input subjecting to an identical excitation, only one excitation time history will be echoed in the output followed by a series of summaries of the responses of the family of systems. The computed responses can be presented at two levels of detail depending on the

needs of the user. When complete histories of the responses are desired, the user can specify in the input complete time histories of the response displacement, the response velocity, the response acceleration, the input energy, the kinetic energy, the recoverable energy, the damping energy, the ground acceleration, the ground velocity and the ground displacement. For input containing more than one structures, seperate sets of time histories will be generated for each structure defined in the input and for each excitation record specified. Alternatively, the output will present only summaries of the maximum and the minimum of the above mentioned responses as well as the times of their occurance.

Following either one of the presentations of the computed responses, a short summary of the system properties and response envelopes is tabulated. The information in the summary include the η-value of the system, maximum positive and negative displacement ductilities, cyclic ductility, accumulative ductility, normalized hysteretic energy ductility, number of positive and negative yield excursions, number of yield reversals, number of zero crossing, residual displacement, and absolute maximum response acceleration, velocity and displacement.

Whenever the responses of more than one system are computed, a summary of selected responses of all systems is listed in a seperate table in the order of the computation. This is the spectra referred to in Appendix A, Section A.1, Card B.2. The responses are the maximum and minimum displacement ductilities, cyclic ductility, normalized hysteretic energy, accumulative ductility, the magnitude and the time of occurance of the maximum and minimum displacement normalized by the peak ground acceleration, the residual displacement, the number of positive and negative yield excursions and zero crossings.

APPENDIX B : EQUIVALENT SINGLE-DEGREE-OF-FREEDOM SYSTEMS

As mentioned in Section 1.1, it is sometimes advantageous and convenient to represent a nonlinear multiple-degree-of-freedom (MDOF) structure as one or more equivalent nonlinear single-degree-of-freedom (SDOF) systemss. For linear elastic multiple-degree-of-freedom system, it is often useful to decompose such systems into their modal components and use the principle of superposition to take advantage of the resulting decoupled equations of motion. Even though modal analysis does not apply in nonlinear cases, design forces for nonlinear multiple-degree-of-freedom systems have been determined using inelastic response spectra with elastic mode shapes and periods in conjunction with modal analysis methods [3]. Iterative procedure have been proposed [24] for analysis which require computation of modified mode shapes, modal frequencies, modal ductilities and modal bilinear hardening ratios for multiple-degree-of-freedom systems with bilinear stiffness characteristics.

Alternatively, it has been proposed that an equivalent nonlinear single-degree-of-freedom system be substituted for the original multiple-degree-of-freedom structure. The Q-model [21,22] is an example of such a simplified approach. The model can be used to calculate the displacement time histories of multi-story structures subjected to seismic motions. Even though the stresses and forces of the original structure can not be inferred directly from those calculated for the equivalent structure, they can be computed readily from the displacements estimated for the original structure.

The Q-model is basically an one-mode approximation of the response. The equivalent system (Fig. B1) is selected so that the deflection of the equivalent system is the same as that for some significant point on the original structure. Furthermore, the constants and resistance force function are evaluated on the basis of an assumed deflected shape of the actual structure. Many choices for this shape function are possible. It might be taken as the fundemental mode shape of the actual structure; or it might be taken as the same as that resulting from the static application of the dynamic load which for earthquake ground motions may be taken as

$$\underline{M}\,\hat{1}=\underline{M}\begin{Bmatrix}1\\1\\\cdot\\\cdot\\1\end{Bmatrix}=\begin{Bmatrix}m_1\\m_2\\\cdot\\\cdot\\m_n\end{Bmatrix} \tag{B.1}$$

if diagonal mass matrix and unit influence vector are assumed with m_i denoting the mass in the ith degree-of-freedom and n denoting the total number of degree-of-freedoms. However, in developing the Q-model, it was found [22] advantageous to compute the assumed deflected shape shape, $\hat{x}$, as follows. First, the structure's lateral resistance function is idealized by its base overturning moment versus roof deflection relationship. This is established by performing an inelastic analysis of the structure with monotonically increasing lateral forces. The forces are assumed to have a "triangular" force distribution: the lateral force at a given level is proportional ot the product of the height and mass at that level. Such a base moment-roof displacement curve will be curvilinear in general due to the nonlinearities in the structure. For simplicity, the curve may be idealized by two straight lines, the knee of the resulting bilinear relationship implying a synthetic yield point [22], see Fig. B2. The shape function, $\hat{x}$, is taken as the deflected shape when the knee of the bilinear force-displacement curve occurs.

With the shape function calculated as just described, the equivalent mass, damping and loading can be computed as follow:

$$M_e=\hat{x}^t \underline{M}\hat{x} \tag{B.2}$$

$$C_e=\hat{x}^t \underline{C}\hat{x} \tag{B.3}$$

$$F_e=-\hat{x}^t \underline{M}\hat{1}\ddot{u}_g(t) \tag{B.4}$$

where M_e, C_e and F_e are the effective mass, damping and loading associated with the equivalent system. The mass and damping matrices of the actual structure and the ground acceleration are denoted as $\underline{M}$, $\underline{C}$ and $\ddot{u}_g(t)$ respectively. The resistance of the equivalent structure can be computed as the modal transformation of the applied lateral forces on the actual structure and can be written as

$$R_e=\hat{x}^t \hat{R} \tag{B.5}$$

where R_e is the lateral resistance forces of the equivalent structure and $\hat{R}$ is the applied lateral force vector on the actual structure.

With the actual structure represented as just described, the equation of motion becomes

$$M_e\ddot{u}+C_e\dot{u}+R_e=F_e \tag{B.6}$$

where u is the displacement of the equivalent structure. The displacement of the actual

structure can be obtained by multiplying the assumed deflected shape vector by the solution of Eqn. B.6. Numerical solution of Eqn. B.6 can be obtained by the computer program described in this report.

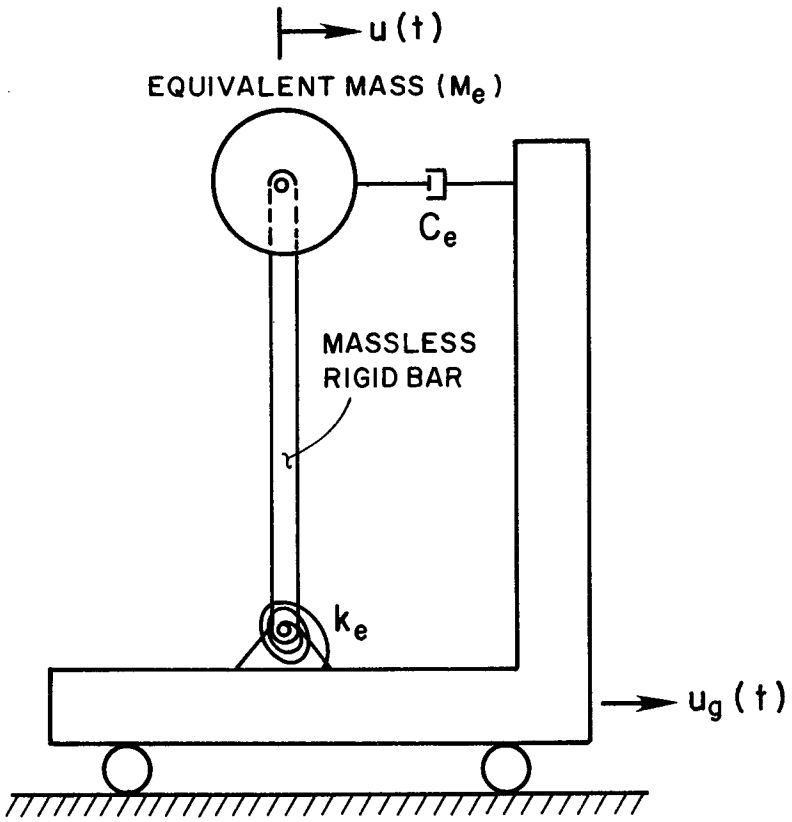

FIG. B.1 The Q-Model (From Ref. 21)

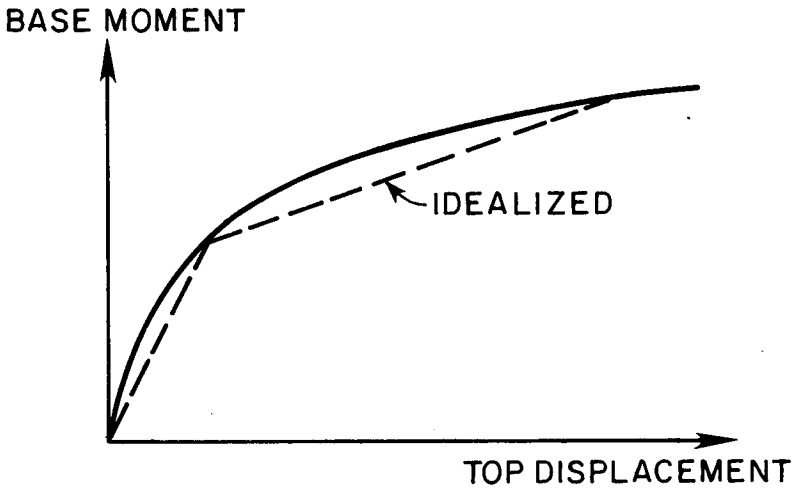

FIG. B.2 Force-Displacement Curve Used To Determine The Characteristic Vibration Shape

EARTHQUAKE ENGINEERING RESEARCH CENTER REPORTS

NOTE: Numbers in parentheses are Accession Numbers assigned by the National Technical Information Service; these are followed by a price code. Copies of the reports may be ordered from the National Technical Information Service, 5285 Port Royal Road, Springfield, Virginia, 22161. Accession Numbers should be quoted on orders for reports (PB --- ---) and remittance must accompany each order. Reports without this information were not available at time of printing. The complete list of EERC reports (from EERC 67-1) is available upon request from the Earthquake Engineering Research Center, University of California, Berkeley, 47th Street and Hoffman Boulevard, Richmond, California 94804.

UCB/EERC-77/01 "PLUSH - A Computer Program for Probabilistic Finite Element Analysis of Seismic Soil-Structure Interaction," by M.P. Romo Organista, J. Lysmer and H.B. Seed - 1977 (PB81 177 651)A05

UCB/EERC-77/02 "Soil-Structure Interaction Effects at the Humboldt Bay Power Plant in the Ferndale Earthquake of June 7, 1975," by J.E. Valera, H.B. Seed, C.F. Tsai and J. Lysmer - 1977 (PB 265 795)A04

UCB/EERC-77/03 "Influence of Sample Disturbance on Sand Response to Cyclic Loading," by K. Mori, H.B. Seed and C.K. Chan - 1977 (PB 267 352)A04

UCB/EERC-77/04 "Seismological Studies of Strong Motion Records," by J. Shoja-Taheri - 1977 (PB 269 655)A10

UCB/EERC-77/05 Unassigned

UCB/EERC-77/06 "Developing Methodologies for Evaluating the Earthquake Safety of Existing Buildings," by No. 1 - B. Bresler; No. 2 - B. Bresler, T. Okada and D. Zisling; No. 3 - T. Okada and B. Bresler; No. 4 - V.V. Bertero and B. Bresler - 1977 (PB 267 354)A08

UCB/EERC-77/07 "A Literature Survey - Transverse Strength of Masonry Walls," by Y. Omote, R.L. Mayes, S.W. Chen and R.W. Clough - 1977 (PB 277 933)A07

UCB/EERC-77/08 "DRAIN-TABS: A Computer Program for Inelastic Earthquake Response of Three Dimensional Buildings," by R. Guendelman-Israel and G.H. Powell - 1977 (PB 270 693)A07

UCB/EERC-77/09 "SUBWALL: A Special Purpose Finite Element Computer Program for Practical Elastic Analysis and Design of Structural Walls with Substructure Option," by D.Q. Le, H. Peterson and E.P. Popov - 1977 (PB 270 567)A05

UCB/EERC-77/10 "Experimental Evaluation of Seismic Design Methods for Broad Cylindrical Tanks," by D.P. Clough (PB 272 280)A13

UCB/EERC-77/11 "Earthquake Engineering Research at Berkeley - 1976," - 1977 (PB 273 507)A09

UCB/EERC-77/12 "Automated Design of Earthquake Resistant Multistory Steel Building Frames," by N.D. Walker, Jr. - 1977 (PB 276 526)A09

UCB/EERC-77/13 "Concrete Confined by Rectangular Hoops Subjected to Axial Loads," by J. Vallenas, V.V. Bertero and E.P. Popov - 1977 (PB 275 165)A06

UCB/EERC-77/14 "Seismic Strain Induced in the Ground During Earthquakes," by Y. Sugimura - 1977 (PB 284 201)A04

UCB/EERC-77/15 Unassigned

UCB/EERC-77/16 "Computer Aided Optimum Design of Ductile Reinforced Concrete Moment Resisting Frames," by S.W. Zagajeski and V.V. Bertero - 1977 (PB 280 137)A07

UCB/EERC-77/17 "Earthquake Simulation Testing of a Stepping Frame with Energy-Absorbing Devices," by J.M. Kelly and D.F. Tsztoo - 1977 (PB 273 506)A04

UCB/EERC-77/18 "Inelastic Behavior of Eccentrically Braced Steel Frames under Cyclic Loadings," by C.W. Roeder and E.P. Popov - 1977 (PB 275 526)A15

UCB/EERC-77/19 "A Simplified Procedure for Estimating Earthquake-Induced Deformations in Dams and Embankments," by F.I. Makdisi and H.B. Seed - 1977 (PB 276 820)A04

UCB/EERC-77/20 "The Performance of Earth Dams during Earthquakes," by H.B. Seed, F.I. Makdisi and P. de Alba - 1977 (PB 276 821)A04

UCB/EERC-77/21 "Dynamic Plastic Analysis Using Stress Resultant Finite Element Formulation," by P. Lukkunapvasit and J.M. Kelly - 1977 (PB 275 453)A04

UCB/EERC-77/22 "Preliminary Experimental Study of Seismic Uplift of a Steel Frame," by R.W. Clough and A.A. Huckelbridge 1977 (PB 278 769)A08

UCB/EERC-77/23 "Earthquake Simulator Tests of a Nine-Story Steel Frame with Columns Allowed to Uplift," by A.A. Huckelbridge - 1977 (PB 277 944)A09

UCB/EERC-77/24 "Nonlinear Soil-Structure Interaction of Skew Highway Bridges," by M.-C. Chen and J. Penzien - 1977 (PB 276 176)A07

UCB/EERC-77/25 "Seismic Analysis of an Offshore Structure Supported on Pile Foundations," by D.D.-N. Liou and J. Penzien 1977 (PB 283 180)A06

UCB/EERC-77/26 "Dynamic Stiffness Matrices for Homogeneous Viscoelastic Half-Planes," by G. Dasgupta and A.K. Chopra - 1977 (PB 279 654)A06

UCB/EERC-77/27 "A Practical Soft Story Earthquake Isolation System," by J.M. Kelly, J.M. Eidinger and C.J. Derham - 1977 (PB 276 814)A07

UCB/EERC-77/28 "Seismic Safety of Existing Buildings and Incentives for Hazard Mitigation in San Francisco: An Exploratory Study," by A.J. Meltsner - 1977 (PB 281 970)A05

UCB/EERC-77/29 "Dynamic Analysis of Electrohydraulic Shaking Tables," by D. Rea, S. Abedi-Hayati and Y. Takahashi 1977 (PB 282 569)A04

UCB/EERC-77/30 "An Approach for Improving Seismic - Resistant Behavior of Reinforced Concrete Interior Joints," by B. Galunic, V.V. Bertero and E.P. Popov - 1977 (PB 290 870)A06

UCB/EERC-78/01 "The Development of Energy-Absorbing Devices for Aseismic Base Isolation Systems," by J.M. Kelly and D.F. Tsztoo - 1978 (PB 284 978)A04

UCB/EERC-78/02 "Effect of Tensile Prestrain on the Cyclic Response of Structural Steel Connections, by J.G. Bouwkamp and A. Mukhopadhyay - 1978

UCB/EERC-78/03 "Experimental Results of an Earthquake Isolation System using Natural Rubber Bearings," by J.M. Eidinger and J.M. Kelly - 1978 (PB 281 686)A04

UCB/EERC-78/04 "Seismic Behavior of Tall Liquid Storage Tanks," by A. Niwa - 1978 (PB 284 017)A14

UCB/EERC-78/05 "Hysteretic Behavior of Reinforced Concrete Columns Subjected to High Axial and Cyclic Shear Forces," by S.W. Zagajeski, V.V. Bertero and J.G. Bouwkamp - 1978 (PB 283 858)A13

UCB/EERC-78/06 "Three Dimensional Inelastic Frame Elements for the ANSR-I Program," by A. Riahi, D.G. Row and G.H. Powell - 1978 (PB 295 755)A04

UCB/EERC-78/07 "Studies of Structural Response to Earthquake Ground Motion," by O.A. Lopez and A.K. Chopra - 1978 (PB 282 790)A05

UCB/EERC-78/08 "A Laboratory Study of the Fluid-Structure Interaction of Submerged Tanks and Caissons in Earthquakes," by R.C. Byrd - 1978 (PB 284 957)A08

UCB/EERC-78/09 Unassigned

UCB/EERC-78/10 "Seismic Performance of Nonstructural and Secondary Structural Elements," by I. Sakamoto - 1978 (PB81 154 593)A05

UCB/EERC-78/11 "Mathematical Modelling of Hysteresis Loops for Reinforced Concrete Columns," by S. Nakata, T. Sproul and J. Penzien - 1978 (PB 298 274)A05

UCB/EERC-78/12 "Damageability in Existing Buildings," by T. Blejwas and B. Bresler - 1978 (PB 80 166 978)A05

UCB/EERC-78/13 "Dynamic Behavior of a Pedestal Base Multistory Building," by R.M. Stephen, E.L. Wilson, J.G. Bouwkamp and M. Button - 1978 (PB 286 650)A08

UCB/EERC-78/14 "Seismic Response of Bridges - Case Studies," by R.A. Imbsen, V. Nutt and J. Penzien - 1978 (PB 286 503)A10

UCB/EERC-78/15 "A Substructure Technique for Nonlinear Static and Dynamic Analysis," by D.G. Row and G.H. Powell - 1978 (PB 288 077)A10

UCB/EERC-78/16 "Seismic Risk Studies for San Francisco and for the Greater San Francisco Bay Area," by C.S. Oliveira - 1978 (PB 81 120 115)A07

UCB/EERC-78/17 "Strength of Timber Roof Connections Subjected to Cyclic Loads," by P. Gülkan, R.L. Mayes and R.W. Clough - 1978 (HUD-000 1491)A07

UCB/EERC-78/18 "Response of K-Braced Steel Frame Models to Lateral Loads," by J.G. Bouwkamp, R.M. Stephen and E.P. Popov - 1978

UCB/EERC-78/19 "Rational Design Methods for Light Equipment in Structures Subjected to Ground Motion," by J.L. Sackman and J.M. Kelly - 1978 (PB 292 357)A04

UCB/EERC-78/20 "Testing of a Wind Restraint for Aseismic Base Isolation," by J.M. Kelly and D.E. Chitty - 1978 (PB 292 833)A03

UCB/EERC-78/21 "APOLLO - A Computer Program for the Analysis of Pore Pressure Generation and Dissipation in Horizontal Sand Layers During Cyclic or Earthquake Loading," by P.P. Martin and H.B. Seed - 1978 (PB 292 835)A04

UCB/EERC-78/22 "Optimal Design of an Earthquake Isolation System," by M.A. Bhatti, K.S. Pister and E. Polak - 1978 (PB 294 735)A06

UCB/EERC-78/23 "MASH - A Computer Program for the Non-Linear Analysis of Vertically Propagating Shear Waves in Horizontally Layered Deposits," by P.P. Martin and H.B. Seed - 1978 (PB 293 101)A05

UCB/EERC-78/24 "Investigation of the Elastic Characteristics of a Three Story Steel Frame Using System Identification," by I. Kaya and H.D. McNiven - 1978 (PB 296 225)A06

UCB/EERC-78/25 "Investigation of the Nonlinear Characteristics of a Three-Story Steel Frame Using System Identification," by I. Kaya and H.D. McNiven - 1978 (PB 301 363)A05

UCB/EERC-78/26 "Studies of Strong Ground Motion in Taiwan," by Y.M. Hsiung, B.A. Bolt and J. Penzien - 1978 (PB 298 436)A06

UCB/EERC-78/27 "Cyclic Loading Tests of Masonry Single Piers: Volume 1 - Height to Width Ratio of 2," by P.A. Hidalgo, R.L. Mayes, H.D. McNiven and R.W. Clough - 1978 (PB 296 211)A07

UCB/EERC-78/28 "Cyclic Loading Tests of Masonry Single Piers: Volume 2 - Height to Width Ratio of 1," by S.-W.J. Chen, P.A. Hidalgo, R.L. Mayes, R.W. Clough and H.D. McNiven - 1978 (PB 296 212)A09

UCB/EERC-78/29 "Analytical Procedures in Soil Dynamics," by J. Lysmer - 1978 (PB 298 445)A06

UCB/EERC-79/01 "Hysteretic Behavior of Lightweight Reinforced Concrete Beam-Column Subassemblages," by B. Forzani, E.P. Popov and V.V. Bertero - April 1979(PB 298 267)A06

UCB/EERC-79/02 "The Development of a Mathematical Model to Predict the Flexural Response of Reinforced Concrete Beams to Cyclic Loads, Using System Identification," by J. Stanton & H. McNiven - Jan. 1979(PB 295 875)A10

UCB/EERC-79/03 "Linear and Nonlinear Earthquake Response of Simple Torsionally Coupled Systems," by C.L. Kan and A.K. Chopra - Feb. 1979(PB 298 262)A06

UCB/EERC-79/04 "A Mathematical Model of Masonry for Predicting its Linear Seismic Response Characteristics," by Y. Mengi and H.D. McNiven - Feb. 1979(PB 298 266)A06

UCB/EERC-79/05 "Mechanical Behavior of Lightweight Concrete Confined by Different Types of Lateral Reinforcement," by M.A. Manrique, V.V. Bertero and E.P. Popov - May 1979(PB 301 114)A06

UCB/EERC-79/06 "Static Tilt Tests of a Tall Cylindrical Liquid Storage Tank," by R.W. Clough and A. Niwa - Feb. 1979 (PB 301 167)A06

UCB/EERC-79/07 "The Design of Steel Energy Absorbing Restrainers and Their Incorporation into Nuclear Power Plants for Enhanced Safety: Volume 1 - Summary Report," by P.N. Spencer, V.F. Zackay, and E.R. Parker - Feb. 1979(UCB/EERC-79/07)A09

UCB/EERC-79/08 "The Design of Steel Energy Absorbing Restrainers and Their Incorporation into Nuclear Power Plants for Enhanced Safety: Volume 2 - The Development of Analyses for Reactor System Piping,""Simple Systems" by M.C. Lee, J. Penzien, A.K. Chopra and K, Suzuki "Complex Systems" by G.H. Powell, E.L. Wilson, R.W. Clough and D.G. Row - Feb. 1979(UCB/EERC-79/08)A10

UCB/EERC-79/09 "The Design of Steel Energy Absorbing Restrainers and Their Incorporation into Nuclear Power Plants for Enhanced Safety: Volume 3 - Evaluation of Commercial Steels," by W.S. Owen, R.M.N. Pelloux, R.O. Ritchie, M. Faral, T. Ohhashi, J. Toplosky, S.J. Hartman, V.F. Zackay and E.R. Parker - Feb. 1979(UCB/EERC-79/09)A04

UCB/EERC-79/10 "The Design of Steel Energy Absorbing Restrainers and Their Incorporation into Nuclear Power Plants for Enhanced Safety: Volume 4 - A Review of Energy-Absorbing Devices," by J.M. Kelly and M.S. Skinner - Feb. 1979(UCB/EERC-79/10)A04

UCB/EERC-79/11 "Conservatism In Summation Rules for Closely Spaced Modes," by J.M. Kelly and J.L. Sackman - May 1979(PB 301 328)A03

UCB/EERC-79/12 "Cyclic Loading Tests of Masonry Single Piers; Volume 3 - Height to Width Ratio of 0.5," by P.A. Hidalgo, R.L. Mayes, H.D. McNiven and R.W. Clough - May 1979(PB 301 321)A08

UCB/EERC-79/13 "Cyclic Behavior of Dense Course-Grained Materials in Relation to the Seismic Stability of Dams," by N.G. Banerjee, H.B. Seed and C.K. Chan - June 1979(PB 301 373)A13

UCB/EERC-79/14 "Seismic Behavior of Reinforced Concrete Interior Beam-Column Subassemblages," by S. Viwathanatepa, E.P. Popov and V.V. Bertero - June 1979(PB 301 326)A10

UCB/EERC-79/15 "Optimal Design of Localized Nonlinear Systems with Dual Performance Criteria Under Earthquake Excitations," by M.A. Bhatti - July 1979(PB 80 167 109)A06

UCB/EERC-79/16 "OPTDYN - A General Purpose Optimization Program for Problems with or without Dynamic Constraints," by M.A. Bhatti, E. Polak and K.S. Pister - July 1979(PB 80 167 091)A05

UCB/EERC-79/17 "ANSR-II, Analysis of Nonlinear Structural Response, Users Manual," by D.P. Mondkar and G.H. Powell July 1979(PB 80 113 301)A05

UCB/EERC-79/18 "Soil Structure Interaction in Different Seismic Environments," A. Gomez-Masso, J. Lysmer, J.-C. Chen and H.B. Seed - August 1979(PB 80 101 520)A04

UCB/EERC-79/19 "ARMA Models for Earthquake Ground Motions," by M.K. Chang, J.W. Kwiatkowski, R.F. Nau, R.M. Oliver and K.S. Pister - July 1979(PB 301 166)A05

UCB/EERC-79/20 "Hysteretic Behavior of Reinforced Concrete Structural Walls," by J.M. Vallenas, V.V. Bertero and E.P. Popov - August 1979(PB 80 165 905)A12

UCB/EERC-79/21 "Studies on High-Frequency Vibrations of Buildings - 1: The Column Effect," by J. Lubliner - August 1979 (PB 80 158 553)A03

UCB/EERC-79/22 "Effects of Generalized Loadings on Bond Reinforcing Bars Embedded in Confined Concrete Blocks," by S. Viwathanatepa, E.P. Popov and V.V. Bertero - August 1979(PB 81 124 018)A14

UCB/EERC-79/23 "Shaking Table Study of Single-Story Masonry Houses, Volume 1: Test Structures 1 and 2," by P. Gülkan, R.L. Mayes and R.W. Clough - Sept. 1979 (HUD-000 1763)A12

UCB/EERC-79/24 "Shaking Table Study of Single-Story Masonry Houses, Volume 2: Test Structures 3 and 4," by P. Gülkan, R.L. Mayes and R.W. Clough - Sept. 1979 (HUD-000 1836)A12

UCB/EERC-79/25 "Shaking Table Study of Single-Story Masonry Houses, Volume 3: Summary, Conclusions and Recommendations," by R.W. Clough, R.L. Mayes and P. Gülkan - Sept. 1979 (HUD-000 1837)A06

UCB/EERC-79/26 "Recommendations for a U.S.-Japan Cooperative Research Program Utilizing Large-Scale Testing Facilities," by U.S.-Japan Planning Group - Sept. 1979(PB 301 407)A06

UCB/EERC-79/27 "Earthquake-Induced Liquefaction Near Lake Amatitlan, Guatemala," by H.B. Seed, I. Arango, C.K. Chan, A. Gomez-Masso and R. Grant de Ascoli - Sept. 1979(NUREG-CR1341)A03

UCB/EERC-79/28 "Infill Panels: Their Influence on Seismic Response of Buildings," by J.W. Axley and V.V. Bertero Sept. 1979(PB 80 163 371)A10

UCB/EERC-79/29 "3D Truss Bar Element (Type 1) for the ANSR-II Program," by D.P. Mondkar and G.H. Powell - Nov. 1979 (PB 80 169 709)A02

UCB/EERC-79/30 "2D Beam-Column Element (Type 5 - Parallel Element Theory) for the ANSR-II Program," by D.G. Row, G.H. Powell and D.P. Mondkar - Dec. 1979(PB 80 167 224)A03

UCB/EERC-79/31 "3D Beam-Column Element (Type 2 - Parallel Element Theory) for the ANSR-II Program," by A. Riahi, G.H. Powell and D.P. Mondkar - Dec. 1979(PB 80 167 216)A03

UCB/EERC-79/32 "On Response of Structures to Stationary Excitation," by A. Der Kiureghian - Dec. 1979(PB 80166 929)A03

UCB/EERC-79/33 "Undisturbed Sampling and Cyclic Load Testing of Sands," by S. Singh, H.B. Seed and C.K. Chan Dec. 1979(ADA 087 298)A07

UCB/EERC-79/34 "Interaction Effects of Simultaneous Torsional and Compressional Cyclic Loading of Sand," by P.M. Griffin and W.N. Houston - Dec. 1979(ADA 092 352)A15

UCB/EERC-80/01 "Earthquake Response of Concrete Gravity Dams Including Hydrodynamic and Foundation Interaction Effects," by A.K. Chopra, P. Chakrabarti and S. Gupta - Jan. 1980(AD-A087297)A10

UCB/EERC-80/02 "Rocking Response of Rigid Blocks to Earthquakes," by C.S. Yim, A.K. Chopra and J. Penzien - Jan. 1980 (PB80 166 002)A04

UCB/EERC-80/03 "Optimum Inelastic Design of Seismic-Resistant Reinforced Concrete Frame Structures," by S.W. Zagajeski and V.V. Bertero - Jan. 1980(PB80 164 635)A06

UCB/EERC-80/04 "Effects of Amount and Arrangement of Wall-Panel Reinforcement on Hysteretic Behavior of Reinforced Concrete Walls," by R. Iliya and V.V. Bertero - Feb. 1980(PB81 122 525)A09

UCB/EERC-80/05 "Shaking Table Research on Concrete Dam Models," by A. Niwa and R.W. Clough - Sept. 1980(PB81 122 368)A06

UCB/EERC-80/06 "The Design of Steel Energy-Absorbing Restrainers and their Incorporation into Nuclear Power Plants for Enhanced Safety (Vol 1A): Piping with Energy Absorbing Restrainers: Parameter Study on Small Systems," by G.H. Powell, C. Oughourlian and J. Simons - June 1980

UCB/EERC-80/07 "Inelastic Torsional Response of Structures Subjected to Earthquake Ground Motions," by Y. Yamazaki April 1980(PB81 122 327)A08

UCB/EERC-80/08 "Study of X-Braced Steel Frame Structures Under Earthquake Simulation," by Y. Ghanaat - April 1980 (PB81 122 335)A11

UCB/EERC-80/09 "Hybrid Modelling of Soil-Structure Interaction," by S. Gupta, T.W. Lin, J. Penzien and C.S. Yeh May 1980(PB81 122 319)A07

UCB/EERC-80/10 "General Applicability of a Nonlinear Model of a One Story Steel Frame," by B.I. Sveinsson and H.D. McNiven - May 1980(PB81 124 877)A06

UCB/EERC-80/11 "A Green-Function Method for Wave Interaction with a Submerged Body," by W. Kioka - April 1980 (PB81 122 269)A07

UCB/EERC-80/12 "Hydrodynamic Pressure and Added Mass for Axisymmetric Bodies," by F. Nilrat - May 1980(PB81 122 343)A08

UCB/EERC-80/13 "Treatment of Non-Linear Drag Forces Acting on Offshore Platforms," by B.V. Dao and J. Penzien May 1980(PB81 153 413)A07

UCB/EERC-80/14 "2D Plane/Axisymmetric Solid Element (Type 3 - Elastic or Elastic-Perfectly Plastic) for the ANSR-II Program," by D.P. Mondkar and G.H. Powell - July 1980(PB81 122 350)A03

UCB/EERC-80/15 "A Response Spectrum Method for Random Vibrations," by A. Der Kiureghian - June 1980(PB81 122 301)A03

UCB/EERC-80/16 "Cyclic Inelastic Buckling of Tubular Steel Braces," by V.A. Zayas, E.P. Popov and S.A. Mahin June 1980(PB81 124 885)A10

UCB/EERC-80/17 "Dynamic Response of Simple Arch Dams Including Hydrodynamic Interaction," by C.S. Porter and A.K. Chopra - July 1980(PB81 124 000)A13

UCB/EERC-80/18 "Experimental Testing of a Friction Damped Aseismic Base Isolation System with Fail-Safe Characteristics," by J.M. Kelly, K.E. Beucke and M.S. Skinner - July 1980(PB81 148 595)A04

UCB/EERC-80/19 "The Design of Steel Energy-Absorbing Restrainers and their Incorporation into Nuclear Power Plants for Enhanced Safety (Vol 1B): Stochastic Seismic Analyses of Nuclear Power Plant Structures and Piping Systems Subjected to Multiple Support Excitations," by M.C. Lee and J. Penzien - June 1980

UCB/EERC-80/20 "The Design of Steel Energy-Absorbing Restrainers and their Incorporation into Nuclear Power Plants for Enhanced Safety (Vol 1C): Numerical Method for Dynamic Substructure Analysis," by J.M. Dickens and E.L. Wilson - June 1980

UCB/EERC-80/21 "The Design of Steel Energy-Absorbing Restrainers and their Incorporation into Nuclear Power Plants for Enhanced Safety (Vol 2): Development and Testing of Restraints for Nuclear Piping Systems," by J.M. Kelly and M.S. Skinner - June 1980

UCB/EERC-80/22 "3D Solid Element (Type 4-Elastic or Elastic-Perfectly-Plastic) for the ANSR-II Program," by D.P. Mondkar and G.H. Powell - July 1980(PB81 123 242)A03

UCB/EERC-80/23 "Gap-Friction Element (Type 5) for the ANSR-II Program," by D.P. Mondkar and G.H. Powell - July 1980 (PB81 122 285)A03

UCB/EERC-80/24 "U-Bar Restraint Element (Type 11) for the ANSR-II Program," by C. Oughourlian and G.H. Powell July 1980(PB81 122 293)A03

UCB/EERC-80/25 "Testing of a Natural Rubber Base Isolation System by an Explosively Simulated Earthquake," by J.M. Kelly - August 1980(PB81 201 360)A04

UCB/EERC-80/26 "Input Identification from Structural Vibrational Response," by Y. Hu - August 1980(PB81 152 308)A05

UCB/EERC-80/27 "Cyclic Inelastic Behavior of Steel Offshore Structures," by V.A. Zayas, S.A. Mahin and E.P. Popov August 1980(PB81 196 180)A15

UCB/EERC-80/28 "Shaking Table Testing of a Reinforced Concrete Frame with Biaxial Response," by M.G. Oliva October 1980(PB81 154 304)A10

UCB/EERC-80/29 "Dynamic Properties of a Twelve-Story Prefabricated Panel Building," by J.G. Bouwkamp, J.P. Kollegger and R.M. Stephen - October 1980(PB82 117 128)A06

UCB/EERC-80/30 "Dynamic Properties of an Eight-Story Prefabricated Panel Building," by J.G. Bouwkamp, J.P. Kollegger and R.M. Stephen - October 1980(PB81 200 313)A05

UCB/EERC-80/31 "Predictive Dynamic Response of Panel Type Structures Under Earthquakes," by J.P. Kollegger and J.G. Bouwkamp - October 1980(PB81 152 316)A04

UCB/EERC-80/32 "The Design of Steel Energy-Absorbing Restrainers and their Incorporation into Nuclear Power Plants for Enhanced Safety (Vol 3): Testing of Commercial Steels in Low-Cycle Torsional Fatigue," by P. Spencer, E.R. Parker, E. Jongewaard and M. Drory

UCB/EERC-80/33 "The Design of Steel Energy-Absorbing Restrainers and their Incorporation into Nuclear Power Plants for Enhanced Safety (Vol 4): Shaking Table Tests of Piping Systems with Energy-Absorbing Restrainers," by S.F. Stiemer and W.G. Godden - Sept. 1980

UCB/EERC-80/34 "The Design of Steel Energy-Absorbing Restrainers and their Incorporation into Nuclear Power Plants for Enhanced Safety (Vol 5): Summary Report," by P. Spencer

UCB/EERC-80/35 "Experimental Testing of an Energy-Absorbing Base Isolation System," by J.M. Kelly, M.S. Skinner and K.E. Beucke - October 1980(PB81 154 072)A04

UCB/EERC-80/36 "Simulating and Analyzing Artificial Non-Stationary Earthquake Ground Motions," by R.F. Nau, R.M. Oliver and K.S. Pister - October 1980(PB81 153 397)A04

UCB/EERC-80/37 "Earthquake Engineering at Berkeley - 1980," - Sept. 1980(PB81 205 374)A09

UCB/EERC-80/38 "Inelastic Seismic Analysis of Large Panel Buildings," by V. Schricker and G.H. Powell - Sept. 1980 (PB81 154 338)A13

UCB/EERC-80/39 "Dynamic Response of Embankment, Concrete-Gravity and Arch Dams Including Hydrodynamic Interaction," by J.F. Hall and A.K. Chopra - October 1980(PB81 152 324)A11

UCB/EERC-80/40 "Inelastic Buckling of Steel Struts Under Cyclic Load Reversal," by R.G. Black, W.A. Wenger and E.P. Popov - October 1980(PB81 154 312)A08

UCB/EERC-80/41 "Influence of Site Characteristics on Building Damage During the October 3, 1974 Lima Earthquake," by P. Repetto, I. Arango and H.B. Seed - Sept. 1980(PB81 161 739)A05

UCB/EERC-80/42 "Evaluation of a Shaking Table Test Program on Response Behavior of a Two Story Reinforced Concrete Frame," by J.M. Blondet, R.W. Clough and S.A. Mahin

UCB/EERC-80/43 "Modelling of Soil-Structure Interaction by Finite and Infinite Elements," by F. Medina - December 1980(PB81 229 270)A04

UCB/EERC-81/01 "Control of Seismic Response of Piping Systems and Other Structures by Base Isolation," edited by J.M. Kelly - January 1981 (PB81 200 735)A05

UCB/EERC-81/02 "OPTNSR - An Interactive Software System for Optimal Design of Statically and Dynamically Loaded Structures with Nonlinear Response," by M.A. Bhatti, V. Ciampi and K.S. Pister - January 1981 (PB81 218 851)A09

UCB/EERC-81/03 "Analysis of Local Variations in Free Field Seismic Ground Motions," by J.-C. Chen, J. Lysmer and H.B. Seed - January 1981 (AD-A099508)A13

UCB/EERC-81/04 "Inelastic Structural Modeling of Braced Offshore Platforms for Seismic Loading," by V.A. Zayas, P.-S.B. Shing, S.A. Mahin and E.P. Popov - January 1981(PB82 138 777)A07

UCB/EERC-81/05 "Dynamic Response of Light Equipment in Structures," by A. Der Kiureghian, J.L. Sackman and B. Nour-Omid - April 1981 (PB81 218 497)A04

UCB/EERC-81/06 "Preliminary Experimental Investigation of a Broad Base Liquid Storage Tank," by J.G. Bouwkamp, J.P. Kollegger and R.M. Stephen - May 1981(PB82 140 385)A03

UCB/EERC-81/07 "The Seismic Resistant Design of Reinforced Concrete Coupled Structural Walls," by A.E. Aktan and V.V. Bertero - June 1981(PB82 113 358)A11

UCB/EERC-81/08 "The Undrained Shearing Resistance of Cohesive Soils at Large Deformations," by M.R. Pyles and H.B. Seed - August 1981

UCB/EERC-81/09 "Experimental Behavior of a Spatial Piping System with Steel Energy Absorbers Subjected to a Simulated Differential Seismic Input," by S.F. Stiemer, W.G. Godden and J.M. Kelly - July 1981

UCB/EERC-81/10 "Evaluation of Seismic Design Provisions for Masonry in the United States," by B.I. Sveinsson, R.L. Mayes and H.D. McNiven - August 1981 (PB82 166 075)A08

UCB/EERC-81/11 "Two-Dimensional Hybrid Modelling of Soil-Structure Interaction," by T.-J. Tzong, S. Gupta and J. Penzien - August 1981(PB82 142 118)A04

UCB/EERC-81/12 "Studies on Effects of Infills in Seismic Resistant R/C Construction," by S. Brokken and V.V. Bertero - September 1981 (PB82 166 190)A09

UCB/EERC-81/13 "Linear Models to Predict the Nonlinear Seismic Behavior of a One-Story Steel Frame," by H. Valdimarsson, A.H. Shah and H.D. McNiven - September 1981(PB82 138 793)A07

UCB/EERC-81/14 "TLUSH: A Computer Program for the Three-Dimensional Dynamic Analysis of Earth Dams," by T. Kagawa, L.H. Mejia, H.B. Seed and J. Lysmer - September 1981(PB82 139 940)A06

UCB/EERC-81/15 "Three Dimensional Dynamic Response Analysis of Earth Dams," by L.H. Mejia and H.B. Seed - September 1981 (PB82 137 274)A12

UCB/EERC-81/16 "Experimental Study of Lead and Elastomeric Dampers for Base Isolation Systems," by J.M. Kelly and S.B. Hodder - October 1981 (PB82 166 182)A05

UCB/EERC-81/17 "The Influence of Base Isolation on the Seismic Response of Light Secondary Equipment," by J.M. Kelly - April 1981 (PB82 255 266)A04

UCB/EERC-81/18 "Studies on Evaluation of Shaking Table Response Analysis Procedures," by J. Marcial Blondet - November 1981 (PB82 197 278)A10

UCB/EERC-81/19 "DELIGHT.STRUCT: A Computer-Aided Design Environment for Structural Engineering," by R.J. Balling, K.S. Pister and E. Polak - December 1981 (PB82 218 496)A07

UCB/EERC-81/20 "Optimal Design of Seismic-Resistant Planar Steel Frames," by R.J. Balling, V. Ciampi, K.S. Pister and E. Polak - December 1981 (PB82 220 179)A07

UCB/EERC-82/01 "Dynamic Behavior of Ground for Seismic Analysis of Lifeline Systems," by T. Sato and A. Der Kiureghian - January 1982 (PB82 218 926)A05

UCB/EERC-82/02 "Shaking Table Tests of a Tubular Steel Frame Model," by Y. Ghanaat and R. W. Clough - January 1982 (PB82 220 161)A07

UCB/EERC-82/03 "Behavior of a Piping System under Seismic Excitation: Experimental Investigations of a Spatial Piping System supported by Mechanical Shock Arrestors and Steel Energy Absorbing Devices under Seismic Excitation," by S. Schneider, H.-M. Lee and W. G. Godden - May 1982 (PB83 172 544)A09

UCB/EERC-82/04 "New Approaches for the Dynamic Analysis of Large Structural Systems," by E. L. Wilson - June 1982 (PB83 148 080)A05

UCB/EERC-82/05 "Model Study of Effects of Damage on the Vibration Properties of Steel Offshore Platforms," by F. Shahrivar and J. G. Bouwkamp - June 1982 (PB83 148 742)A10

UCB/EERC-82/06 "States of the Art and Practice in the Optimum Seismic Design and Analytical Response Prediction of R/C Frame-Wall Structures," by A. E. Aktan and V. V. Bertero - July 1982 (PB83 147 736)A05

UCB/EERC-82/07 "Further Study of the Earthquake Response of a Broad Cylindrical Liquid-Storage Tank Model," by G. C. Manos and R. W. Clough - July 1982 (PB83 147 744)A11

UCB/EERC-82/08 "An Evaluation of the Design and Analytical Seismic Response of a Seven Story Reinforced Concrete Frame - Wall Structure," by F. A. Charney and V. V. Bertero - July 1982(PB83 157 628)A09

UCB/EERC-82/09 "Fluid-Structure Interactions: Added Mass Computations for Incompressible Fluid," by J. S.-H. Kuo - August 1982 (PB83 156 281)A07

UCB/EERC-82/10 "Joint-Opening Nonlinear Mechanism: Interface Smeared Crack Model," by J. S.-H. Kuo - August 1982 (PB83 149 195)A05

UCB/EERC-82/11 "Dynamic Response Analysis of Techi Dam," by R. W. Clough, R. M. Stephen and J. S.-H. Kuo - August 1982 (PB83 147 496)A06

UCB/EERC-82/12 "Prediction of the Seismic Responses of R/C Frame-Coupled Wall Structures," by A. E. Aktan, V. V. Bertero and M. Piazza - August 1982 (PB83 149 203)A09

UCB/EERC-82/13 "Preliminary Report on the SMART 1 Strong Motion Array in Taiwan," by B. A. Bolt, C. H. Loh, J. Penzien, Y. B. Tsai and Y. T. Yeh - August 1982 (PB83 159 400)A10

UCB/EERC-82/14 "Shaking-Table Studies of an Eccentrically X-Braced Steel Structure," by M. S. Yang - September 1982 (PB83 260 778)A12

UCB/EERC-82/15 "The Performance of Stairways in Earthquakes," by C. Roha, J. W. Axley and V. V. Bertero - September 1982 (PB83 157 693)A07

UCB/EERC-82/16 "The Behavior of Submerged Multiple Bodies in Earthquakes," by W.-G. Liao - Sept. 1982 (PB83 158 709)A07

UCB/EERC-82/17 "Effects of Concrete Types and Loading Conditions on Local Bond-Slip Relationships," by A. D. Cowell, E. P. Popov and V. V. Bertero - September 1982 (PB83 153 577)A04

UCB/EERC-82/18 "Mechanical Behavior of Shear Wall Vertical Boundary Members: An Experimental Investigation," by M. T. Wagner and V. V. Bertero - October 1982 (PB83 159 764)A05

UCB/EERC-82/19 "Experimental Studies of Multi-support Seismic Loading on Piping Systems," by J. M. Kelly and A. D. Cowell - November 1982

UCB/EERC-82/20 "Generalized Plastic Hinge Concepts for 3D Beam-Column Elements," by P. F.-S. Chen and G. H. Powell - November 1982 (PB83 247 981)A13

UCB/EERC-82/21 "ANSR-III: General Purpose Computer Program for Nonlinear Structural Analysis," by C. V. Oughourlian and G. H. Powell - November 1982 (PB83 251 330)A12

UCB/EERC-82/22 "Solution Strategies for Statically Loaded Nonlinear Structures," by J. W. Simons and G. H. Powell - November 1982 (PB83 197 970)A06

UCB/EERC-82/23 "Analytical Model of Deformed Bar Anchorages under Generalized Excitations," by V. Ciampi, R. Eligehausen, V. V. Bertero and E. P. Popov - November 1982 (PB83 169 532)A06

UCB/EERC-82/24 "A Mathematical Model for the Response of Masonry Walls to Dynamic Excitations," by H. Sucuoğlu, Y. Mengi and H. D. McNiven - November 1982 (PB83 169 011)A07

UCB/EERC-82/25 "Earthquake Response Considerations of Broad Liquid Storage Tanks," by F. J. Cambra - November 1982 (PB83 251 215)A09

UCB/EERC-82/26 "Computational Models for Cyclic Plasticity, Rate Dependence and Creep," by B. Mosaddad and G. H. Powell - November 1982 (PB83 245 829)A08

UCB/EERC-82/27 "Inelastic Analysis of Piping and Tubular Structures," by M. Mahasuverachai and G. H. Powell - November 1982 (PB83 249 987)A07

UCB/EERC-83/01 "The Economic Feasibility of Seismic Rehabilitation of Buildings by Base Isolation," by J. M. Kelly - January 1983 (PB83 197 988)A05

UCB/EERC-83/02 "Seismic Moment Connections for Moment-Resisting Steel Frames," by E. P. Popov - January 1983 (PB83 195 412)A04

UCB/EERC-83/03 "Design of Links and Beam-to-Column Connections for Eccentrically Braced Steel Frames," by E. P. Popov and J. O. Malley - January 1983 (PB83 194 811)A04

UCB/EERC-83/04 "Numerical Techniques for the Evaluation of Soil-Structure Interaction Effects in the Time Domain," by E. Bayo and E. L. Wilson - February 1983 (PB83 245 605)A09

UCB/EERC-83/05 "A Transducer for Measuring the Internal Forces in the Columns of a Frame-Wall Reinforced Concrete Structure," by R. Sause and V. V. Bertero - May 1983 (PB84 119 494)A06

UCB/EERC-83/06 "Dynamic Interactions between Floating Ice and Offshore Structures," by P. Croteau - May 1983 (PB84 119 486)A16

UCB/EERC-83/07 "Dynamic Analysis of Multiply Tuned and Arbitrarily Supported Secondary Systems," by T. Igusa and A. Der Kiureghian - June 1983 (PB84 118 272)A11

UCB/EERC-83/08 "A Laboratory Study of Submerged Multi-body Systems in Earthquakes," by G. R. Ansari - June 1983 (PB83 261 842)A17

UCB/EERC-83/09 "Effects of Transient Foundation Uplift on Earthquake Response of Structures," by C.-S. Yim and A. K. Chopra - June 1983 (PB83 261 396)A07

UCB/EERC-83/10 "Optimal Design of Friction-Braced Frames under Seismic Loading," by M. A. Austin and K. S. Pister - June 1983 (PB84 119 288)A06

UCB/EERC-83/11 "Shaking Table Study of Single-Story Masonry Houses: Dynamic Performance under Three Component Seismic Input and Recommendations," by G. C. Manos, R. W. Clough and R. L. Mayes - June 1983

UCB/EERC-83/12 "Experimental Error Propagation in Pseudodynamic Testing," by P. B. Shing and S. A. Mahin - June 1983 (PB84 119 270)A09

UCB/EERC-83/13 "Experimental and Analytical Predictions of the Mechanical Characteristics of a 1/5-scale Model of a 7-story R/C Frame-Wall Building Structure," by A. E. Aktan, V. V. Bertero, A. A. Chowdhury and T. Nagashima - August 1983 (PB84 119 213)A07

UCB/EERC-83/14 "Shaking Table Tests of Large-Panel Precast Concrete Building System Assemblages," by M. G. Oliva and R. W. Clough - August 1983

UCB/EERC-83/15 "Seismic Behavior of Active Beam Links in Eccentrically Braced Frames," by K. D. Hjelmstad and E. P. Popov - July 1983 (PB84 119 676)A09

UCB/EERC-83/16 "System Identification of Structures with Joint Rotation," by J. S. Dimsdale and H. D. McNiven - July 1983

UCB/EERC-83/17 "Construction of Inelastic Response Spectra for Single-Degree-of-Freedom Systems," by S. Mahin and J. Lin - July 1983